CRANFIELD UNIVERSITY

Wenfang Dong

ATC Constraints and Modelling in Global ATM Environment

SCHOOL OF ENGINEERING

MSc by Research Thesis

January 2011

Cranfield University

School of Engineering

MSc by Research Thesis

Academic Year 2010 - 2011

Wenfang Dong

ATC Constraints and Modelling in Global ATM Environment

Supervisor: Dr. Huamin Jia

January 2011

ABSTRACT

The United Kingdom's Civil Aviation Authority published the national aviation forecast in 2008. The forecast predicts that domestic traffic will increase by 3.5% per year, and that international traffic will grow, on average, by 4.5% during 2010-2020. Based on this prediction, the traffic density will increase dramatically in the future, and airspace will be more and more congested. Usually, there are two potential solutions to deal with this situation: improving the ability of air traffic flow management is one solution; reducing the separation minimum of aircraft is another solution. However, this thesis focuses on the second solution, based on constraints of communication, navigation and surveillance systems (CNS). The separation minimum evaluation procedure can be divided into four steps: firstly, models or parameters are developed to describe the performance of CNS, such as navigation accuracy, communication transaction time and surveillance delay time; secondly, a Kalman filter prediction architecture, based on the CNS performance parameters, is built to improve the performance of aircraft's position estimation; then, a Reich model is used to evaluate the collision risk probability of parallel air route separation minimum; finally, the collision risk probability is compared to target level of safety (TLS) of 5×10^{-9} to ascertain whether the separation minimum can satisfy safety requirements or not.

On the basis of the above models, the air route separation minimum assessment has been completed. The results indicate that the method proposed in this thesis provides a feasible method for safety assessment of parallel route separation minimum.

Keywords: Safety Assessment, CNS Systems, Kalman Filter, Separation Minimum, Target Level of Safety.

ACKNOWLEDGEMENTS

First of all I would like to express my sincere thanks to my supervisor Dr. Huamin Jia for his advising, guidance and teaching during the research.

Special thanks are extended to Professor John Fielding, Dr. Craig Lawson, Dr. Shijun Guo, Dr. Howard Smith, and other staff in School of Engineering for their encouragements and advices.

My thanks would like to go to the AVIC of China and First Aircraft Design Institute, the company where I work, for the opportunity and support they offer to me to study in CRANFIELD UNIVERSITY.

Moreover I would like to acknowledge the help from my classmates with whom I work. My team learning capacity is greatly improved due to their help.

Finally, I give my best appreciation to my family members in China. I can not finish my work without their support.

TABLE OF CONTENTS

LIST OF FIGURES

LIST OF TABLES

LIST OF ABBREVIATIONS

ADS	Automatic dependent surveillance
ADS-B	Automatic dependent surveillance-broadcast
ATC	Air Traffic Control
ATN	Aeronautical Telecommunications Network
CNS/ATM	Communication, Navigation, Surveillance/ Air Traffic Management
CPDLC	Controller Pilot Data Link Communications
DME	Distance measuring equipment
ECEF	Earth-Centered, Earth-Fixed
FAA	Federal Aviation Administration
FANS	Future Air Navigation System
FTE	Flight Technical Error
FL 390	Flight Level
GPS	Global Positioning System
GNSS	Global Navigation Satellite Systems
HF	High Frequency
ICAO	International Civil Aviation Organization
ILS	Instrument Landing System
INS	Inertial Navigation System

NUCp	Navigation Uncertainty Category Position
NUCv	Navigation Uncertainty Category Velocity
PSR	Primary Surveillance Radar
RCP	Required Communication Performance
RSP	Required Surveillance Performance
RNP	Required Navigation Performance
RTSP	Requited Total System Performance
RNAV	Area Navigation
SSR	Secondary Surveillance Radar
VHF	Very High Frequency
VOR	VHF omnidirectional range
TLS	Target Level of Safety
TSE	Total System Error
TVE	Total Vertical Error
WGS-84	World Geodetic System of 1984

1 Introduction

In the past decades, the civil aviation industry has developed rapidly. According to the United Kingdom's Civil Aviation Authority report, the number of passengers who took flights at UK airports was 112 million in 1994 [1]. As Figure 1-1 shows, although there was a large decrease of passengers travelling by plane at UK airports between 2002 and 2003, the passengers had a 4% year-on-year increase between 1994 and 2007. A large number of aircraft are needed to meet the growth in air passengers, so the air space gets congested. As a consequence, airline delays become worse; for example, Heathrow airport has the worst delays in Europe, with passengers usually experiencing a delay of half an hour, and it is also implied in Figure 1.2 that 1/4 of flights in Europe are not on time, and the average delay is about 30-40 minutes [1].

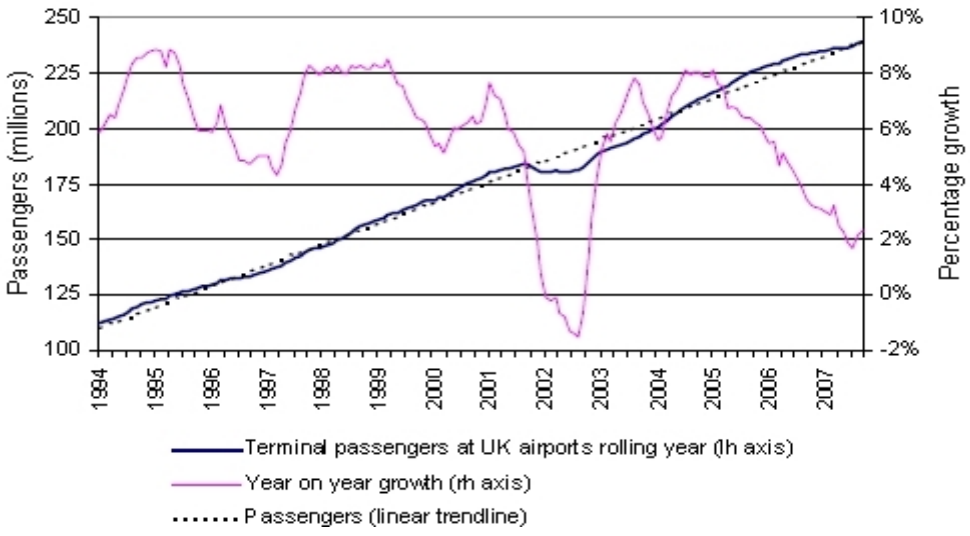

Figure 1-1 Passengers Growth [1]

The civil aviation industry will continue to increase in the future. The United Kingdom's Civil Aviation Authority published the national aviation forecast in 2008. The forecast shows a prediction that domestic traffic will increase 3.5% per year and international traffic will grow, on average, by 4.5% during 2010-2020 [1]. Based on this prediction, the traffic density will increase dramatically in the future, and airspace will be more and more congested.

Airline delay rates

AEA carriers at:	Flights %	minutes (avg)	AEA carriers at:	Flights %	minutes (avg)
London Heathrow	33.8	34.6	Milan Malpensa	20.8	36.7
Rome	31.2	40.9	Zurich	20.8	34.9
Paris CDG	27.8	38.7	Paris Orly	20.5	39.4
Larnaca	27.6	55.1	Lisbon	20.4	35.7
London Gatwick	27.4	33.8	Amsterdam	20.1	50.4
Madrid	26.7	38.0	Istanbul	19.9	38.5
Barcelona	26.5	40.3	Helsinki	19.5	37.5
Dublin	26.2	37.8	Geneva	19.3	32.7
Athens	25.9	42.5	Dusseldorf	18.9	36.2
Manchester	24.9	42.0	Oslo	18.0	35.7
Frankfurt	24.8	39.8	Vienna	16.9	36.3
Stockholm	23.9	36.3	Brussels	15.5	37.8
Milan Linate	23.0	37.9			
Munich	22.1	37.3	April - June 2007		

Figure 1-2 Airline Delay Rates [1]

As described, congestion of air space will become worse, and as a consequence, customers may suffer longer delays in the future. The main reasons contributing to the airline delay are shown as follows [1] - [2]:

- ◆Congestion of airspace;
- ◆Inefficient way to use airspace;
- ◆Low inefficient ATM;
- ◆Low ability of CNS;
- ◆Low capacity of airport.

In order to ease the air congestion, International Civil Aviation Organization (ICAO) introduced a new system, named as Communication, Navigation, Surveillance / Air Traffic Management (CNS/ATM) systems, which depended on the technologies in computers, satellites, advanced avionics and data links [2]. Based on the constraints of CNS systems, this thesis discusses the method, used to reduce the separation minimum to ease the air congestion.

1.1 Project Background

In the current ATC system, there are two types of instrument flight procedure as shown in Figure 1.3. The first one is ground-based radio navigation aids air route, shown in Figure 1.3a. In this architecture, many navigation aids are built along air routes. Aircraft must pass navigation aids one by one. This procedure

is being widely used nowadays, but has some significant disadvantages. Firstly, many navigation aids and air traffic control units should be built along air routes. Because of limited working range of the navigation aids, this air route architecture uses a small portion of airspace and the airspace can not be expanded. Some areas along the air route, such as mountains and oceanic areas are hard to build navigation aids on, so this air route architecture usually has longer flight distance than the optimum air route. Secondly, an aircraft's position estimation errors depend on the range between aircraft and navigation aids - the longer the range, the bigger the error. The second instrument flight procedure, shown in Figure 1.3b, is performance-based RNAV/RNP procedure. In this architecture, satellite navigation methods, such as GPS, which have world wide coverage, are selected. Therefore, the pilot can choose the optimum air route to follow, which results in shorter flight distance, lower fuel-cost and lower possibility of delay. Meanwhile, the separation minimum between aircraft of RNAV/RNP air route is smaller than that of the ground aids air route [3].

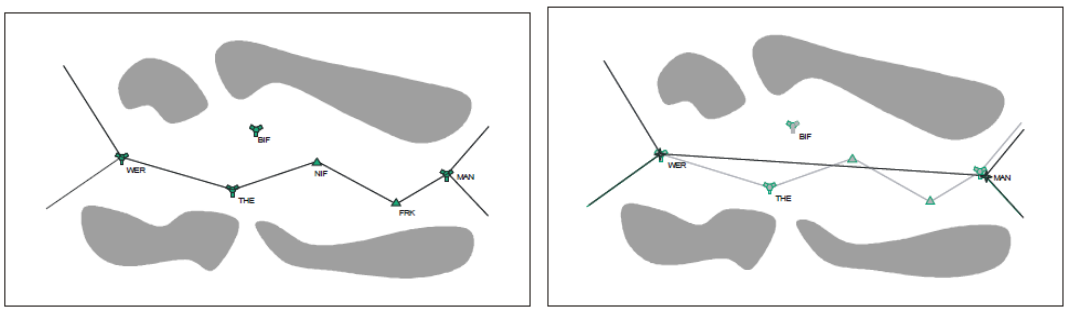

(a) (b)

Figure 1-3 Instrument Flight Procedure

Conventional Route, (b) Performance-based RNP Route [3]

In order to evaluate the separation minimum collision risk probability to satisfy the target level of safety (TLS) of 5×10^{-9}, Reich provided a model to evaluate safety issues of long range air traffic routes ([4]-[6]), and then this model was named as the Reich model and had a wide effect on the separation minimum estimation, which can be seen in the ICAO DOC 9426 [7]. In the Reich model, factors such as traffic density and navigation performance are considered. In

1977 and 1978, Brooker and Penna used the Reich model to evaluate the longitudinal separation of North Atlantic Air Traffic ([8]-[9]). Moek used the Reich model to conduct risk assessment of RNP 10 and RVSM in the South Atlantic Flight Identification Regions, and eventually the lateral separation was reduced from 100 NMI to 50 NMI after the air route was deployed the RNP 10 navigation ability [10]. In 2010, Zhang used the Reich model to estimate the collision risk in cross air routes in Shanghai areas in China, and the results showed that the separation minimum could satisfy the requirement of TLS ([10]-[13]. Radar surveillance sensor errors, including PSR and SSR sensor errors, have been carefully analysed [14]. The position errors and display errors have been evaluated in the activity. In 1995, Rockman developed a simple model to describe the radar separation minimum. 3 NMI separation minimum has been analysed, based on several factors such as surveillance position accuracy, radar antenna scan time, and human reaction time [15]. For 3 NMI and 5 NMI separations, Thompson and Andrews evaluate RSP needed to support the separation minimum [16]. Eventually, the RSP has been defined. Sakae Nagaoka estimated a radar separation minimum based on the long-range secondary surveillance radar. In his work, position errors mainly depend on the azimuth of the aircraft, and the separation minimum is evaluated [17]. Gazit discussed the probability that the separation minimum can be reduced when GPS is used as the main navigation sensors [18]. The result is that the GPS sensor can provide a smaller separation minimum than the radar sensors does. Jones provided an idea that ADS-B can be used to support the 3 NMI and 5 NMI separation minimum [19]. Michael evaluated separation though the ADS-B in LOUISVILLE, in 2009 [20]. The result shows that the ADS-B can satisfy the requirements used to set a 5 NMI separation minimum.

As the existing separation minimum risk assessment model is based on ground aids technology, or the model considers navigation performance only, it is suggested to develop an assessment model not only considering navigation performance, but also considering communication performance and surveillance performance.

Another motivation is that trajectory prediction methods are widely used in air traffic controller areas at current time. By using trajectory tracking methods, more accurate aircraft position estimation can be achieved. As a result, the separation minimum can be reduced. The research follows the procedure shown in Figure 1-4.

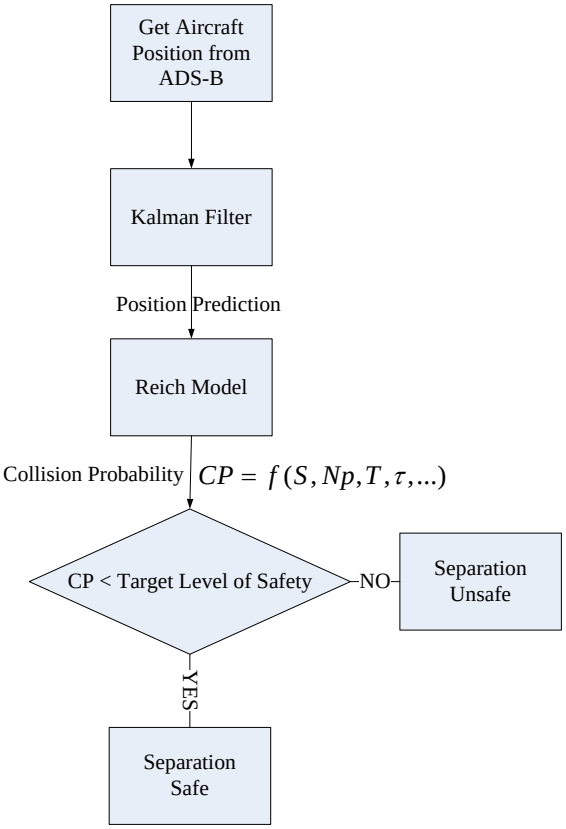

Figure 1-4 Procedure of Research

1.2 Objectives

The Objectives of this thesis are shown as follows:

- ◆Study of advanced CNS/ATM technologies.
- ◆Study of performance-based CNS/ATM, including Requited Navigation Performance (RNP), Required Communication Performance (RCP) and Required Surveillance Performance (RSP).
- ◆Analyse constraints of CNS/ATM.
- ◆Develop an algorithm to improve aircraft tracking performance in global

ATM environment.

- ◆Calculate aircraft's lateral, longitudinal and vertical separation minimum of parallel air routes.

1.3 Outline of the Thesis

Chapter 2 reviews development of CNS systems, including conventional CNS systems, FANS CNS systems and performance based CNS systems. The advantages and shortcomings of these systems are discussed. At the end of this chapter, the separation minimum, including air route separation minimum and radar separation minimum, are studied.

Chapter 3 gives a brief introduction to the safety assessment model of the separation minimum. The main task of this chapter is to introduce the separation minimum safety assessment model and analyse which parameter in the model has large effect on safety assessment issues.

Chapter 4 introduces the method that is used in modelling the aircraft's position uncertainty. Firstly, this chapter analyses the uncertainty sources. Then coordinate transformations, aircraft dynamic model and Kalman filter used in this thesis, are introduced. Finally, simulation and results shows that the position uncertainty is reduced by using the Kalman filter.

Chapter 5 calculates lateral, longitudinal and vertical separation minimum by using the Reich model. The main purpose of this chapter is to use a case study to demonstrate effectiveness of the method proposed in this thesis.

Chapter 6 concludes the work of this thesis. Also future work is recommended.

2 Study of CNS/ATM

2.1 Introduction

This chapter introduces the development of CNS systems. A special committee was built by ICAO for the FANS in 1983. Originally, this committee focused on the next navigation system, but in 1991, ICAO expanded its mission to CNS/ATM in the global environment. At the same time, ICAO recognised that there was not a normalized set of standards to describe the ability of airspace and aircraft. So firstly, ICAO proposed RNP to define operational requirements for a navigation system in different airspace. Then, RCP and RSP were proposed. Finally, a new concept of Required Total System Performance (RTSP) was developed. Based on the RTSP, it is easy to classify airspace into different levels, and determine the aircraft's CNS systems performance. Section 2.2, Section 2.3, and Section 2.4 discuss development of the communication system, navigation system and surveillance system, respectively. Meanwhile, the advantages and disadvantages are discussed. Section 2.5 describes air traffic management systems. Aircraft separation minimum are presented in Section 2.5. Finally, a summary is given in Section 2.7.

2.2 Communication System

Future CNS/ATM systems will be hybrid systems. Conventional voice communication continues to be used via existing high frequency (HF) radios and very high frequency (VHF) radios. However, more and more communication will be based on digital data links such as digital HF radios and VHF radios. Another big change is that communication based on satellite technology will be introduced, especially in some remote air routes, for

example, oceanic areas where it is difficult to build HF and VHF ground stations used to support communication between aircraft and ATM controllers.

Many advantages can be gained from the future communication system. Pilots and air traffic controllers can send digital data information to each other in a more efficient way, using data displays instead of voice. Also, based on digital data link, many control functions can be implemented in an automatic way which can reduce controllers' workload.

Another motivation of the development of the communication system is that automatic surveillance technologies rely on digital data communication. In order to achieve the surveillance functions, some special digital communications are introduced, such as VHF Data Link (VDL Mode 4), Universal Access Transceiver (978 MHz UAT) and Mode-S Extended Squitter (1090 MHz, 1090 ES). 1090 ES data link, proposed by ICAO, is based on Mode-S and Secondary Surveillance Radar (SSR) technologies. UAT is a standard data link, proposed by FAA [21]-[24]. The future communication system is shown in Figure 2-1.

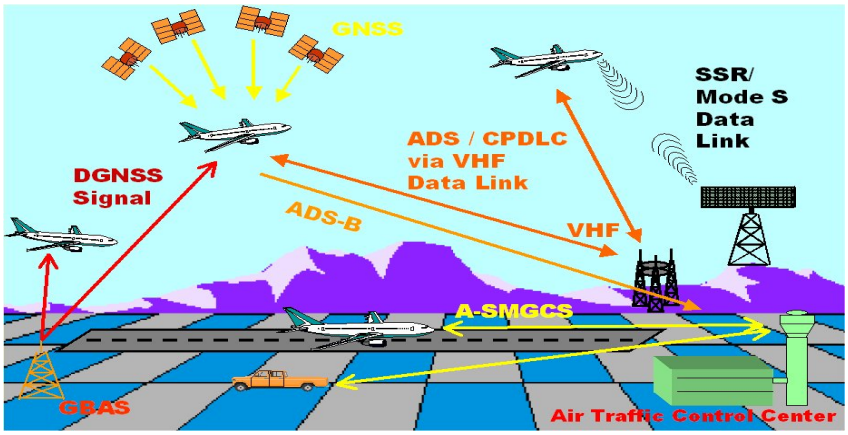

Figure 2-1 Communication System [21]

2.2.1 Conventional Communication System

Communication systems are used to connect between pilots and air traffic controllers, because the controllers need to know states of aircraft during all phases of flight. For example, when the controllers detect a potential collision happening between aircraft, they will use the communication systems to notify the pilots to perform a resolution manoeuvre. At the current time, connections between pilots and controllers are usually via HF and VHF voice communication. Current voice communication architecture is shown in Figure 2.2.

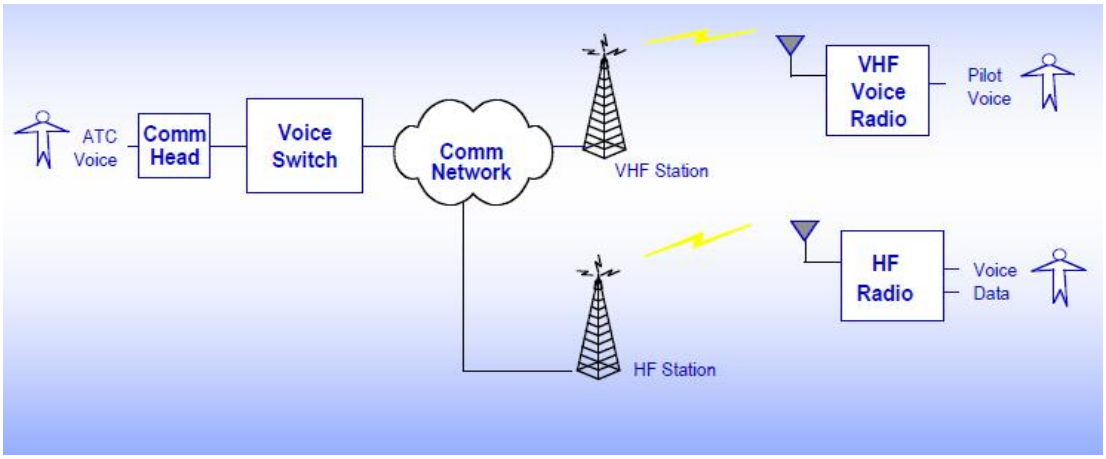

Figure 2-2 Voice Communication Architecture

VHF voice communication: VHF communication can be used for air to ground and air to air communication. However, the communication range of the VHF radio is affected by the Earth's curvature. Usually, the working range is line of sight (LOS). Because of the high reliability and high availability of the VHF, the VHF voice communication will be kept in use in the future CNS/ATM, especially in terminal areas.

The frequency band of VHF is limited - which is from 118MHZ to 137MHZ. As the number of aircraft increase, ICAO expanded the VHF frequency band and reduced channel spacing several times, as shown in Table 2.1.

Table 2-1 VHF Frequency and Channel Spacing [22]

Date	Frequency Band	Channel Spacing (kHz)	Number of Channels
1947	118-132 MHz	200	70
1958	118-132 MHz	100	140
1959	118-136 MHz	100	180
1964	118-136 MHz	50	360
1972	118-136 MHz	25	720
1979	118-137 MHz	25	760
1995	118-137 MHz	8.33	2280

HF voice communication: HF communication can provide communication service between pilots and controllers beyond the line of sight. Pilots use HF communication when VHF can not provide service in some remote and oceanic areas where it is hard to build VHF ground stations.

HF signal transmits long range, depending on the ionised layers reflecting (Figure 2-3). However, the ionised layers are unstable - at different times, the ionised layers have different optimum reflecting frequency. Therefore, HF communication needs to use adaptive frequency to get high quality communication. The quality of communication also depends on the different seasons in a year; for example, in summer it is better than in winter [23]. Frequency band of HF is from 2 MHZ to 30 MHZ.

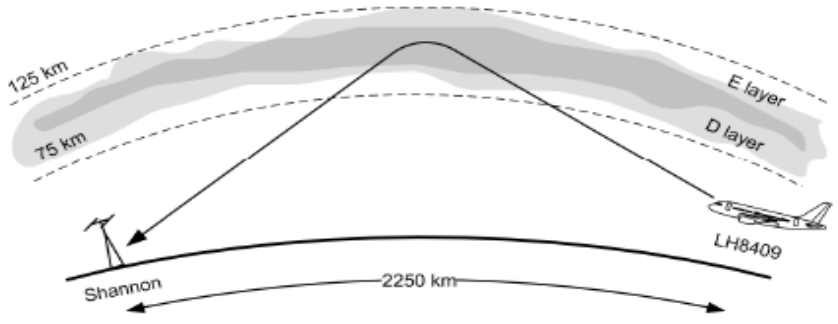

Figure 2-3 HF Communication Model [24]

2.2.2 FANS communication System

FANS communication system is a communication network system, named as aeronautical telecommunications network (ATN). In the ATN, every user, such as aircraft pilot, air traffic controller and airline operator, is considered as an end-system. These end systems share information through the ATN. For ground application, the biggest benefit expected from ATN is that the system can share all distributed computer resources. It means that ATM will be more powerful and efficient. For aircraft application, the ability to transfer data can serve to achieve the automatic functions in flight management systems, which can reduce the workload of pilots, and improve the ability of the flight management system. Four types of transceivers, which are HF digital radio, VHF digital radio, satellite digital transceivers and 1090 ES, are used to communicate between airplane and ground station. Each radio can be used to achieve functions which are Automatic Dependent Surveillance (ADS), Controller Pilot Data Link Communications (CPDLC), Flight Information services and Context Management. Figure 2.4 shows the ATN architecture.

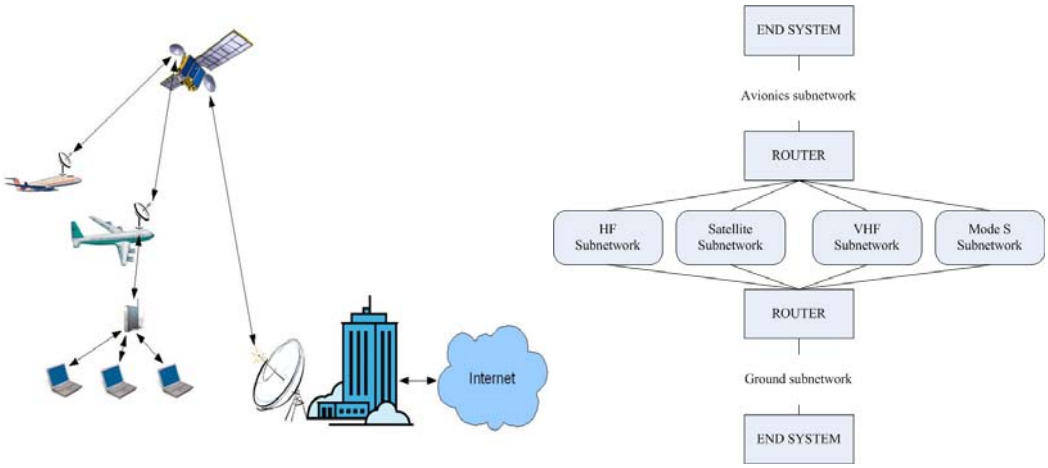

Figure 2-4 ATN Architecture

“Aeronautical Telecommunication Network (ATN): An inter-network architecture that allows ground, air to ground, and avionic data sub-networks

to inter operate by adopting common interface services and protocols based on the international organization for standardization (ISO) open systems interconnection (OSI) reference model" [21].

VHF digital link (VDL): VDL is a main system used to achieve advanced ATM. Voice radio will serve as a back up for digital radio, especially in some high density airspaces which need high quality and quick response communication. Until now, ICAO has recommended four types of VHF digital radios [24].

- ◆VDL-1: VDL-1 is widely used at the current time. This radio is used to achieve the functions of Aircraft Communications Addressing and Reporting System (ACARS). Technology is AM-ASK, and channel space is 25 kHz.
- ◆VDL-2: Technology is D8PSK, which is totally different from VDL-1. Of course, VDL-2 can provide faster data rates than VDL-1 does. Average data rate is about 31.5 kbps, and channel space is 25 kHz.
- ◆VDL-3: New technologies, such as time division multiple accesses (TDMA) and Differential 8-ary Phase Shift Keying (D8PSK), are used in this radio. Data rate is round 31.5 kbps, and channel space is 25 kHz.
- ◆VDL-4: It is a more advanced digital radio. Self-organizing time division multiple access (STDMA), which is a more advanced and complicated technology, has been used in this radio. Data rate is about 19.2 Kbps, and channel space is 25 kHz.

Satellite digital communication: The advantage of this system, compared with other methods of long-range communications, is its ability to permit global coverage. Satellite communications, combined with satellite navigation system, are making new concepts of air traffic control and operation possible; for example ADS, CPDLC and automatic air traffic control.

HF digital radio: HF digital radio is also called HF data link (HFDL). In some remote and oceanic areas where VHF data link can not provide coverage, this data link can provide service. Besides this, HFDL has some other benefits: firstly, cost is lower than satellite data link; secondly, some aircraft without satellite equipment can use HFDL; finally, HFDL can serve as a back up system for satellite data link.

1090 ES: 1090 ES is a data link based on technology of MODE-S. Until now, this link has only been used to support ADS-B function. Broadcast frequency is 1090 MHz, and information transmitted in this data link is aircraft's state data, such as position, velocity and heading angle.

Controller and pilot data link communication: CPDLC and ADS are two typical applications of the digital data links which have been introduced above. Via CPDLC, a traffic control system can build a link to aircraft. Using this link, the automatic air traffic control system can send control data to the aircraft without the controller's involvement. This means that by using this automatic control procedure, the workload of the controller and pilot can be reduced sharply. Meanwhile, performance of ATM will be improved. Figure 2.5 shows the architecture of CPDLC.

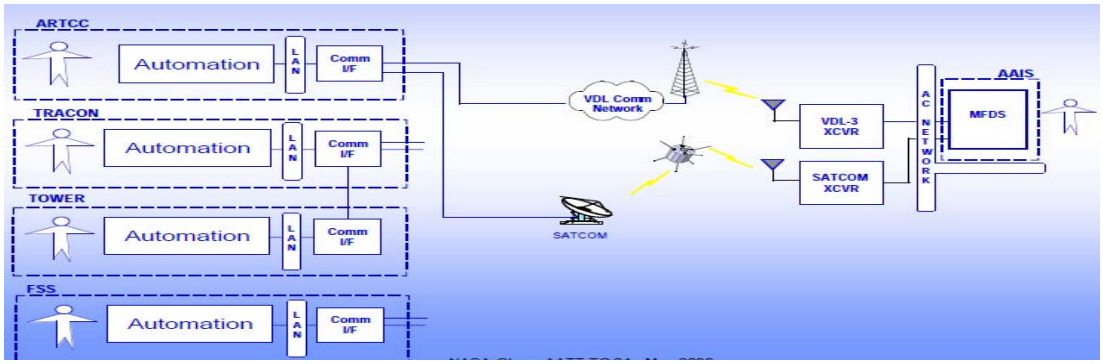

Figure 2-5 CPDLC Procedure

2.2.3 Performance Based Communication System

RCP is a set of standards to define operational requirements for communication systems. It is a concept of how to specify the requirements for communication systems that support ATM functions.

ICAO uses four key parameters to specify RCP (Transaction time, Continuity, Availability, Integrity). [24]

- ◆Transaction time: The maximum time for communication system to finish an operational transaction.
- ◆Continuity: Probability of the communication system finishing an operational transaction within the transaction time.
- ◆Availability: Probability of the communication system being available when an operational transaction needs to be start.
- ◆Integrity: Probability of the communication system finishing an operational transaction within the transaction time with errors undetected.

For different applications, RCP has different types. The detail is shown in Table 2.2.

Table 2-2 RNP Types [24]

RCP type	Transaction time (sec)	Continuity (probability/ flight hour)	Availability (probability/ flight hour)	Integrity (acceptable rate/ flight hour)
RCP 10	10	0.995	0.99998	10^{-5}
RCP 60	60	0.99	0.9995	10^{-5}
RCP 120	120	0.99	0.9995	10^{-5}
RCP 240	240	0.99	0.9995	10^{-5}
RCP 400	400	0.99	0.999	10^{-5}

2.3 Navigation System

Conventional ground station aided navigational methods will continue to be used in the future FANS navigation systems. However, as satellite navigational technologies develop, more and more navigation will depend on global satellite navigation system (GNSS). GNSS covers worldwide airspace, and in the future, GNSS can be used to navigate aircraft not only for en-route, but also for approaches. Eventually, GNSS could be a replacement for ground station aided navigation methods used at the current time.

The advantages gained from the GNSS are that receivers installed on aircraft are very simple and can provide worldwide coverage. For example, in some remote continental area and oceanic airspace, ground aided navigation can not be built, so no navigation function can be provided. However, GNSS overcomes this limitation.

Figure 2.6 shows a view that as CNS technologies develop, the separation minimum of air routes reduces. Figure 2-6 (a) is the conventional air route, which is based on ground navigation aids. Because of limited navigation accuracy, the separation minimum is the largest among the three air routes. Figure 2-6 (b) and Figure 2-6 (c) which are partly performance-based air routes have the smaller separation minimum. This means that in the same airspace, using RNP air route can accommodate more aircraft than using the conventional air route.

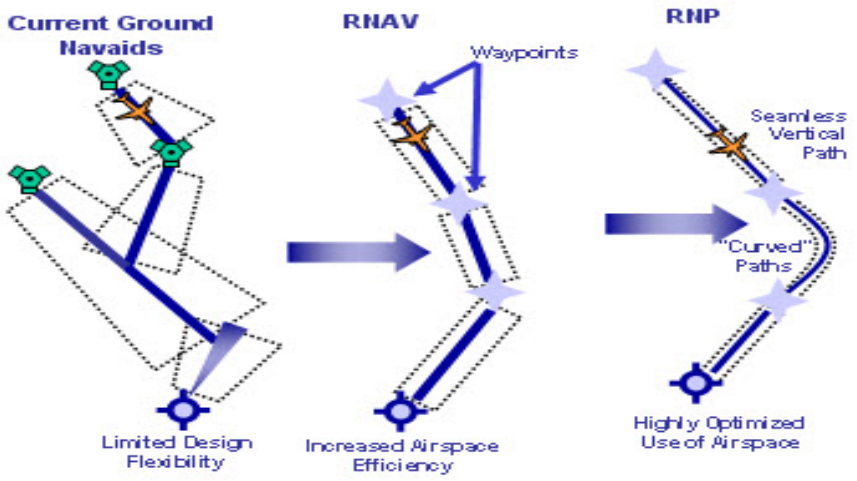

(a) Conventional Air Route (b) RNAV Air Route (c) RNP Air Route

Figure 2-6 Conventional Air Route, RNAV Air Route, RNP Air Route [25]

2.3.1 Conventional Navigation System

Based on different applications, navigation systems can be divided into several types. VOR and DME often provide bearing and distance measurements relative to ground stations in the en-route phase. ILS and Marker Beacon are used in the descending and landing phases. INS is a self-contained long-range navigation aid, independent of external signal inputs.

VHF Omnidirectional Range (VOR): This navigation radio aid is the system widely used in en-route and terminal areas currently. VOR operates in frequency range 108 MHz to 117.95 MHz, and work range is Line-of-Sight. Ground station sends two signals: one is a reference signal whose phase does not vary; another one is a variable phase signal whose phase varies accordance to signal direction. The receivers, installed on aircraft, compare the two signals to get the aircraft's bearing, relative to the VOR ground station (Figure 2-7).

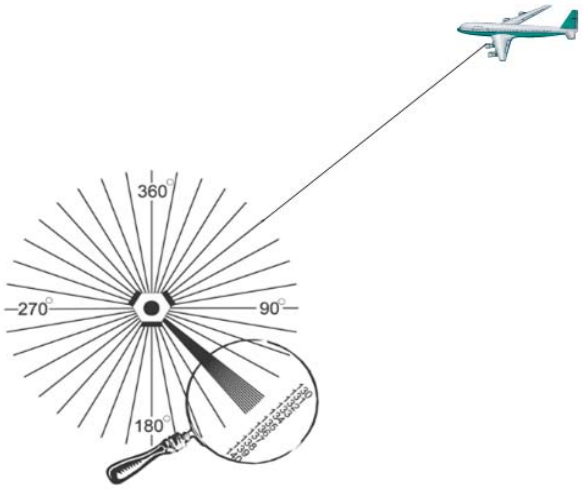

Figure 2-7 VOR Navigation

Distance Measuring System (DME): DME is used to measure distance in nautical miles to a DME ground station. Distance measuring equipment is normally located with or close to VOR navigation transmitters on the ground. The DME system operates in frequency range 960 MHz to 1215 MHz. A DME transmitter is fitted on aircraft and is called an interrogator. The airborne interrogator is used to interrogate a system in the DME ground station called a transponder. A system of distance and time measurement by the interrogator results in slant range measurement to the DME ground station. Figure 2.8 shows the work procedure of DME.

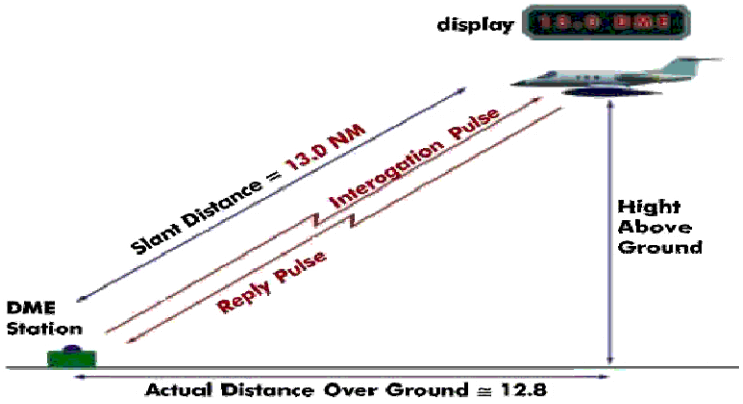

Figure 2-8 DME Navigation

Marker Beacon: This system work with instrument landing system (ILS) as a landing aid. A series of marker radio beacon transmitters have been located to help pilots, when a land approaching is being made.

Ground marker radio beacon signals are transmitted at different locations along an instrument landing system approach. When an aircraft is en route to an airport runway, the ground maker beacon will provide the pilot with the exact point where that specific beacon is located.

Often, according to the location, marker beacon can be divided into three types, outer beacon, middle beacon and inner beacon. They have the same work frequency - 75 MHz.

The work procedure is shown in Figure 2.9.

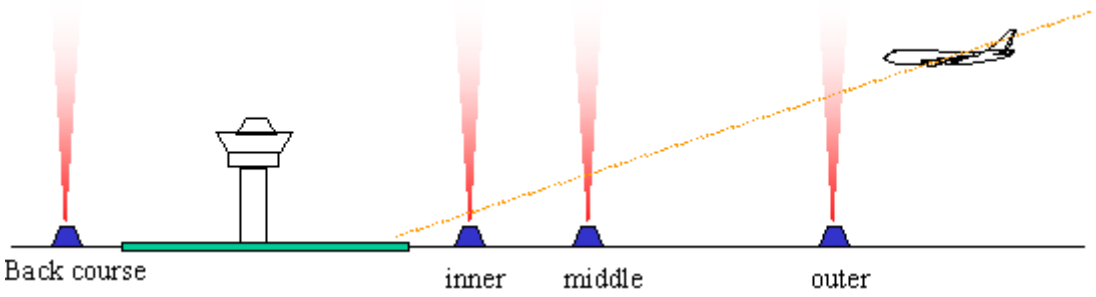

Figure 2-9 Marker Beacon

Instrument Landing System (ILS): The ILS signal is transmitted in frequency range of 108.1 MHz to 111.9 MHz. Ground transmitter which is located close to the runway radiates signal towards incoming aircraft. Two directional slopes are sent out. One to the left directional slope is modulated with a 90 Hz audio signal. The right slope is modulated with a 150 Hz audio signal. The centreline of the runway is where both signals are equal. When an aircraft is on approach and is left of the runway the 90 Hz predominates, right of the runway the 150 Hz beam is stronger (Figure 2-10). On board the aircraft a

radio navigation radio receiver is able to process the signal to guide the aircraft along the centreline of the localiser and glide slope radio beam.

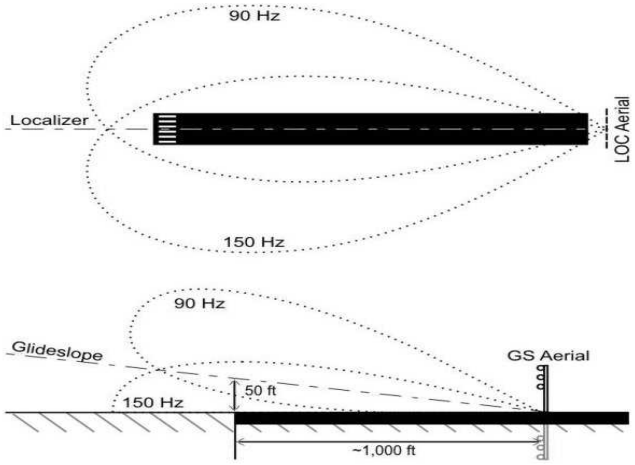

Figure 2-10 ILS Approaching

Inertial Navigation System (INS): INS is a self-contained system, which can be used for long-range navigation. Navigation performance can be improved by other systems, such as GPS and air data system.

2.3.2 FANS Navigation System

FANS navigation system mainly depends on satellite navigation technology. Currently, Satellite Navigation System often contains three parts – a space part, control part, and a user part (Figure 2.11). The space part is comprised of the satellite constellation, made up of multiple satellites. The satellites provide the basic navigation frame of reference, and transmit the radio signals from which the users can collect measurements required for this navigation solution. Knowledge of the satellites' position and time history is also required for the user's solution, and the satellites also transmit that information via data modulation of the signals.

The control part includes three major segments:

◆Monitor stations which track the signal transmitted by satellites and

pick up measurements.

- ◆A master control station that uses these measurements to determine and predict the satellite health.
- ◆Ground antennas that perform the upload and general control of the satellite.

The user segment is comprised of the receiving equipment and processors that perform the navigation solution.

The basic satellite theory is illustrated in Figure 2.12. Because of the errors, the measurements are not range, but pseudo range. If only range is measured, the equations are as follows:

$$PR_i = R_i + c\Delta t_{si} - c\Delta t_u + \varepsilon pr_i$$

PR_i is the pseudorange to the satellite i.

R_i is the real range to the satellite.

Δt_{si} is the clock error in the satellite.

Δt_u is the receiver clock error.

c is the velocity of light.

$\varepsilon pr_i i$ are the others errors, such as atmospheric delays, the Earth's rotation correction, multi path noise and receiver noise.

If the errors are neglected, the range is given as:

$$R_i = \sqrt{(X_{si} - X_u)^2 + (Y_{si} - Y_u)^2 + (Z_{si} - Z_u)^2}$$

X_{si}, Y_{si}, Z_{si} are the position of the satellite.

X_u, Y_u, Z_u are the position of the user.

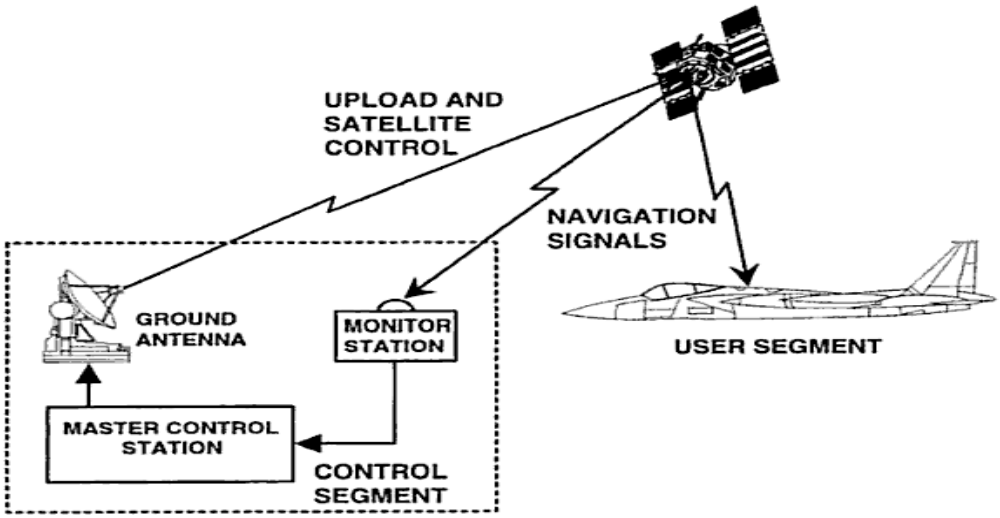

Figure 2-11 Satellite Navigation System Architecture [25]

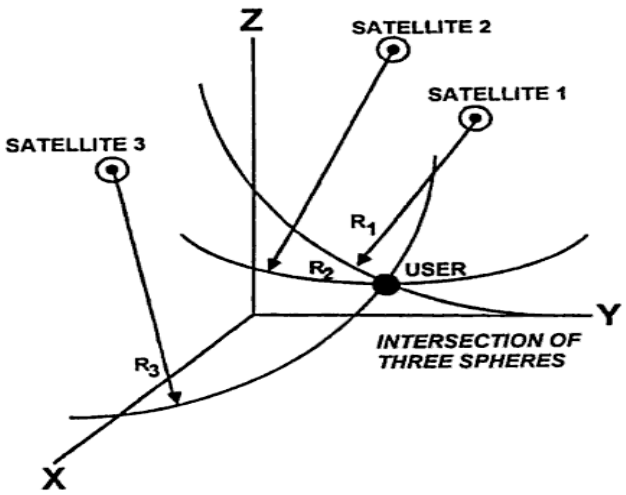

Figure 2-12 Ranging Solution [25]

There are three major satellite navigation systems, GPS, GLONASS and GALILEO.

2.3.3 Performance Based Navigation System

There are several reasons which result in the emergence of RNP concepts. Firstly, the aviation industries continue to increase rapidly, and as a result, air space gets more congested. Secondly, the method which is used to track

aircraft has been enhanced. Lastly, new navigation systems, such as satellite navigation, have improved navigation performance. Based on these reasons, ICAO developed new performance based navigation concepts, such as RNAV and RNP. The biggest difference between RNP and RNAV is that the RNP has receiver autonomous integrity monitoring function, but the RNAV does not.

Area Navigation (RNAV): RNAV is a navigation method. It enables aircraft to fly a preferred air route in range of navigation signals. In other words, the RNAV integrates multi navigation sensors to give out estimation of the aircraft, then build the preferred flight route, and navigate the aircraft to fly along the route. Unlike conventional navigation methods that the aircraft must fly navigation aids one by one, which results in a small part of airspace being used, RNAV can make full use of the airspace and improve the efficiency of aircraft ability. The sensors used by RNAV are INS/IRS, VOR/DME/, DME/DME, LORAN C, GNSS. A complex RNAV architecture of aircraft is shown in Figure 2.13. RNP types and applications are shown in Table 2-3.

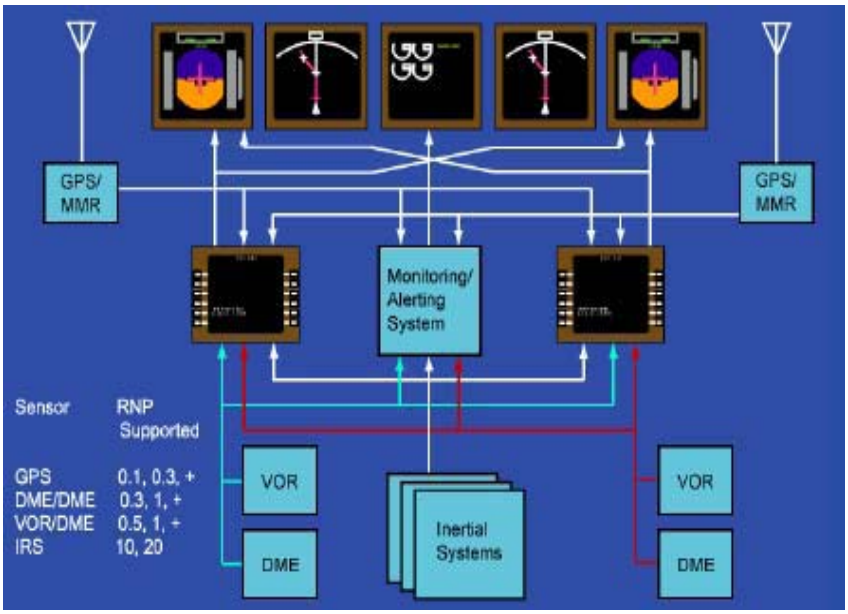

Figure 2-13 RNAV and RNP Navigation Architecture [26]

Table 2-3 RNAV Types and Applications [26]

Navigation Specification	Navigation resource	Application area
RNAV 10 RNP 10	GNSS, INS/IRS	Oceanic and remote continental
RNAV 4. 5 RNP 4, 5	GNSS, DME/DME, VOR/DME, INS/IRS	Continental en-route
RNAV 2 RNP 2	GNSS, DME/DME,, INS/IRS	Continental en-route
RNAV 1 RNP1	GNSS	Terminal airspace: arrival and departure

Required Navigation Performance RNP: RNP is a concept to describe the accuracy of a navigation system in a particular airspace. Aircraft that want to fly in a particular airspace must have specific RNP type. The RNP type is defined as a 95% containment value and a measure of navigation performance accuracy (Figure 2-14). RNP types used present, are shown in Table 2-4.

ICAO uses 4 key parameters, which are accuracy, integrity, continuity and availability, to describe the navigation system performance.

- ◆Accuracy: the ability of the system to maintain the position within a specified error with 95% probability.
- ◆Integrity: the quality which related to the thrust that can be placed in the correctness of the information. Integrity risk is the probability of an undetected failure of the specified accuracy.
- ◆Continuity: the ability of the system to perform its function without unscheduled interruptions.
- ◆Availability: the ability of the system to provide the required guidance at

the initiation of the intend operation.

Table 2-4 RNP Types and Applications

Navigation Specification	Navigation resource	Application area	Horizontal Error (95%)
RNP 10	GNSS, INS/IRS	Oceanic and remote continental	<10 NM
RNP 5	GNSS, DME/DME, VOR/DME, INS/IRS	Continental en-route	<5 NM
RNP 4	GNSS, DME/DME, VOR/DME, INS/IRS	Oceanic and remote continental	<4 NM
RNP 1	GNSS	Terminal airspace: arrival and departure	<1 NM
RNP APCH	GNSS	Approach	<0.3 NM
RNP AR APCH	GNSS	Approach	<0.1 NM

[26]

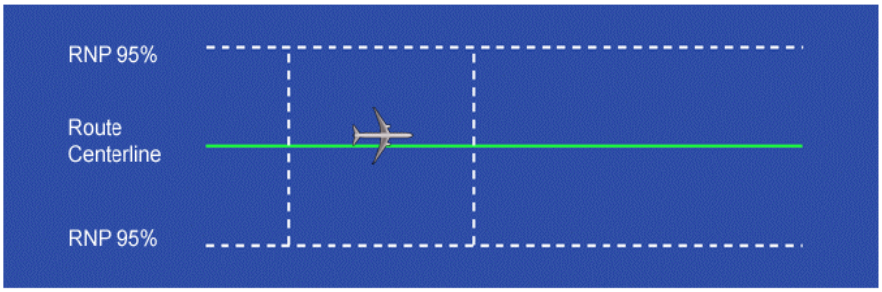

Figure 2-14 RNP Containment [26]

2.4 Surveillance System

The future Surveillance system is a hybrid system. ADS technology will be widely used in the future. However, in some busy areas, such as terminal areas and congestion en-route areas, PSR and SSR are going to be used to monitor aircraft. The hybrid surveillance system is shown in Figure 2-15.

The main function of ADS is to broadcast the host state vectors to other users, such as vicinity aircraft and ground traffic control stations. When ground traffic control stations receive these state vectors, they can use these data to predict the aircraft's position in the future, and they also can use the data to improve the surveillance ability of SSR and PSR via data fusion.

ADS can also be seen as a communications application that represents the true merging of communications and navigation technologies. ADS state vectors come from GNSS, and ADS use digital data communication methods (satellite, 1090 ES, UAT, VDL-4) to send these data. Current ADS version in usage is ADS-B. Benefits would come from ADS in oceanic and some continental areas that currently have no radar coverage.

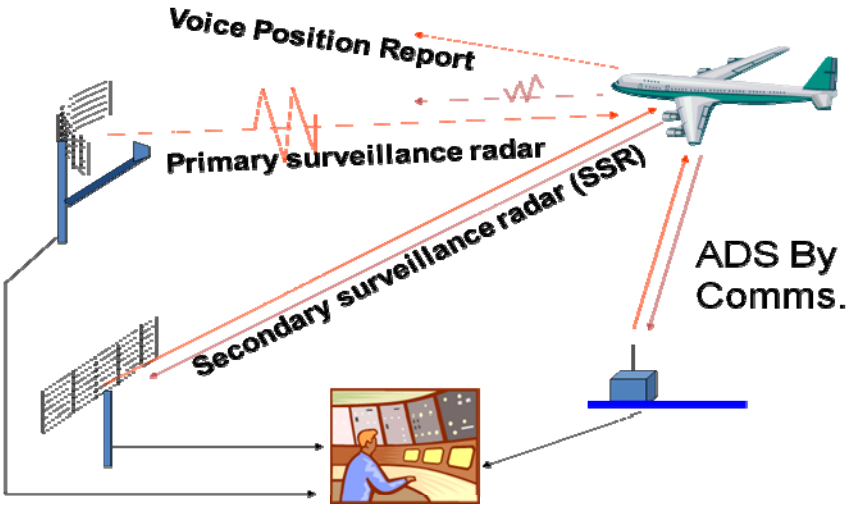

Figure 2-15 Future Surveillance Architecture

2.4.1 Conventional Surveillance System

Traditional SSR and PSR are widely used to monitor aircraft.

PSR: this ground based radar is a system which sends out radio frequency waves in a narrow directed beam. This beam strikes the aircraft. Part of the beam signal is reflected off the outer skin of the aircraft. This reflected signal

is picked up by a ground radar antenna and coupled to a ground radar receiver. After the signal being processed, the range and azimuth information between aircraft and radar can be deduced, and then the information is displayed on the air traffic controller's radar display screen. This display is known as planned position indicator (PPI). PSR is important but the information given to a ground controller is not enough; for example, the controller has no way of knowing what aircraft he is watching and how high it is flying.

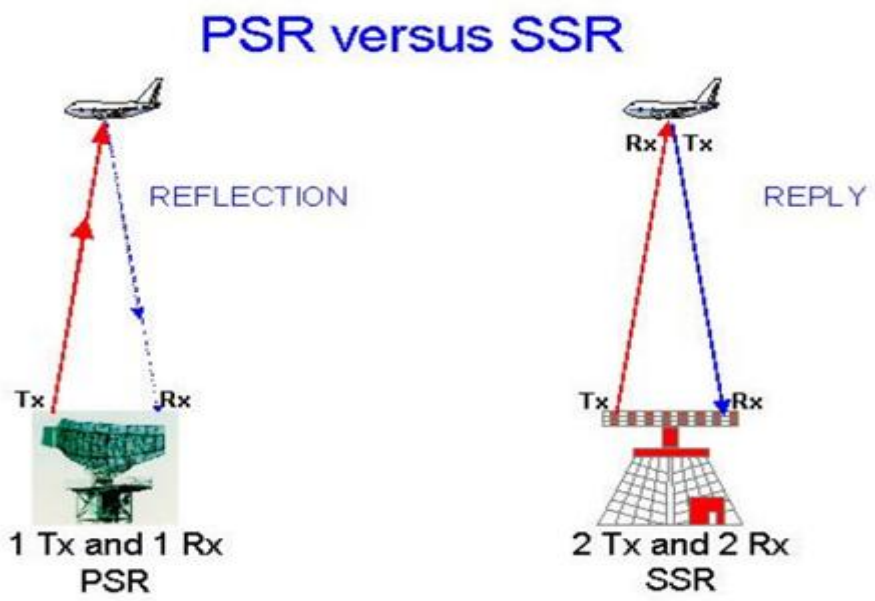

Figure 2-16 PSR and SSR

Secondary Surveillance Radar (SSR): The secondary radar is different from the primary in that it uses a transponder installed on the aircraft to produce the information needed. The ground receiver called the "interrogator" transmits coded radio frequency pulses to an aircraft. The interrogator signals trigger an aircraft's transponder to reply. This reply from the aircraft is picked up at the ground radar receiver. The reply is decoded by equipment at the ground station and coupled to a display monitor screen. An air traffic controller will now have displayed on his screen the identity and altitude of the aircraft.

When the PSR and SSR information are combined, they give the controller all the information necessary: altitude, bearing, range and location.

2.4.2 FANS Surveillance System

The conventional surveillance system mainly relies on PSR and SSR, but this architecture has some significant shortcomings. For example, many PSR or SSR should be built to support the surveillance function; however, oceanic areas and remote areas are not suitable for building PSR or SSR ground stations.

Automatic dependent surveillance (ADS) has been defined by ICAO as a function used by ATS in the future. Through data link, aircraft automatically send states data, such as three-dimensional position, which come from on-board navigation system to vicinity users. Using satellite communications, ADS will allow aircraft to be monitored and controlled when they are outside the work range of air traffic radar. It is planned that anywhere in the world, when flying in airspace over large areas of desert and sea, air traffic control can obtain an aircraft's current position, intended flight path and other information held in the onboard navigation systems. These functions can be achieved automatically, without the need for direct pilot's and controller's involvement (Figure 2-17). The states information contains:

- ◆Position information
- ◆Route information
- ◆Meteorological information

Communication interface: ADS use different communication systems: HF, VHF, Satellite, Mode S.

ATM automation and ADS: Via ADS, ATM can get many benefits, shown as follows:

◆Flight data validation,

◆Conformance monitoring,

◆Automated tracking,

◆Conflict detection,

◆Conflict resolution.

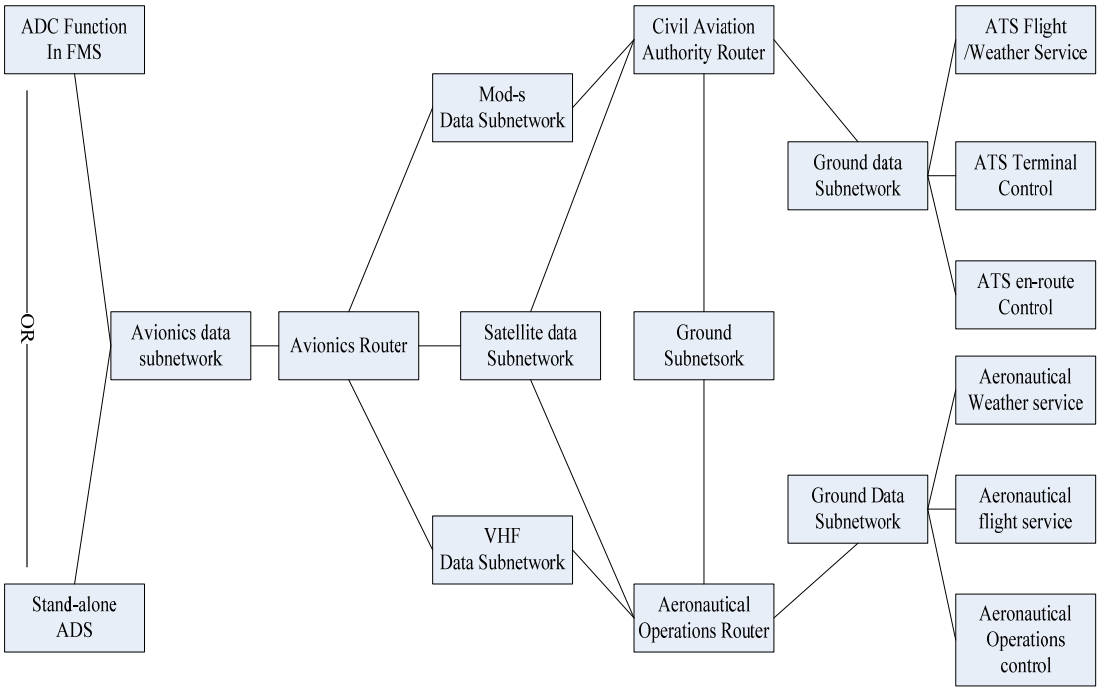

Figure 2-17 ADS Applications [27]

Auto dependant surveillance-broadcast (ADS-B): ADS-B is to broadcast state information to the nearby aircraft via communication medium. As shown in Figure 2.18, the ADS-B application gets data from different sources, and sends these data to other aircraft or ground stations; therefore, the aircraft can be monitored.

The data transmitted via ADS-B are identification, state vector, status, intent information, and class code.

Besides the 3D position data, the navigation uncertainty category position (NUCp) is sent. Therefore, when users receive the ADS-B information, they can determine whether position data can be trusted or not, and errors of

position can be calculated based on the NUCp (Table 2.5). Similar to the NUCp parameter which is used to describe the velocity, Navigation Uncertainty Categories Velocity (NUCv) is broadcasted too (Table2.6).

ICAO uses some key parameters to define performance of ADS-B system, such as update time, latency, availability, continuity and integrity.

Table 2-5 NUCp [27]

NUCp	Horizontal Protection Level (10^{-7})	Horizontal Error (95%)	Vertical Error (95%)	Comment
0	No integrity	Unknown	Unknown	No Integrity
1	<20 nmi	<10 nmi	Baro Alt	RNP 10
2	<10 nmi	<5 nmi	Baro Alt	RNP 5
3	<2 nmi	<1 nmi	Baro Alt	RNP 1
…				

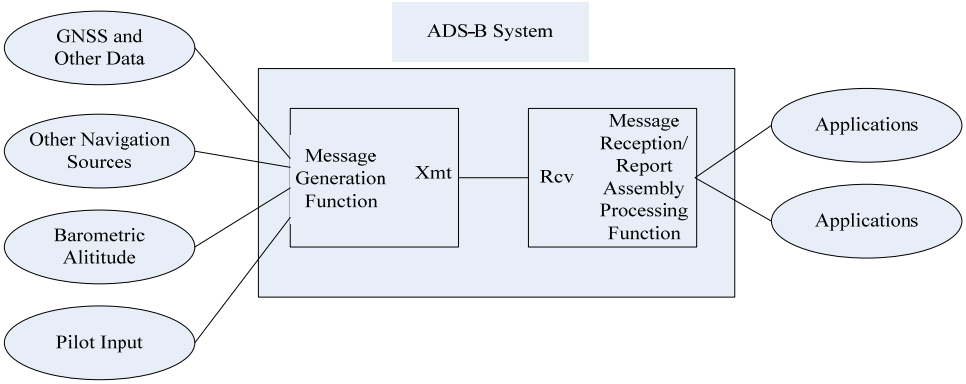

Figure 2-18 ADS-B System

Table 2-6 NUCv [27]

NUCv	Horizontal Velocity Error (95%)	Vertical Velocity Error (95%)
0	Unknown	Unknown
1	<10 m/s	<50 fps
2	<3 m/s	<15 fps
3	<1 m/s	<5 fps
4	<0.3 m/s	<1.5 fps

2.4.3 Performance Based Surveillance System

RSP: It is a set of performance requirements for surveillance systems. A surveillance system is used to ensure that aircraft are separated correctly. Aircraft's position information needs to be updated every 4 seconds in high-traffic airspace. However, in low-traffic airspace such as oceanic and remote airspace, the updating time is slightly longer, so position information needs to be updated every 12 seconds. Another usage of a surveillance system is that the system should have the ability to support free flight in the future [27].

ICAO uses 5 key parameters, which are accuracy, update time, integrity, continuity and availability, to describe the surveillance system performance. Some papers discuss RSP based on some particular application ([16], [27]-[28]). Accuracy and update time of ADS-B are taken into account in this thesis.

- ◆Accuracy: the ability of the surveillance system to measure the aircraft's position.
- ◆Update time: the maximum time used to update the measurement to controller.
- ◆Integrity: Integrity risk is the probability of an undetected failure of the

specified accuracy.

◆Continuity: the ability of the system to perform its function within the update time without errors undetected.

◆Availability: the ability of the system to provide the required surveillance function at the initiation of the intend operation.

2.5 Air Traffic Management Systems

Functions of ATM are airspace management (ASM), air traffic flow management (ATFM), air traffic information service (ATS), air traffic control (ATC) and flight operations. Based on new CNS technologies described above, the ability of ATM can receive a direct enhancement. More appropriately, advancements in CNS technologies will serve to support ATM.

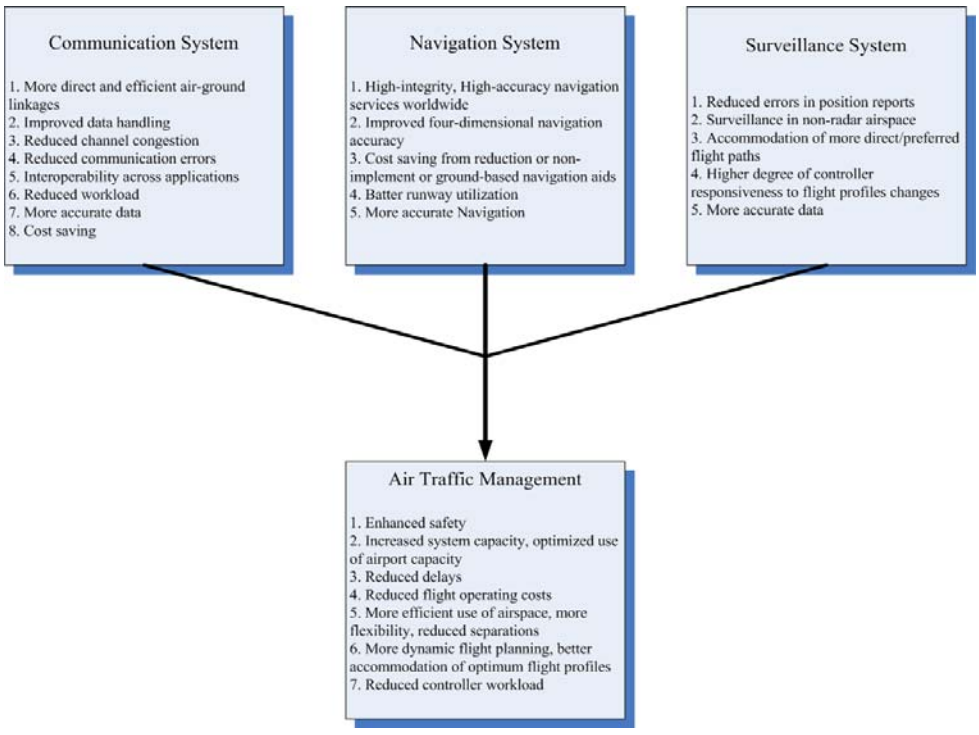

Figure 2-19 CNS/ATM Advantages: a high level view [29]

Combined benefits gained from the advanced CNS technologies, together with increasing use of the automation, will lead to an improved ATM system. Figure 2.19 shows the advantages.

2.6 Separation Minimum

2.6.1 Airspace Concept and ATC Constraints

How many aircraft can be accommodated in airspace? This depends on several factors. The first one is the separation between aircraft (Figure 2.20). When the separation decreases, it means more aircraft can fly in airspace. The second factor is conflict detection and resolution ability of ATC.

The main work of ATC is to ensure separation between adjacent aircraft. The efficiency of ATC depends on the availability of communications and surveillance capabilities. The risk of collision depends on navigation performance, communication performance and surveillance performance, so a model should be used to describe ATC constraints and abilities. This thesis focuses on the effect of ATC constraints on the separation minimum safety assessment issues. Other factors, such as human factors, air route configuration and traffic density, which can affect the separation minimum assessment, are not taken into account.

Figure 2-20 Aircraft Separation: Lateral, Longitudinal and Vertical [27]

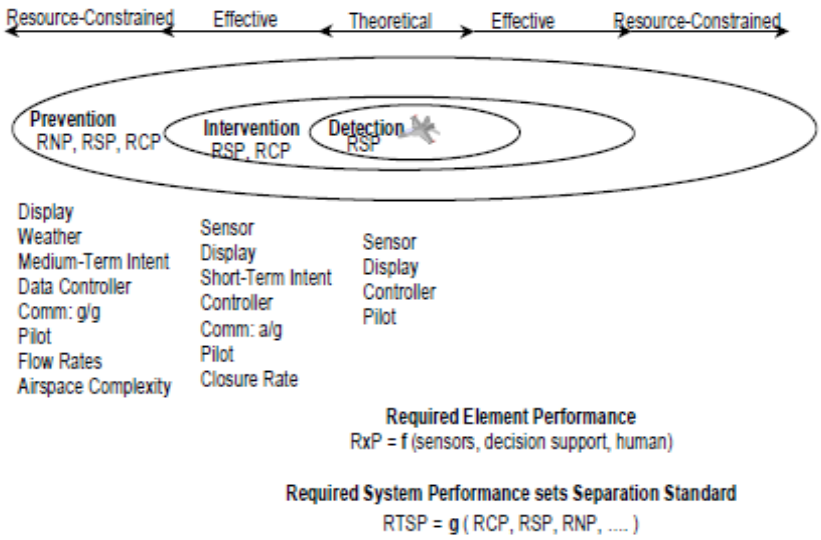

Figure 2-21 CNS/ATM Characteristics [28]

Separation minimum standard was induced from performance of navigation in the past time. However, communication and surveillance ability are important too. Therefore, some researchers provided a new concept of RTSP which integrates RSP, RCP and RNP to describe the ability of CNS/ATM [28].

RTSP: It is a normalized, standard, rational, consistent set of performance metrics, which are used to describe a particular airspace region. Meanwhile, if aircraft want to fly in this region, they must have according system performance. The normalized set of performance requirements regulates the behaviour of air aircraft operators and air traffic control functions providers.

Figure 2-22 shows RTSP of CNS systems and its applications.

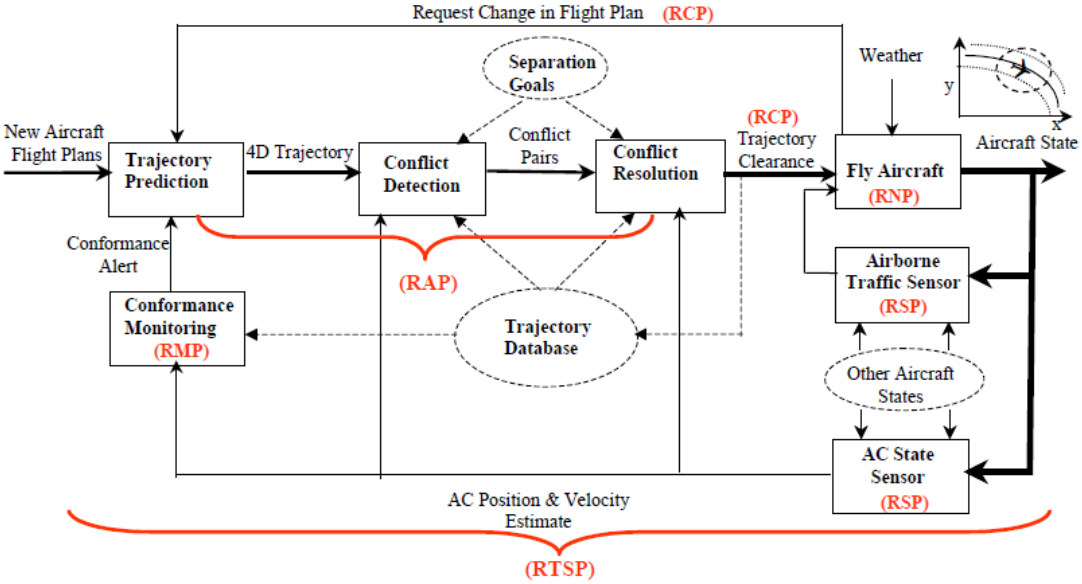

Figure 2-22 Required Total System Performance [28]

2.6.2 Parallel Air Route Separation Minimum

According to reference [30], there are two types of air route architecture - parallel route and cross route. In order to simplify the issue, only parallel air route separation minimum will be discussed here.

As shown in Figure 2.23, two air routes are parallel to each other. Aircraft are expected to fly along the dotted line, and stay within the air route space. How to set the separation minimum S or the air route space to meet the target level of safety (TLS) of 5×10^{-9} [30], based on constraints of current CNS systems, is the main task of this thesis.

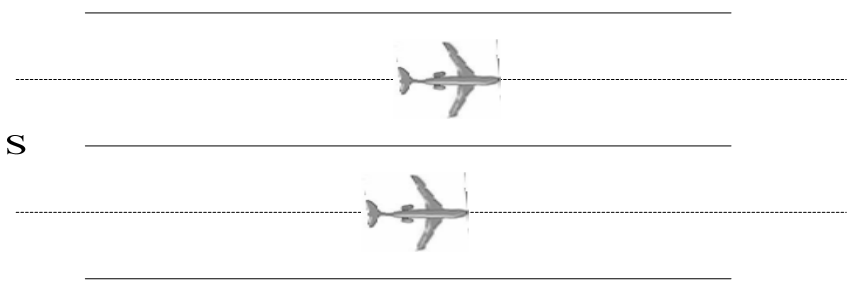

Figure 2-23 Lateral Separation [30]

Air route space or separation is affected by several factors, such as navigation performance, exposure to risk and intervention ability of ATC (Figure 2.24). When a new air route is built, the first work is to estimate the collision risk [24].

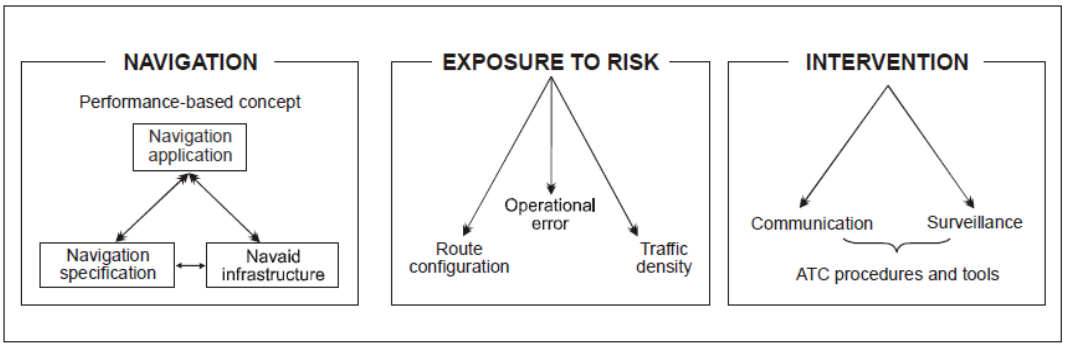

Figure 2-24 Air Route Separation and Space Model [24]

According to different system ability and traffic density, air route space is different. For example, based on navigation type RNP4, usually 50/50 NMI separation minimum can satisfy the requirement of TLS, but for the RNP 2, 10/10 NMI separation minimum is enough [30].

For the vertical separation, the separation minimum is 2000ft above FL290, and under FL290, the separation minimum is 1000ft [43].

2.6.3 Radar Separation Minimum

As described in Section 2.3.1, there are two types of surveillance radar systems - PSR and SSP. Usually, these two radars work together to provide service. Radar separation is mainly affected by 4 factors: estimation accuracy of aircraft position, radar scan time, controller and system reaction time, and time needed to resolve the collision.

The radar separation minimum is different in different areas; for example, in the terminal area, the radar separation minimum is 3 NMI within a range of 40 NMI from surveillance radar, but 3 NMI separation minimum can safely be

expanded to a range of 60 NMI from surveillance radar implemented by using advanced technology. In the en route area, the radar separation minimum is 5 NMI within the range of 200 NMI from surveillance radar - this range can also be extended to 250 NMI [14].

Based on radar surveillance, the vertical separation minimum is 1000ft in en the route area, and this value can be reduced to 500ft in the terminal area.

2.7 Summary

In this chapter, development of CNS systems has been presented, and the advantages and disadvantages have been discussed. The main tasks of this chapter are summarized as follows:

1. Study of the development of CNS systems, including conventional CNS systems, FANS CNS systems and performance based CNS systems.

2. Comparison of different types of CNS systems, and the advantages and disadvantages have been presented.

3. Introduction of air space concept, moreover, how to use the performance based CNS systems (RTSP) to describe the ability of the airspace has been discussed.

4. Review of air route separation minimum and radar surveillance separation minimum.

3 Separation Minimum Safety Assessment Model

3.1 Introduction

This chapter discusses the Reich model used to evaluate the separation minimum safety issues. Firstly, air route architecture, proximity shell, separation vector and slab are introduced in section 3.2.1 and Section 3.2.2; then, the Reich model is described in Section 3.2.3; finally, a summary is given in Section 3.2.

3.2 Reich Model [4]-[6]

3.2.1 Air Route

Air route architecture: Air route architectures include parallel air route and cross air route. In this thesis, parallel air route is discussed. Parallel air route includes traditional and composite architecture shown in Figure 3.1. S_x , S_y and S_z represent the longitudinal separation, lateral separation and vertical separation, respectively.

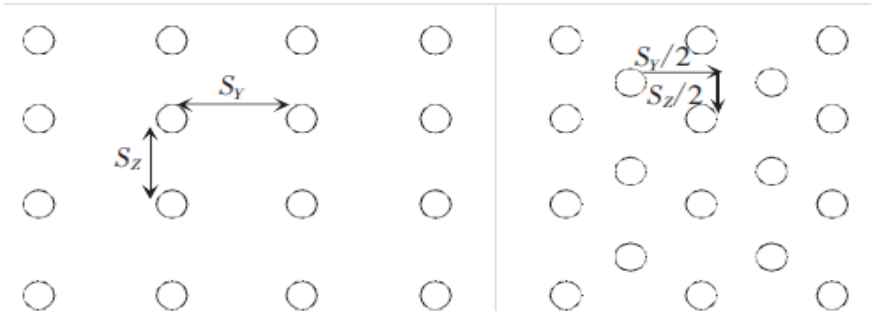

(a)Traditional (b) composite

Figure 3-1 Parallel Air Route

3.2.2 Proximity Shell and Slab

Proximity shell: Separation standards, which are denoted by S_x, S_y and S_z, are shown in Figure 3.2. A box has been built around aircraft A. when aircraft B is

close to or inside the box, the collision risk will increase rapidly. When the aircraft B is outside of the proximity shell, safety between two aircraft is guaranteed.

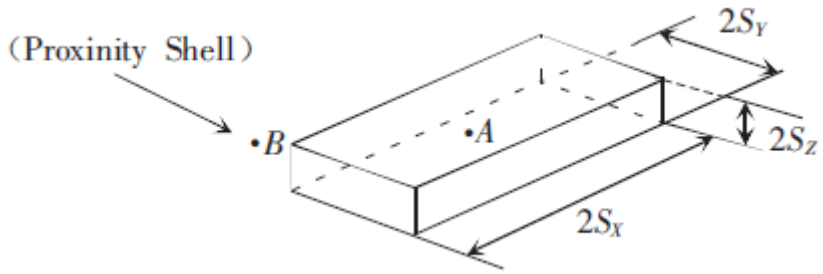

Figure 3-2 Proximity Shell

Separation vector: point A and point B (shown in Figure 3-3) represent intended position of aircraft A and Aircraft B, but because of errors, such as track errors, navigation errors and flight errors, the true positions are point A' and point B'. Vector [AB] is intended separation. Vector [A'B'] is true separation. As the A'B' shrinks to the separation standard, the probability of collision risk will arise. This collision risk depends on the vector [AB] and the position estimation errors. The separation vector is shown in Figure 3-3.

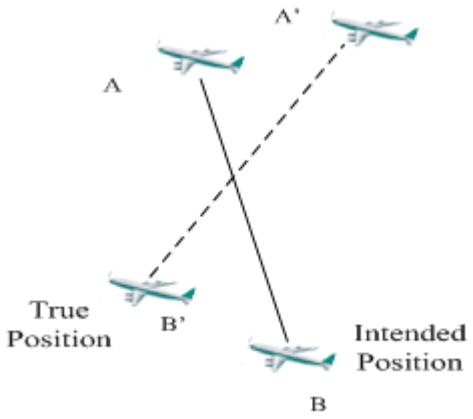

Figure 3-3 Separation Vector

Slab: Assumption that aircraft in air route has the same dimensions. λ_x, λ_y and λ_z are used to describe length, span and thickness of the aircraft. A rectangular box with $2\lambda_x$, $2\lambda_y$ and $2\lambda_z$ has been built. Aircraft A is in centre of the rectangular.

When aircraft B is on the face of or inside the rectangular box (Figure 3-4), a collision happened. So, the collision rate (CR) equals to the times that the aircraft B will fly into the slab.

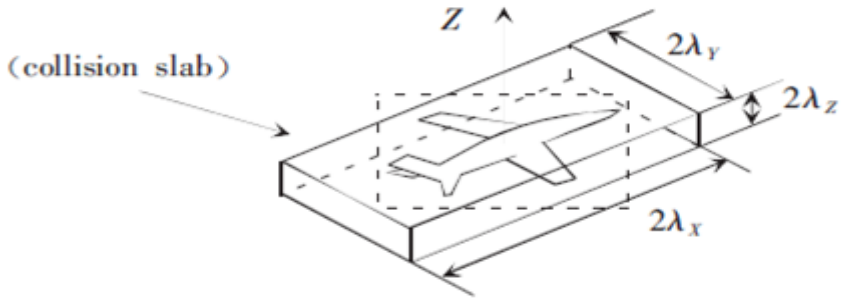

Figure 3-4 Collision Slab

3.2.3 Safety Assessment

Reich model: Before the Reich model is discussed, some assumptions will be defined.

1. Air routes are parallel to each other, and separated by distance S_y .
2. Only adjacent collision is take in account in the parallel air route.
3. Lateral deviations of the aircraft that fly in the adjacent routes are uncorrelated
4. Velocity has no relationship to position.
5. ATC controllers or pilots are not intended to solve collision when the collision happens, but the ability of ATC, required solving the collision, are considered in the model.
6. A rectangular box is used to represent the aircraft in the model.
7. The aircraft fly with a constant velocity during the cruise phase of flight.

Procedure, used to calculate the collision risk, can be divided into two steps: firstly, time T, which is an integral of time that the aircraft B flies in the proximity shell of aircraft A, should be calculated; secondly, the collision rate (CR) per time units is calculated.

Calculating the CR: Following parameters can be defined:

N_x is the frequency that longitudinal separation is less than λ_x

$$N_x = longitudinal\ \ collision\ \ times/duration\ which\ A'B'\ is\ less\ than\ S_x \qquad \textbf{(3-1)}$$

N_y , N_z are the frequency, which lateral separation and vertical separation are less than λ_y , λ_z , respectively.

P_x is the probability which longitudinal separation is less than λ_x

$$P_x = duration\ which\ A'B'\ is\ less\ \lambda_x\ /\ duration\ which\ A'B'\ is\ less\ than\ S_x \qquad \textbf{(3-2)}$$

P_y , P_z are the probability that lateral separation and vertical separation are less than λ_y , λ_z , respectively.

T_x is the time, which is needed for aircraft to pass though the slab, so T_x is given by

$$T_x = 2\lambda_x / V_x$$

V_x is longitudinal relative velocity of aircraft A and aircraft B.

From equation 3-1 and equation 3-2, the following equation can be deduced.

$$\frac{N_x}{P_x} = \frac{longitudinal\ \ collision\ \ times}{duration\ which\ A'B'\ is\ less\ \lambda_x} == \frac{1}{T_x} \qquad \textbf{(3-3)}$$

The frequency, that aircraft A and aircraft B collide from front and end faces (Figure 3.4), is defined by the lateral and vertical collision frequency multiplied by the N_x, which is denoted by $N_x P_y P_z$. So, collision from top and bottom faces

is $N_z P_x P_y$, and collision from either sides is $N_y P_x P_z$. Therefore, the total collision CR is given by

$$CR = N_x P_y P_z + N_y P_x P_z + N_z P_x P_y$$

In this thesis, parallel air route is taken into consideration. P_y , P_z, N_y, N_z are $P_y(S_y)$, $P_z(0)$, $N_y(S_y)$, $N_z(0)$. So, the lateral risk model is shown as follows:

$$CR_y = N_x[P_y(S_y)P_z(0)] + P_x[N_y(S_y)P_z(0) + N_z(0)P_y(S_y)] \quad \textbf{(3-4)}$$

According to equation 3-2, P_x can be rewritten as follows

$$P_x = \frac{2\lambda_x / V_x}{2S_x / V_x}$$

According to equation 3-3, N_x is given by

$$N_x = \frac{P_x}{T_x} = \frac{\lambda_x / S_x}{2\lambda_x / V_x} = \frac{V_x}{2S_x}$$

so the CR_y can be rewritten as follows:

$$CR_y = \frac{1}{S_x}[\frac{V_x}{2} P_y(S_y)P_z(0) + \lambda_x N_y(S_y)P_z(0) + \lambda_x N_z(0)P_y(S_y)]$$

If aircraft, in the same and opposite direction (Figure 3-5), are take into account together, CR_y is as follow:

$$CR_y = \frac{T_y(sam)}{S_x}[\frac{\Delta V_x}{2} P_y(S_y)P_z(0) + \lambda_x N_y(S_y)P_z(0) + \lambda_x N_z(0)P_y(S_y)] + \frac{T_y(opp)}{S_x}[\frac{V_x}{2} P_y(S_y)P_z(0) + \lambda_x N_y(S_y)P_z(0) + \lambda_x N_z(0)P_y(S_y)]$$

(3-5)

ΔV_x is the same direction relative velocity.

V_x is the opposite relative velocity.

Calculating $T_y(sam)$ and $T_y(opp)$:

$$T_y(sam) = aggregate\ of\ times\ spent\ by\ all\ pairs\ in\ the\ configurarion\ of\ Figure 3.5(a)$$

$$T_y(sam) = aggregate\ of\ times\ spent\ by\ all\ pairs\ in\ the\ configurarion\ of\ Figure 3.5(b)$$

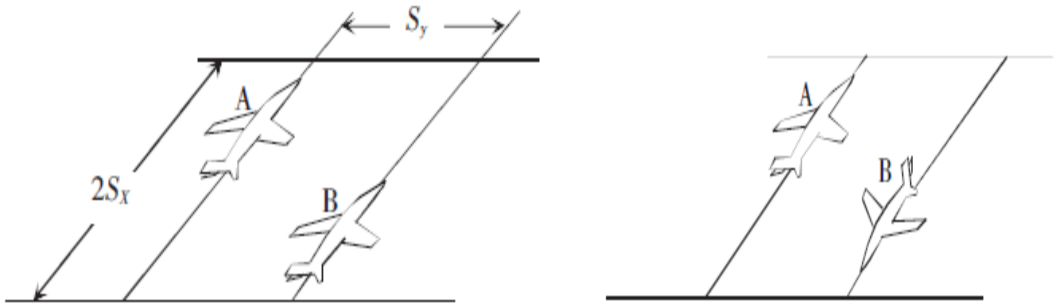

(a) Same Direction (b) Opposite Direction

Figure 3-5 Laterally Proximate Pairs

The parallel air route architecture is shown in Figure 3.6. Let aircraft's flow rate in path (i,j) be

$$M_{ij}$$

For a aircraft in the path (i, j), the maximum number of aircraft within a longitudinal separation $\pm S_x$ of it on path (i-1, j) is

$$\frac{2S_x}{\bar{V}} M_{i-1,j}$$

Therefore, for a long range air route, aircraft proximity rate between path (i, j) and path (i-1, j) is given by

$$\frac{2LS_x}{\bar{V}^2} M_{i-1,j} M_{i,j}$$

Then, $T_y(sam)$ and $T_y(opp)$ can be deduced as follows:

$$T_y(sam) = \frac{2LS_x}{\Delta V^2} \sum_{i=2}^{t} \sum_{j=1}^{f} M_{i-1,j} M_{i,j} \qquad \textbf{(3-6)}$$

$$T_y(opp) = \frac{2LS_x}{V^2} \sum_{i=2}^{t} \sum_{j=1}^{f} M_{i-1,j} M_{i,j}$$

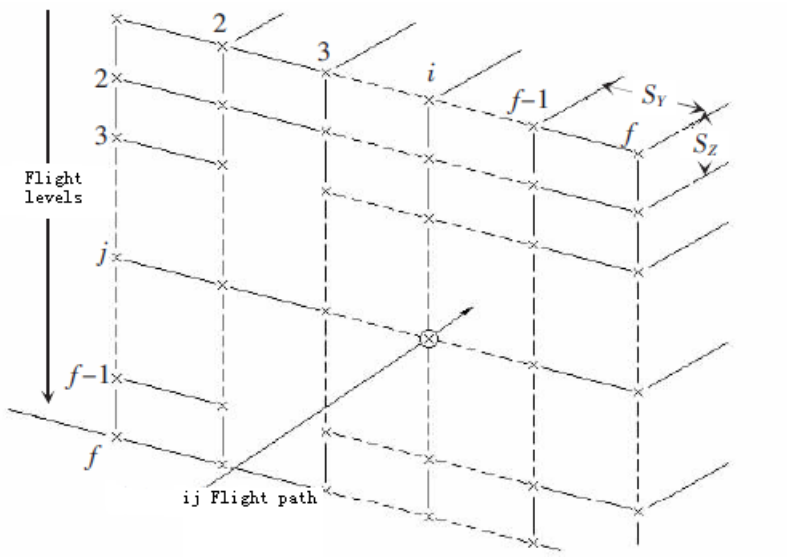

Figure 3-6 Parallel Air Route

To sum up, the lateral collision risk can be derived as follows:

$$N_y = P_y(S_y) P_z(0) \frac{\lambda_x}{\tilde{S}_x} [E_y(same)\{\frac{|\Delta V|}{2\lambda_x} + \frac{|\dot{y}|}{2\lambda_y} + \frac{|\dot{z}|}{2\lambda_z}\} + E_y(opp)\{\frac{|2V|}{2\lambda_x} + \frac{|\dot{y}|}{2\lambda_y} + \frac{|\dot{z}|}{2\lambda_z}\}]$$

(3-7)

The parameters in equation 3-7 are shown in table 3-1.

Table 3-1 Lateral Collision Model Parameters Definition

Parameter	Description
S_y	The lateral separation standard
$P_y(S_y)$	The probability of lateral overlap of aircraft nominally flying on laterally adjacent paths
$P_z(0)$	The probability of vertical overlap of aircraft nominally flying at the same flight level
λ_x	The average length of an aircraft
λ_y	The average width of an aircraft
λ_z	The average height of an aircraft
$\tilde{S}_x$	A parameter used in the calculation of E_y values
$E_y(same)$	The average number of same direction aircraft flying on laterally adjacent tracks at the same flight level within segments of length $2\tilde{S}_x$ centered on the typical aircraft
$E_y(opp)$	The average number of opposite direction aircraft flying on laterally adjacent tracks at the same flight level within segments of length $2\tilde{S}_x$ centered on the typical aircraft
$\lvert\Delta V\rvert$	The average relative along-track speed of two aircraft flying at the same flight level in the same direction
$\lvert V\rvert$	The average ground speed of an aircraft
$\lvert\dot{y}\rvert$	The average relative cross-track speed between aircraft which have lost S_y NM of separation
$\lvert\dot{z}\rvert$	The average relative vertical speed of aircraft flying at the same flight level

The vertical collision risk model can be derived as follows

$$N_z = P_z(S_z)P_y(0)\frac{\lambda_x}{\tilde{S}_x}[E_z(same)\{\frac{|\Delta V|}{2\lambda_x}+\frac{|\dot{y}|}{2\lambda_y}+\frac{|\dot{z}|}{2\lambda_z}\}+E_z(opp)\{\frac{|2V|}{2\lambda_x}+\frac{|\dot{y}|}{2\lambda_y}+\frac{|\dot{z}|}{2\lambda_z}\}] \quad \textbf{(3-8)}$$

Table 3-2 Vertical Collision Model Parameters Definition

Parameter	Description
N_z	The expected number of accidents per flight hour due to the loss of vertical separation
S_z	The vertical separation minimum
$P_z(S_z)$	The probability of vertical overlap of aircraft nominally flying on adjacent flight levels of the same track
$P_y(0)$	The probability of lateral overlap of aircraft nominally flying at the same track
λ_x	The average length of an aircraft
λ_y	The average width of an aircraft
λ_z	The average height of an aircraft
$\tilde{S}_x$	A parameter used in the calculation of E_z values
$E_z(same)$	The average number of same direction aircraft flying on adjacent flight levels of the same track within segments of length $2\tilde{S}_x$ centered on the typical aircraft
$E_z(opp)$	The average number of opposite direction aircraft flying on adjacent flight levels of the same track within segments of length $2\tilde{S}_x$ centered on the typical aircraft
$\lvert\Delta V\rvert$	The average relative along-track speed of two aircraft flying at the same track in the same direction
$\lvert V\rvert$	The average ground speed of an aircraft
$\lvert\dot{y}\rvert$	The average relative cross-track speed of aircraft flying at the same track
$\lvert\dot{z}\rvert$	The average relative vertical speed between aircraft which have lost S_z ft of separation

The longitudinal collision risk model is given by

$$N_x = P_x(S_x)P_z(0)P_y(0)\frac{\lambda_x}{\tilde{S}_x}[E_x(same)\{\frac{|\Delta V|}{2\lambda_x}+\frac{|\dot{y}|}{2\lambda_y}+\frac{|\dot{z}|}{2\lambda_z}\}+E_x(opp)\{\frac{|2V|}{2\lambda_x}+\frac{|\dot{y}|}{2\lambda_y}+\frac{|\dot{z}|}{2\lambda_z}\}] \quad \textbf{(3-9)}$$

Table 3-3 Longitudinal Collision Model Parameters Definition

Parameter	Description
S_x	The lateral separation standard
$P_x(S_x)$	The probability of longitudinal overlap of aircraft nominally flying on laterally adjacent paths
$P_z(0)$	The probability of Vertical overlap of aircraft nominally flying on laterally adjacent paths
$P_y(0)$	The probability of lateral overlap of aircraft nominally flying on laterally adjacent paths
λ_x	The average length of an aircraft
λ_y	The average width of an aircraft
λ_z	The average height of an aircraft
$\tilde{S}_x$	A parameter used in the calculation of E_y values
$E_x(same)$	The average number of same direction aircraft flying on laterally adjacent tracks at the same flight level within segments of length $\tilde{S}_x$ centered on the typical aircraft
$E_x(opp)$	The average number of opposite direction aircraft flying on laterally adjacent tracks at the same flight level within segments of length $\tilde{S}_x$ centered on the typical aircraft
$\lvert\Delta V\rvert$	The average relative along-track speed of two aircraft flying at the same flight level in the same direction
$\lvert V\rvert$	The average ground speed of an aircraft
$\lvert\dot{y}\rvert$	The average relative cross-track speed between aircraft which have lost S_y NM of separation.
$\lvert\dot{z}\rvert$	The average relative vertical speed of aircraft flying at the same flight level

In the Reich model, the main factors contributing to the separation minimum are traffic density and probability of overlap. So, how to calculate the probability of overlap will be discussed.

When two aircraft are intended to be separated by S_0 (Figure 3-7), the probability of overlap is defined by:

$$P(S_0) = \int_{-\lambda}^{\lambda} f^{x_{12}}(x)dx$$

$f^{12}(x)$ denotes the probability density of the separation x_{12} between two aircraft. Deviations of two aircraft from their intended position are denoted by x_1 and x_2 respectively. x_{12} is given by

$$x_{12} = S_0 + x_1 - x_2$$

and

$$f^{x_{12}}(x) = \int_{-\infty}^{\infty} f^{x}(x_1) f^{x}(S_0 + x_1 - x)dx_1$$

Where aircraft's position distributions are independent, $P(S_0)$ can be rewritten as follow

$$P(S_0) = \int_{-\lambda}^{\lambda}\int_{-\infty}^{\infty} f^{x}(x_1) f^{x}(S_0 + x_1 - x)dx_1 dx \quad \textbf{(3-10)}$$

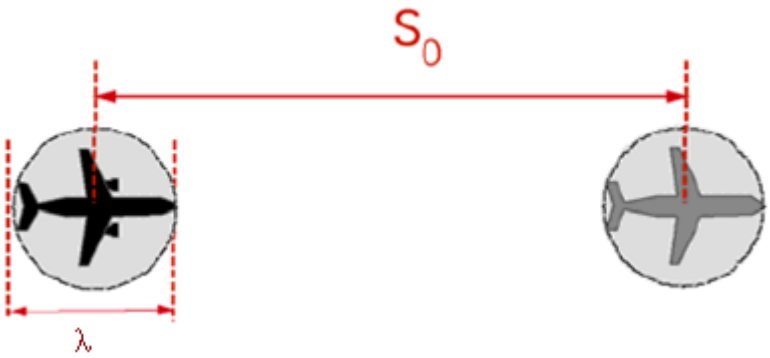

Figure 3-7 Parallel Air Route

3.3 Summary

This chapter has discussed the Reich model used to evaluate separation minimum safety issues. The main missions of this chapter are summarised as follows:

1. Review of cases which use Reich model to evaluate the separation safety issues.

2. Introduction of safety assessment model of the separation minimum.

3. Analysis of the parameters in the Reich model which have a large effect on safety assessment issues.

4 Modelling Aircraft's Position Uncertainty

4.1 Introduction

This chapter introduces the Kalman filter, used to improve aircraft's trajectory tracking performance, and as a result, position uncertainty can be reduced. The Kalman filter, which has been widely used in integrated navigation systems, is a powerful tool used to track manoeuvring aircraft. Section 4.2 describes air route architectures discussed in this thesis. Section 4.3 discusses the ATC services and constraints of the air routes. Section 4.4 gives aircraft's uncertainty sources. Section 4.5 uses the Kalman filter to model the aircraft's horizontal position uncertainty. Section 4.6 models the vertical position uncertainty. Finally, a summary is given in Section 4.7.

4.2 Air route Architectures

According to reference [28], phases of flight can be divided into five parts, which are takeoffs, departures, en route, arrivals and approaches. In different flight phases, aircraft have different navigation performance (shown in Figure 4-1).

Parallel air routes are built for risk assessment. As shown in Figure 4-2, two parallel air routes separated by S_T have been constructed. Aircraft in arrival/departure phases have RNP1 navigation performance, and in en route phase have RNP5 navigation performance. The aircraft's cruising altitude is FL390.

Aircraft flying in the adjacent air routes obey the following assumptions:

- Assumption that positions of the aircraft that are flying in the adjacent air routes are independent.
- Assumption that the aircraft's positions in three dimensions are independent.
- Assumption that the aircraft's velocity and position are independent.

- Assumption that the time of different aircraft entering into the air routes are independent.

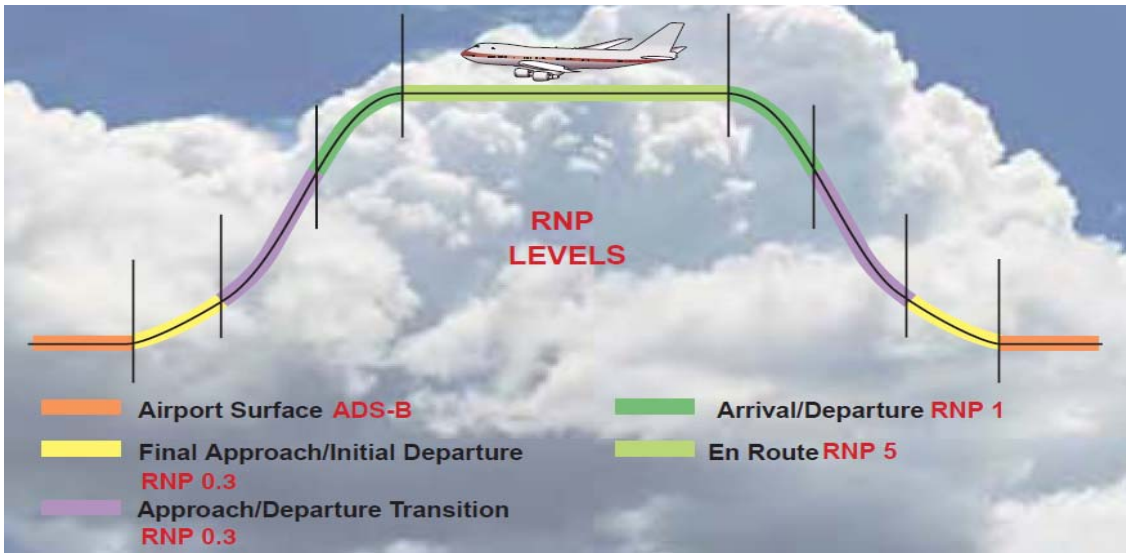

Figure 4-1 Navigation Type

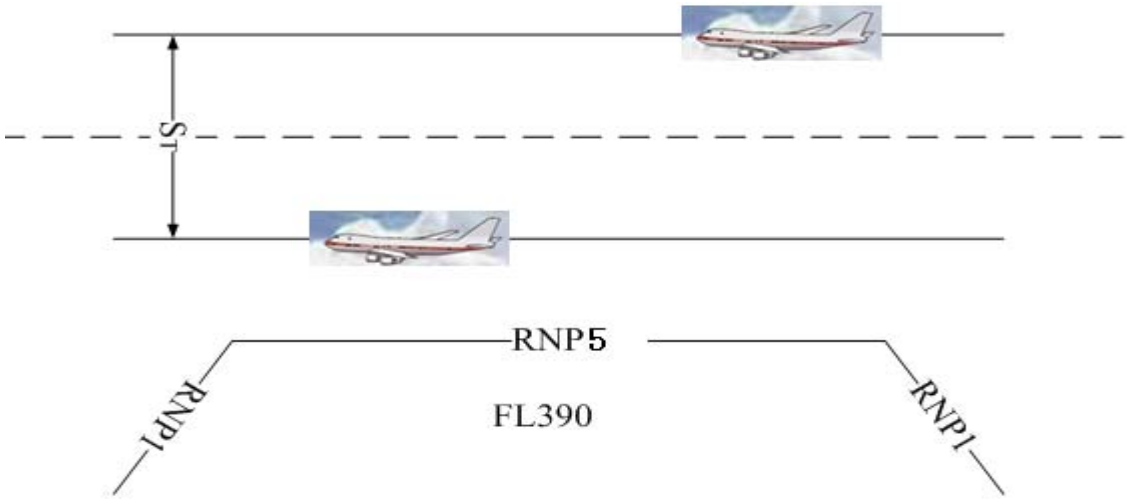

Figure 4-2 Air route Architecture

4.3 ATC Services and Constraints

Airspace in RNP 5 area is navigated by VOR/DME or the navigation tools which have the same performance. Surveillance system, in this area, is based on ADS-B system - aircraft can broadcast their position, position uncertainty,

velocity and velocity uncertainty to controllers. ATC controllers keep receiving and processing the information. If the controllers find a collision in the future, they will use digital communication system (in this thesis, communication system is assumed to be CPDLC system) to contact pilots and give resolution advice. The surveillance procedure is shown in Figure 4-3.

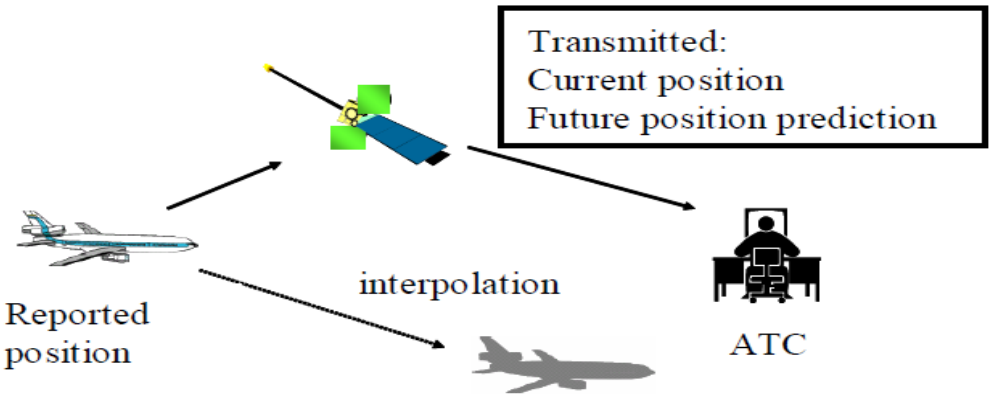

Figure 4-3 Surveillance Architecture

In this thesis, three parameters, which are navigation performance, ADS-B updating time and communication transaction time, are taken into account. In another way, these parameters are a definition of constraints of the CNS systems, because they define the performance of CNS systems used in this thesis. The value of the three parameters is given in Table 4-1.

Table 4-1 CNS Systems Parameters

Parameter	Value
Navigation performance	RNP 5 RNP 1
ADS-B updating time	5 S
Communication transaction time	6 S

4.4 Uncertainty sources

ICAO provides a definition of uncertainty of aircraft's position, which is the difference between the actual aircraft location and the location where the air traffic controller believes the aircraft to be [29].

The total system error (TSE) includes flight technical error (FTE), display system error (DSE), path definition error (PDE), path steering error (PSE), and position estimation error (PEE). [30]

Flight technical error: "The accuracy with which the aircraft is controlled as measured by the indicated aircraft position with respect to the indicated command or desired position."

Display system error: "These errors may include error components contributed by any input, output or signal conversion equipment used by the display as it presents either aircraft position or guidance commands (e.g. course deviation or command heading) and by any course definition entry device employed. For systems in which charts are incorporated as integral parts of the display, the display system error necessarily includes charting errors to the extent that they actually result in errors in controlling the position of the aircraft relative to a desired path over the ground."

Path definition error: "The difference between the defined path and the desired path at a specific point."

Path steering error: "The distance from the estimated position to the defined path. The PSE includes both FTE and display error (e.g., CDI error)."

Position estimation error: "The difference between true position and estimated position."

TSE is a combination of flight technical error, display system error, RNAV/RNP computation error and navigation system error. TSE is given by [30]

$$TSE = \sqrt{(FTE)^2 + (DSE)^2 + (PDE)^2 + (PSE)^2 + (PEE)^2} \quad \textbf{(4-1)}$$

The TSE is demonstrated in Figure 4-4.

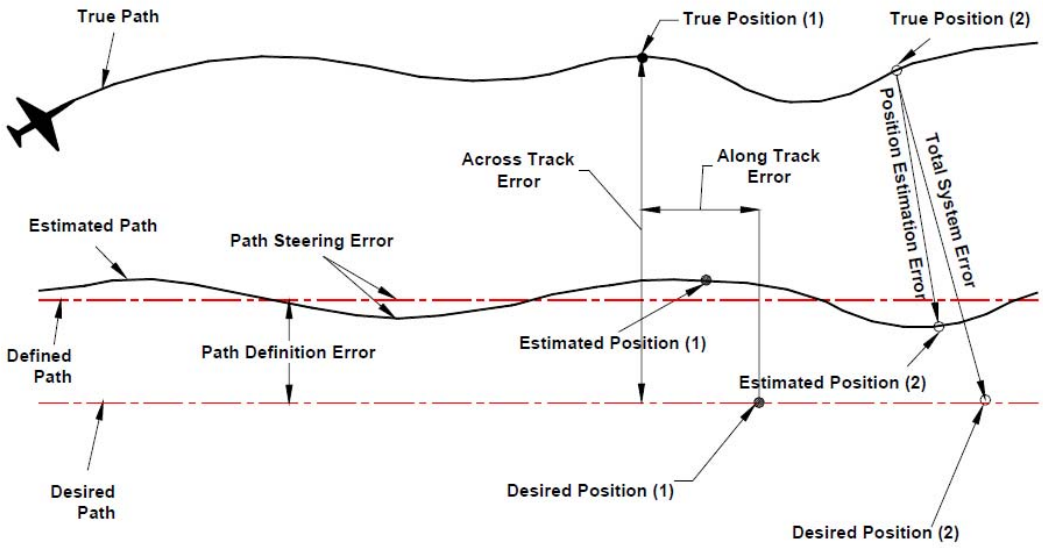

Figure 4-4 Total System Error Demonstration [30]

The distribution of total system error can be modelled by Gaussian or Double Exponential (DE) distributions [18], [25], [34]. Figure 4.5 shows the Gaussian and the Double Exponential (DE) distributions with the same mean value and variance.

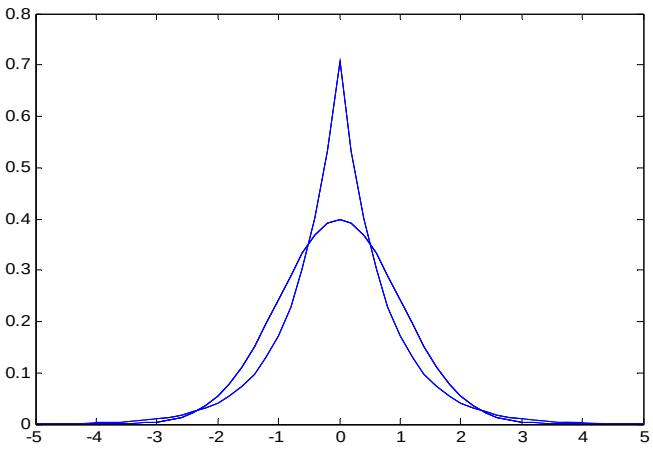

Figure 4-5 Gaussian or Double Exponential (DE) Distributions

The DE distribution, which has a long tail, is more conservative than the Gaussian distribution. In this thesis, the Gaussian distribution is used to model the TSE.

In order to monitor aircraft operation, the aircraft should have the ability to transmit its position information measured by on-board sensors, such as GPS or VOR/DME sensors, periodically to air traffic controllers. ADS-B aircraft has this ability, based on data link communication (e.g. VDL-4, INMARSAT, 1090ES). Also, the ADS-B aircraft send their velocity information to ATC controllers via data link. After receiving this information, ATC controllers make a prediction of the collision probability of two aircraft. If there is a high collision probability in the future, the ATC controller will give a resolution advisory via data link (e.g. CPDLC) to the aircraft to perform an evasive manoeuvre.

The position and velocity comprehension errors by the Air Traffic Controller, which is the difference between the actual aircraft position and the position where ATC consider the aircraft to be, depend on three factors - which are sensor errors, ADS-B updating time and Communication transaction time. As shown in Figure 4-3, the aircraft's position displayed on the ATC console is not the same as the aircraft's actual position, because the position which is measured by the sensors has more or less errors. The second parameter is ADS-B update time. Aircraft's position uncertainty increases until ATC get the next information sent by the ADS-B aircraft. The last parameter that must be considered is communication transactions time needed for the ATC controller to send a resolution advisory to the aircraft.

In the horizontal plane, let (V_a, V_c) denote the along tracking velocity and cross tracking velocity, respectively. The actual position is denoted by (P_{ca}, P_{cc}). The current position which is reported by ADS-B aircraft is denoted by $(\overline{P}_{ca,}\ \overline{P}_{cc})$ for the along tracking and cross tracking respectively, and the predicted position at future time t is denoted by $(P_{ta,}\ P_{tc})$. Similar to the position symbols, velocity in the future is denoted by $(P_{ta,}\ P_{tc})$. The ADS-B update time is denoted by T, and the communication transaction time is represented by τ. The aircraft's position is given by

$$\bar{P}_{ca} = P_{ca} + R$$
$$\bar{P}_{cc} = P_{cc} + R \quad \textbf{(4-2)}$$

Where R is a zero-mean normally distributed random variable whose variance can be calculated by using the ADS-B position uncertainty information.

The aircraft's velocity is given by

$$\bar{V}_{ca} = V_a + W$$
$$\bar{V}_{cc} = V_c + W \quad \textbf{(4-3)}$$

W is a zero-mean normally distributed random variable whose variance can be calculated by using the ADS-B velocity uncertainty information.

Therefore, the position in the future can be induced by

$$P_{ta} = \bar{P}_{ca} + \bar{V}_{ca} * t$$
$$P_{tc} = \bar{P}_{cc} + \bar{V}_{cc} * t \quad \textbf{(4-4)}$$

The mean value of predicted position is denoted by

$$E(P_{ta}) = E(\bar{P}_{ca} + \bar{V}_{ca} * t) = P_{ca} + V_{ca} * t$$
$$E(P_{tc}) = E(\bar{P}_{cc} + \bar{V}_{cc} * t) = P_{cc} + V_{cc} * t \quad \textbf{(4-5)}$$

In Section 3.2.1, an assumption that position and velocity are independent has been made, so the variance of predicted position is given by

$$D(P_{ta}) = D(\bar{P}_{ca} + \bar{V}_{ca} * t) = \sigma^2{}_p + \sigma^2{}_v * t^2$$
$$D(P_{tc}) = D(\bar{P}_{cc} + \bar{V}_{cc} * t) = \sigma^2{}_p + \sigma^2{}_v * t^2 \quad \textbf{(4-6)}$$

σ_p is the variance of R in equation (4-2), and σ_v is the variance of W in equation (4-3). However, $D(P_{ta})$ and $D(P_{tc})$ will saturate to a constant value for a long term prediction [31]-[33]. σ_{pt} is used to denote the variance of predicted position at time t, so for a long term prediction, σ_{pt} is given by

$$\sigma^2_{pt} \sim \min(\sigma^2_p + \sigma^2_v * t^2, \bar{\sigma}^2) \quad \textbf{(4-7)}$$

The long time prediction error is shown in Figure 4-6, and the short term prediction error is shown in Figure 4-8.

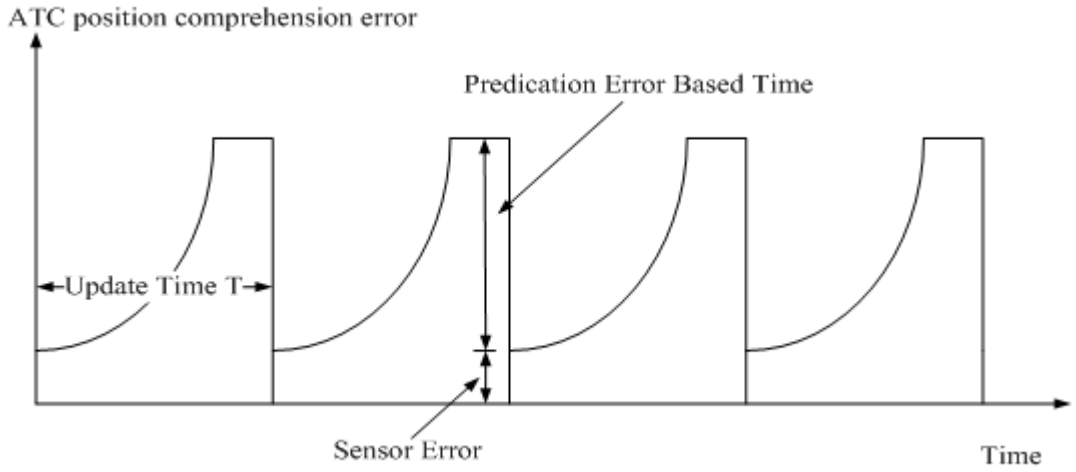

Figure 4-6 Long Time Prediction Error

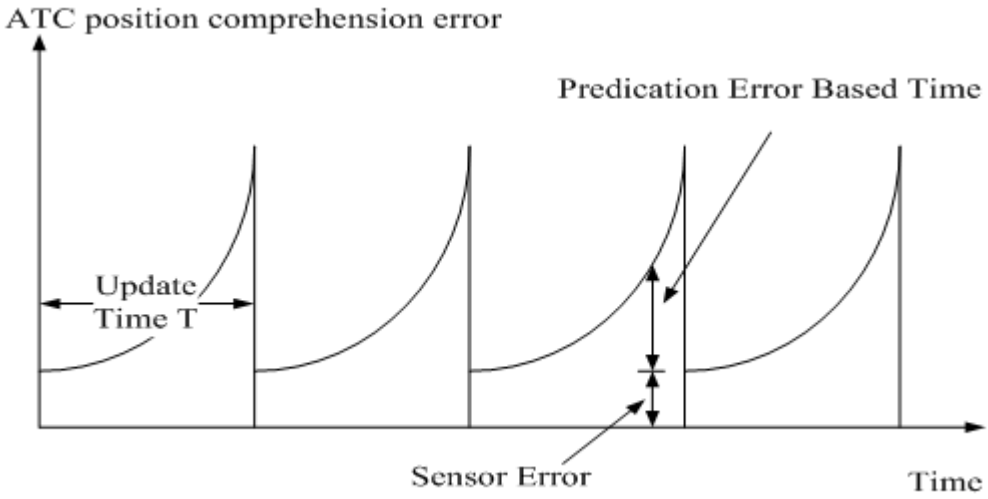

Figure 4-7 Short Time Prediction Error

Navigation Accuracy Code for Position (NAC_P) included in the ADS-B information, indicates how accurate the reported position is. This value has the same meaning as the RNP value, which means that the aircraft is expected to remain within a specific volume of airspace for at least 95 percent of the flight

time. The NAC_P value, transmitted by ADS-B data link, is shown in the Table 2.5. Navigation Uncertainty Categories – Velocity (NUC_V) included in the ADS-B information is used to describe accuracy of the reported velocity. The NUC_V, value, transmitted through ADS-B data link, is shown in Table 2.6.

Calculating position probability density function: the parallel air routes built, in Section 4.2, have RNP 5 navigation performance in en-route areas. In equation 3-2, parameter R is a zero-mean normally distributed random variable whose probability density function is given by

$$f(r) = \frac{1}{\sqrt{2\pi}\sigma} e^{-\frac{(r-\mu)^2}{2\sigma^2}} \quad \textbf{(4-8)}$$

Where μ equals zero. The variance σ can be determined by the RNP value. For RNP 5, the variance σ is given by

$$\int_{-5}^{5} f(r)dr = 0.95 \quad \textbf{(4-9)}$$

So, σ is given by

$$\sigma = 2.551\, nm$$

Calculating the velocity probability density function: in equation 4-2, W is a zero-mean normally distributed random variable, and the probability density function is given by

$$f(w) = \frac{1}{\sqrt{2\pi}\sigma} e^{-\frac{(w-\mu)^2}{2\sigma^2}} \quad \textbf{(4-10)}$$

Where mean value μ equals zero. The variance σ can be determined by the NUC_V value. For NUC_V 3, the variance σ is given by

$$\int_{-1}^{1} f(w)dw = 0.95 \quad \textbf{(4-11)}$$

So, σ is given by

$\sigma = 0.51\, m/s$

4.5 Modelling Horizontal Position Uncertainty

In the last section, aircraft's position uncertainty has been discussed. A long term and short term position prediction has been introduced. By using this prediction method, the position uncertainty increases as time flows. However, this is not true in actual applications, or is not a good prediction method. In this section, a prediction method based on the Kalman filter is presented.

4.5.1 Coordinate Definitions and Transformations

The geometric position information of ADS-B reports is referenced to the WGS-84 frame system [3]. However, trajectory tracking and prediction should be implemented in a local air traffic station frame, which is shown in Figure 4-6. Therefore, the geometric position represented in the latitude and longitude, should be transformed to the local frame. The transformation processes can be divided into two steps: firstly, aircraft position relative to WGS-84 frame is transformed into that relative to Earth-centred Earth-fixed (ECEF) frame; then, position information in ECEF frame should be transformed into that in local North-west Up frame. [34]

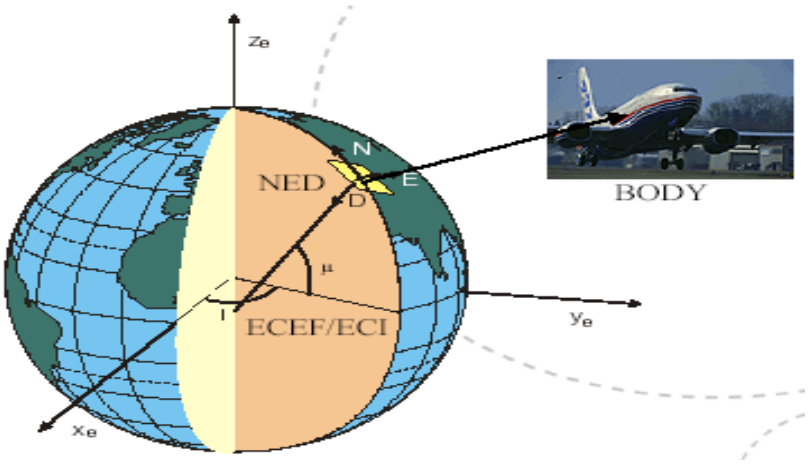

Figure 4-8 Coordinate Systems

Positions, transformed from WGS-84 frame to ECEF frame, are shown as follows [34]:

$$X_{ECEF} = \frac{a\cos\lambda}{\sqrt{1+(1-e^2)\tan^2\psi}} + h\cos\lambda\cos\psi \qquad \textbf{(4-12)}$$

$$Y_{ECEF} = \frac{a\sin\lambda}{\sqrt{1+(1-e^2)\tan^2\psi}} + h\sin\lambda\cos\psi$$

$$Z_{ECEF} = \frac{a(1-e^2)\sin\psi}{\sqrt{1-e^2\sin^2\psi}} + h\sin\psi$$

Where λ, ψ and h are the longitude, latitude and height of aircraft (according to WGS-84). a is the major axis of the Earth ellipsoid and e is its eccentricity (according to WGS-84).

Transformation from ECEF frame to local North-west Up frame is given by [34]:

$$\begin{pmatrix} X_{LNED} \\ Y_{LNED} \end{pmatrix} = \begin{pmatrix} -\sin\psi_s\cos\lambda_s & -\sin\psi_s\sin\lambda_s & \cos\psi_s \\ \sin\lambda_s & -\cos\lambda_s & 0 \end{pmatrix} \left(\begin{pmatrix} X_{ECEF-aircraft} \\ Y_{ECEF-aircraft} \\ Z_{ECEF-aircraft} \end{pmatrix} - \begin{pmatrix} X_{ECEF-station} \\ Y_{ECEF-station} \\ Z_{ECEF-station} \end{pmatrix} \right)$$

(4-13)

Where λ_s, ψ_s are the longitude and latitude of air traffic station (according to WGS-84).

4.5.2 The Kalman Filter

R. E. Kalman's paper describing a recursive solution of the discrete-data linear filtering problem was published in 1960. About this same time, advances in digital computer technology made it possible to consider implementing this recursive solution in a number of real-time applications. [40] - [42].

Random process to be estimated can be modelled in the form

$$x(k+1) = \Phi(k)x(k) + \omega(k) \qquad \textbf{(4-14)}$$

The observation (measurement) of the process is assumed to occur at discrete points in time in accordance with the linear relationship

$$z(k) = H(k)x(k) + v(k) \qquad \textbf{(4-15)}$$

Where

$x(k)$ = (n×1) process state at time t_k

$\phi(k)$ = (n×n) matrix relating $x(k)$ to $x(k+1)$ in the absence of a forcing function (if $x(k)$ is sample of continuous process, $\phi(k)$ is the usual state transition matrix)

$w(k)$ = (n×1) vector-assumed to be a white sequence with known covariance structure

$z(k)$ = (m×1) vector measurement at time t_k

$H(k)$ = (m×n) matrix giving the ideal (noiseless) connection between the measurement and the state vector at time t_k

$v(k)$ = (m×1) measurement error assumed to be a white sequence with known covariance structure having zero cross correlation with the $w(k)$ sequence

The covariance matrices for the $w(k)$ and $v(k)$ vectors are given by

$$E(w_k w_i^T) = \begin{cases} Q_k & k = i \\ 0 & k \neq i \end{cases}$$

$$E(v_k v_i^T) = \begin{cases} R_k & k = i \\ 0 & k \neq i \end{cases}$$

$$E(w_k v_i^T) = 0 \quad \textit{for all } k \textit{ and } i$$

An initial estimate of the process at some point in time t_k has been got, and that this estimate is based on all our knowledge about the process prior to t_k. This prior estimate will be denoted as $\hat{x}(k/k-1)$. The estimation error is given by

$$e(k/k-1) = x(k/k) - \hat{x}(k/k-1) \quad \textbf{(4-16)}$$

and the associated error covariance matrix is shown as follow

$$P_{\hat{x}}(k/k-1) = E(e(k/k-1)e^T(k/k-1)) = E[(x(k) - \hat{x}(k/k-1))(x(k) - \hat{x}(k/k-1))^T] \quad \textbf{(4-17)}$$

With the assumption of a prior estimate $\hat{x}(k/k-1)$, the measurement $z(k)$ is used to improve the prior estimate. The estimated state at the time t_k is given by

$$\hat{x}(k/k) = \hat{x}(k/k-1) + K(k)[y(k) - H(k)\hat{x}(k/k-1)] \quad \textbf{(4-18)}$$

Where $\hat{x}(k/k)$ is the estimated value at time t_k, and $K(k)$ is Kalman filter gain.

The associated error covariance matrix is shown as follows:

$$P_{\hat{x}}(k/k) = E(e(k/k)e^T(k/k)) = E[(x(k) - \hat{x}(k/k))(x(k) - \hat{x}(k/k))^T]$$

$$P_{\hat{x}}(k/k) = (I - K(k)H(k))P_{\hat{x}}(k/k-1)(I - K(k)H(k))^T + K(k)R(k)K^T(k) \quad \textbf{(4-19)}$$

There is a wish to find the particular $K(k)$ that minimizes the individual terms along the major diagonal of $P_{\hat{x}}(k/k)$, because these terms represent the estimation error variances for the elements of the state vector. So the $K(k)$ is given by

$$K(k) = P_{\hat{x}}(k/k-1)H^T(k)[H(k)P_{\hat{x}}(k/k-1)H^T(k) + R)(k)]^{-1} \quad \textbf{(4-20)}$$

Substituting equation 4-20 into equation 4-19, the estimated variance matrix is shown as follows:

$$P_{\hat{x}}(k/k) = [I - K(k)H(k)]P_{\hat{x}}(k/k-1) \quad \textbf{(4-21)}$$

The state is predicted by

$$\hat{x}(k/k-1) = \Phi(k/k-1)\hat{x}(k-1/k-1) \quad \textbf{(4-22)}$$

Substituting equation 4-22 into equation 4-17, the $P_{\hat{x}}(k/k-1)$ is denoted by

$$P_{\hat{x}}(k/k-1) = \Phi(k/k-1)P_{\hat{x}}(k-1/k-1)\Phi^T(k/k-1) + Q_{k-1} \quad \textbf{(4-23)}$$

To sum up, the Kalman filter estimates a process by using a form of feedback control: the process state at a time is estimated by the filter, and then feedback in the form of measurements are obtained. So, the equations for the Kalman filter divide into two sections: time update equations and measurement update equations. The time update equations are used to project forward (in time) the current state and error covariance estimates to get the a priori estimates for the next time step. The measurement update equations are used for the feedback. The time update equations can also be considered as predictor equations, while the measurement update equations can be considered as corrector equations. Indeed a predictor-corrector algorithm is integrated in the final estimation algorithm for solving numerical problems, as shown below in Figure 4-9.

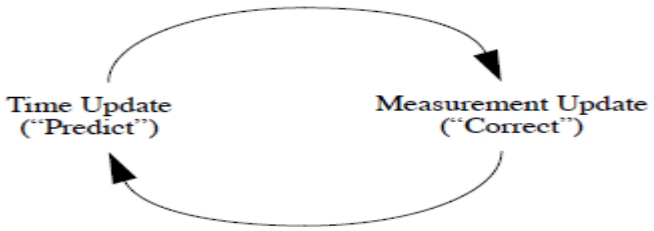

Figure 4-9 Kalman Filter Updating

Discrete Kalman filter time updating equations are given by

$$\begin{aligned}\hat{x}(k/k-1) &= \Phi(k/k-1)\hat{x}(k-1/k-1)\\ P_{\hat{x}}(k/k-1) &= \Phi(k/k-1)P_{\hat{x}}(k-1/k-1)\Phi^T(k/k-1) + Q_{k-1}\end{aligned} \quad \textbf{(4-24)}$$

Discrete Kalman filter measurement update equations are shown as follows

$$K(k) = P_{\hat{x}}(k/k-1)H^T(k)[H(k)P_{\hat{x}}(k/k-1)H^T(k)+R)(k)]^{-1}$$
$$\hat{x}(k/k) = \hat{x}(k/k-1) + K(k)[y(k) - H(k)\hat{x}(k/k-1)] \quad \textbf{(4-25)}$$
$$P_{\hat{x}}(k/k) = [I - K(k)H(k)]P_{\hat{x}}(k/k-1)$$

The matrix Q and R are the process noise covariance and measurement noise covariance.

$$p(w) \sim N(0, Q)$$
$$p(v) \sim N(0, R)$$

The standard Kalman filter is summarised in Figure 4-10.

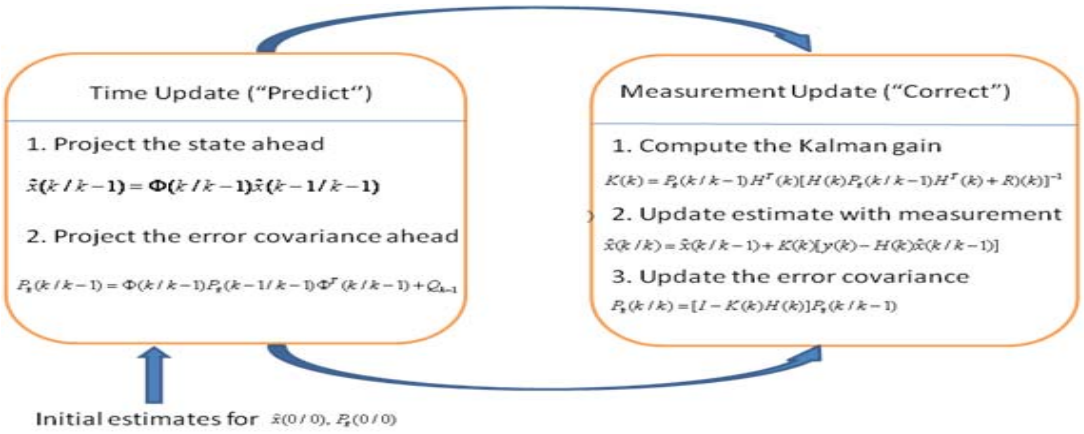

Figure 4-10 Kalman Filter Process

The Kalman filter prediction equations are summarised as follows

$$\hat{x}(k+1/k) = \Phi(k+1/k)\hat{x}(k/k-1) + K(k)[y(k) - H(k)\hat{x}(k/k-1)]$$
$$K(k) = \Phi(k+1/k)P(k/k-1)H^T(k)[H(k)P(k/k-1)H^T(k) + R(k)]^{-1} \quad \textbf{(4-26)}$$
$$P(k+1/k) = [\Phi(k+1/k) - K(k)H(k)]P(k/k-1) + Q(k)$$

4.5.3 Aircraft Dynamic Model

Many aircraft dynamic models have been developed [36]. To estimate state trajectories of a target is the main objective of aircraft tracking. An aircraft is usually treated as a point object without a shape in tracking, especially in aircraft dynamic models, although an aircraft is almost never really a point in the

space and the information about its orientation is valuable for tracking. An aircraft dynamic model or motion model describes the evolution of the aircraft state with respect to time.

The aircraft dynamic model used here is constant velocity (CV) model which has been widely used for civil aircraft tracking [35]-[41]. Using CV model is reasonable for civil aircraft tracking, because civil aircraft has low dynamic performance, especially during the cruising phase where they usually have constant cruise speed.

The aircraft's state transition equation is given by

$$x(k+1) = \Phi(k)x(k) + \omega(k)$$

$$\begin{pmatrix} X(k+1) \\ V_x(k+1) \\ a_x(k+1) \\ Y(k+1) \\ V_y(k+1) \\ a_y(k+1) \end{pmatrix} = \begin{pmatrix} 1 & T & T^2/2 & 0 & 0 & 0 \\ 0 & 1 & T & 0 & 0 & 0 \\ 0 & 0 & 1 & 0 & 0 & 0 \\ 0 & 0 & 0 & 1 & T & T^2/2 \\ 0 & 0 & 0 & 0 & 1 & T \\ 0 & 0 & 0 & 0 & 0 & 1 \end{pmatrix} \begin{pmatrix} X(k) \\ V_x(k) \\ a_x(k) \\ Y(k) \\ V_y(k) \\ a_y(k) \end{pmatrix} + \begin{pmatrix} T^2/2 & 0 \\ T & 0 \\ 1 & 0 \\ 0 & T^2/2 \\ 0 & T \\ 0 & 1 \end{pmatrix} \begin{pmatrix} w_x(k) \\ w_y(k) \end{pmatrix}$$

(4-27)

Table 4-2 Transition Equation Parameters Description

Parameters	Description
X , Y	Aircraft position along X axis and Y axis.
V_x , V_y	Aircraft velocity along X axis and Y axis.
a_x , a_y	Aircraft acceleration along X axis and Y axis.
T	ADS-B updating time.
w_x , w_y	Independent process noise (White Gaussian noise) because

	of atmospheric turbulence. $\sigma_{w_x} = \sigma_{w_y} = 1\,m/s^2$

According to the application of this thesis, only aircraft's position information needs to be measured. Therefore, the observation model is shown as follows

$$y(k) = H(k)x(k) + v(k)$$

$$\begin{pmatrix} X(k) \\ Y(k) \end{pmatrix} = \begin{pmatrix} 1 & 0 & 0 & 0 & 0 & 0 \\ 0 & 0 & 0 & 1 & 0 & 0 \end{pmatrix} \begin{pmatrix} X(k) \\ V_x(k) \\ a_x(k) \\ Y(k) \\ V_y(k) \\ a_y(k) \end{pmatrix} + \begin{pmatrix} 1 & 0 \\ 0 & 1 \end{pmatrix} \begin{pmatrix} v_x(k) \\ v_y(k) \end{pmatrix}$$

(4-28)

Where $v_x(k)$ and $v_y(k)$ are measured noises which are White Gaussian noise.

ADS-B information contains RNP types. According to reference [42], the variances of $v_x(k)$ and $v_y(k)$ are given by

$$\sigma_{v_x} = \sigma_{v_y} = 0.3RNP \qquad \textbf{(4-29)}$$

4.5.4 Simulation and Discussion

MATLAB has been used to conduct simulation work. The architecture of the simulation is shown in Figure 4-11. Monte Carlo method is used in the simulation. For a particular trajectory, the Kalman filter prediction is repeated 100,000 times. Three functions, trajectory function, Kalman function and result function, are built. Firstly, an aircraft trajectory is constructed in the trajectory function. Secondly, the Kalman filter prediction is implemented in the Kalman function. Lastly, the variance of the estimated trajectory is generated in the result function.

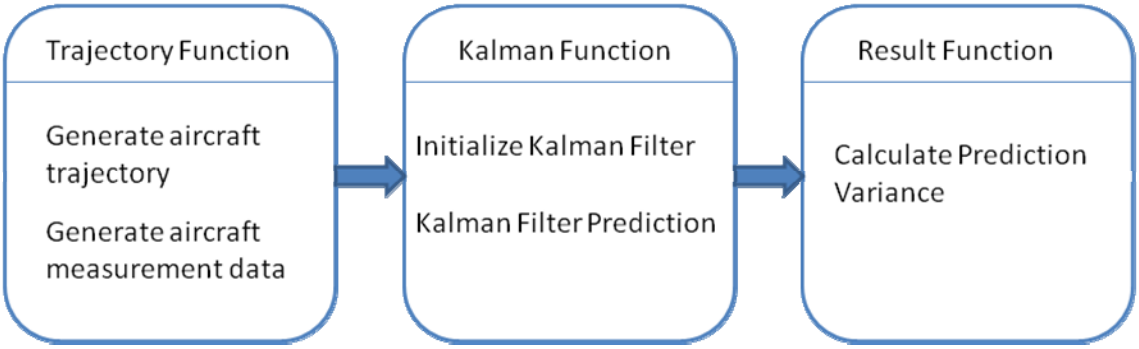

Figure 4-11 Simulation Architecture

The Kalman filter prediction equations are initialized as follows.

The initialized state matrix is given by

$$\begin{pmatrix} \hat{X}(2/2) \\ \hat{V}_x(2/2) \\ \hat{a}_x(2/2) \\ \hat{Y}(2/2) \\ \hat{V}_y(2/2) \\ \hat{a}_y(2/2) \end{pmatrix} = \begin{pmatrix} X(2) \\ (X(2)-X(1))/T \\ (X(2)-X(1))/T^2 \\ Y(2) \\ (Y(2)-Y(1))/T \\ (Y(2)-Y(1))/T^2 \end{pmatrix}$$

The initialized process noise matrix is given by

$$Q = \begin{pmatrix} \frac{T^4}{4}\sigma_{w_x} & \frac{T^3}{2}\sigma_{w_x} & \frac{T^2}{2}\sigma_{w_x} & 0 & 0 & 0 \\ \frac{T^2}{2}\sigma_{w_x} & T^2\sigma_{w_x} & T\sigma_{w_x} & 0 & 0 & 0 \\ \frac{T^2}{2}\sigma_{w_x} & T\sigma_{w_x} & \sigma_{w_x} & 0 & 0 & 0 \\ 0 & 0 & 0 & \frac{T^4}{4}\sigma_{w_y} & \frac{T^3}{2}\sigma_{w_y} & \frac{T^2}{2}\sigma_{w_y} \\ 0 & 0 & 0 & \frac{T^2}{2}\sigma_{w_y} & T^2\sigma_{w_y} & T\sigma_{w_y} \\ 0 & 0 & 0 & \frac{T^2}{2}\sigma_{w_y} & T\sigma_{w_y} & \sigma_{w_y} \end{pmatrix}$$

The initialized measured noise matrix is shown as follows

$$R = diag[\sigma_{v_x}, \sigma_{v_y}]$$

The initialized covariance matrix is denoted by

$$P(2/2) = \begin{pmatrix} P_{11} & P_{12} \\ P_{21} & P_{22} \end{pmatrix}$$

$$P_{ij} = \begin{pmatrix} r_{ij}(2) & \frac{r_{ij}(2)}{T} & \frac{r_{ij}(2)}{T^2} \\ \frac{r_{ij}(2)}{T} & \frac{r_{ij}(2)+r_{ij}(1)}{T^2} & \frac{r_{ij}(2)+2r_{ij}(1)}{T^3} \\ \frac{r_{ij}(2)}{T^2} & \frac{r_{ij}(2)+2r_{ij}(1)}{T^3} & \frac{r_{ij}(2)+4r_{ij}(1)+r_{ij}(0)}{T^4} \end{pmatrix} \qquad i, j = 1, 2$$

T is position information updating time.

Four trajectories are simulated.

The results of the first trajectory, whose RNP type is RNP 5 and velocity is $250\,m/s^2$, are shown as follows

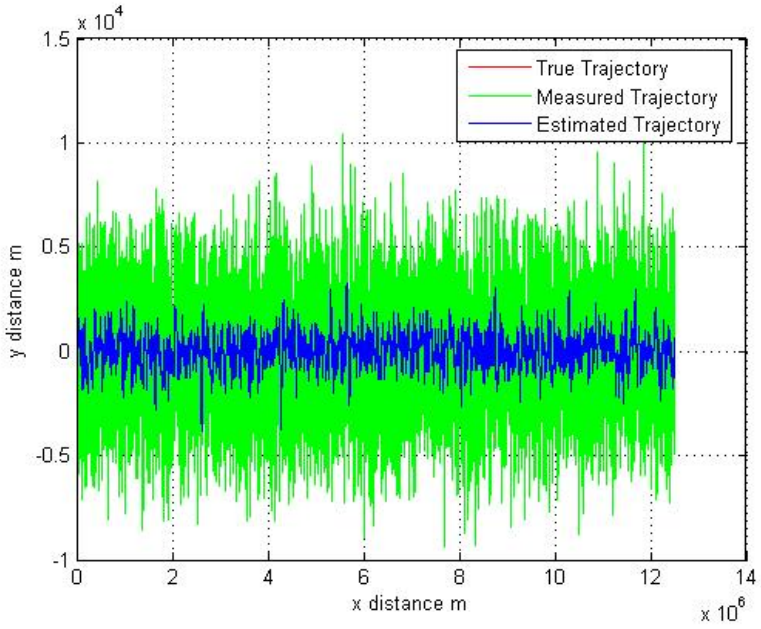

(a) Measured and Estimated Trajectories

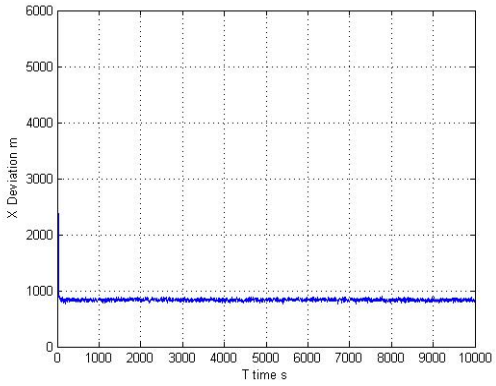

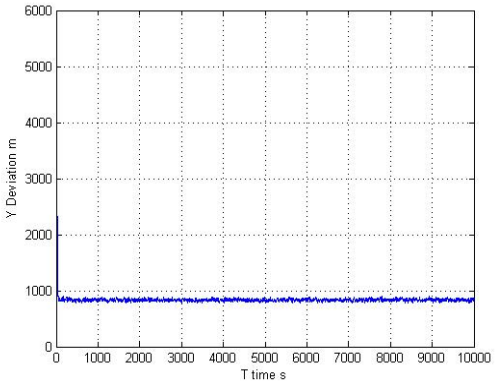

(b) Along Tracking Variance **(b) Cross Tracking Variance**

Figure 4-12 Simulation Results with RNP 5 and Velocity $250 m/s^2$

The results of the second trajectory, whose RNP type is RNP 5 and velocity is $220 m/s^2$, are given by

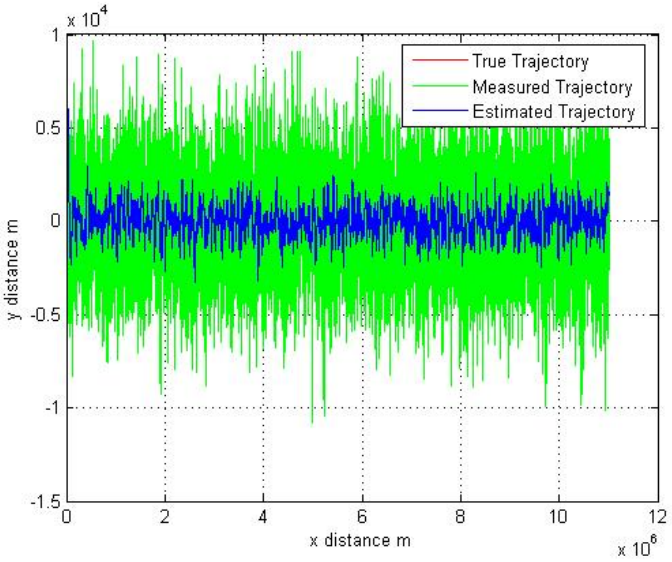

(b) Measured and Estimated Trajectories

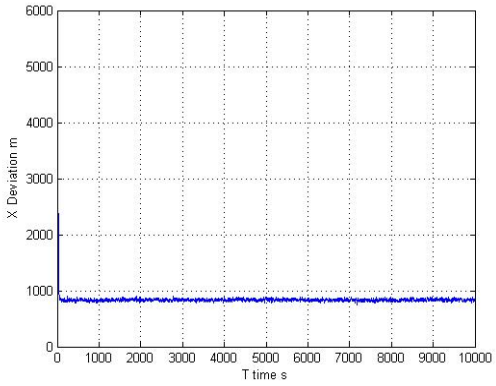

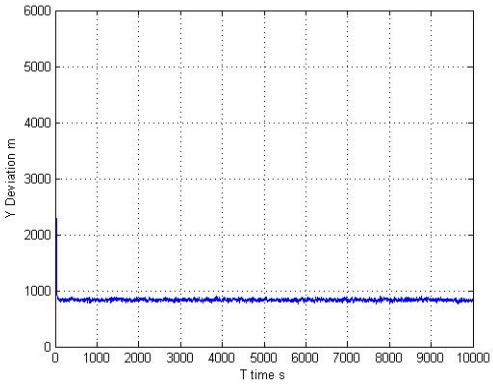

(b) Along Tracking Variance **(b) Cross Tracking Variance**

Figure 4-13 Simulation Results with RNP 5 and Velocity $220 m/s^2$

The results of the third trajectory, whose RNP type is RNP 1 and velocity is $250 m/s^2$, are shown as follows

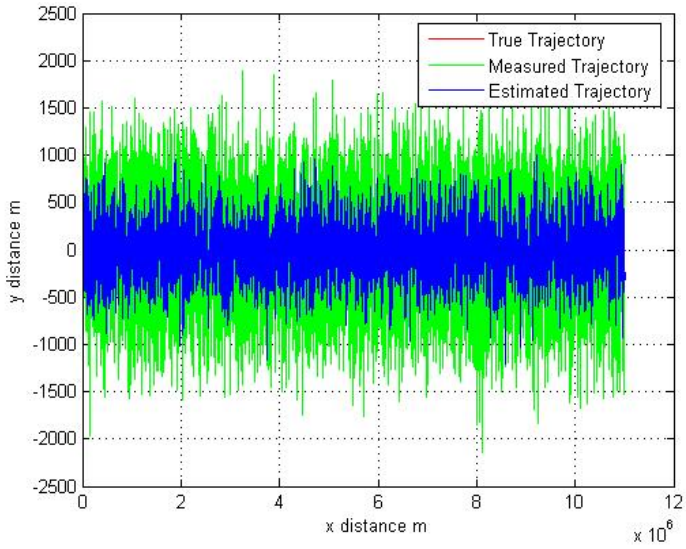

(c) Measured and Estimated Trajectories

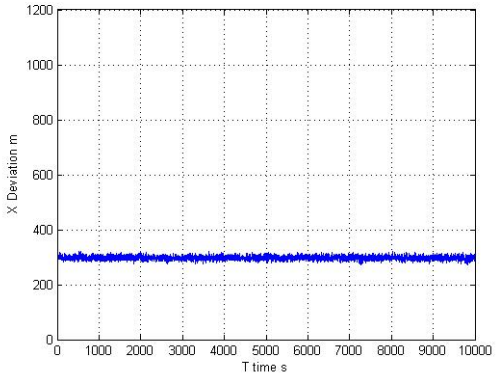

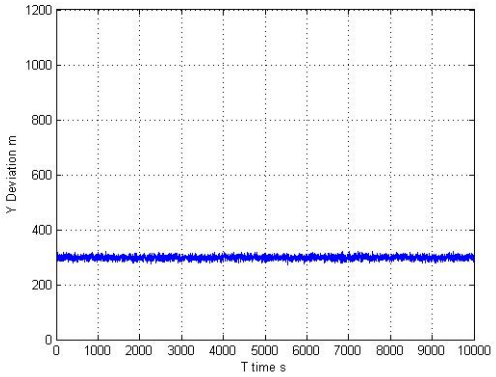

(b) Along Tracking Variance **(b) Cross Tracking Variance**

Figure 4-14 Simulation Results with RNP 1 and Velocity $250 m/s^2$

The results of the second trajectory, whose RNP type is RNP 1 and velocity is $220 m/s^2$, are given by:

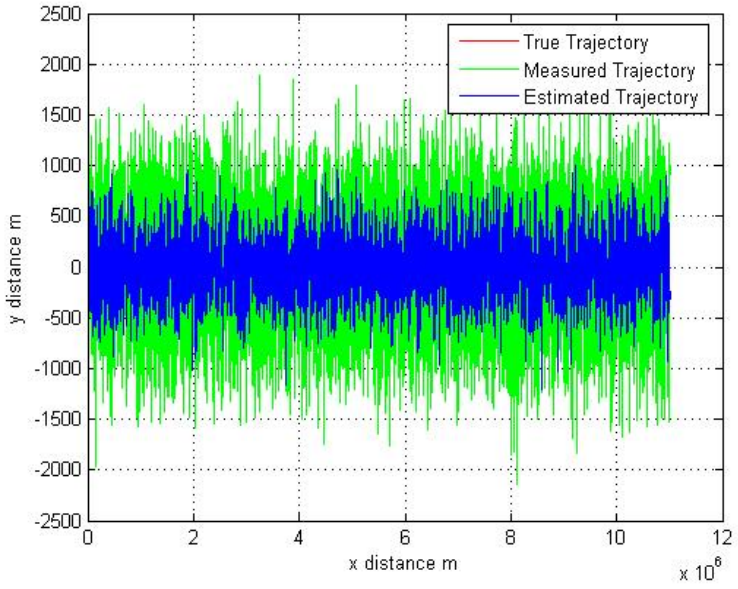

(d) Measured and Estimated Trajectories

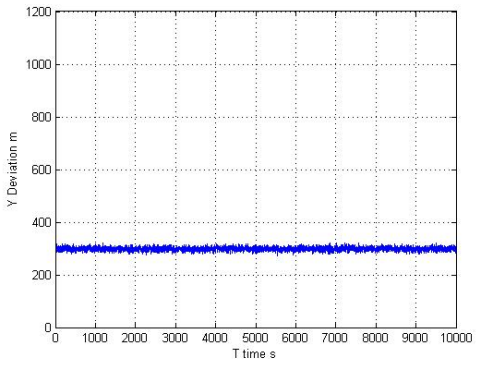

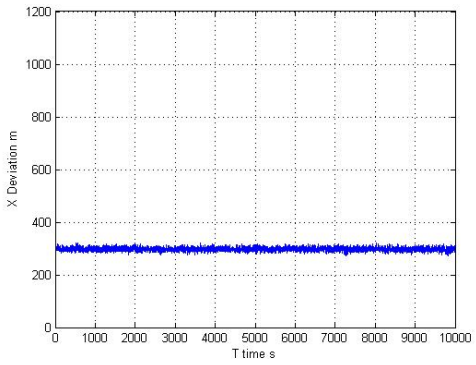

(b) Along Tracking Variance **(b) Cross Tracking Variance**

Figure 4-15 Simulation Results with RNP 1 and Velocity $220 m/s^2$

Green lines in Figures represent reported position which is transmitted by ADS-B, and blue lines are estimated position by using the Kalman filter. It is easy to see that trajectory tracking performance has been improved, because deviations of estimated position are smaller than that of reported position. As a consequence, the measured noise has been reduced. As shown in Figure 4-12 (b)-(c), when the aircraft's velocity is $250 m/s^2$ and RNP type is RNP 5, the maximum variance of along tracking and cross tracking are 908 m and 906 m. In Figure 4-13 (b)-(c), when the aircraft's velocity is $220 m/s^2$, the maximum variance of along tracking and cross tracking is 904 m and 903 m. To be conservative, 908 m and 906 m are selected as the variance of along tracking and cross tracking. Because of the reduction of noise variance, the variance of position distribution will be decreased. According to equation 4-1 and equation 4-16, the variances of estimated position distribution are given by

$$\sigma_x = 2.05\, nmi$$
$$\sigma_y = 2.05\, nmi \qquad \textbf{(4-30)}$$

Compared to equation 4-9, the variance of position distribution has been reduced.

When the RNP type is RNP 1, the variances of estimated position distribution are given by

$$\sigma_x = 0.43 nmi$$
$$\sigma_y = 0.43 nmi \quad \textbf{(4-31)}$$

4.6 Modelling Vertical Position Uncertainty

The sensor which is used to measure flight altitude of aircraft is the barometric altimeter. However, the altitude information included in ADS-B information does not have uncertainty information. Therefore, the uncertainty of aircraft is modelled by zero mean Gaussian distribution, based on the historical observation data [43]-[44]. The uncertainty of aircraft is defined in total vertical error (TVE) where

$$TVE = \text{actual pressure altitude flown by an aircraft} - \text{assigned altitude}$$

TVE contains two types of errors, which are Flight Technical Error (FTE) and Altimetry System Error (ASE). According to equation 4-1, the variance of TVE is given by

$$\sigma_{TVE} = \sqrt{\sigma_{ASE}^2 + \sigma_{FTE}^2}$$

The variance of ASE density is 81.7ft, and the variance of FTE density is 39.8 ft [44]. Therefore, the variance of TVE density is given by

$$\sigma_{TVE} = 90.9 \ ft \quad \textbf{(4-32)}$$

4.7 Summary

The main object of this chapter has been to develop a method to model aircraft's position uncertainty. The work of this chapter is summarized as follows

1. Parallel air routes have been constructed. Navigation performance is RNP 5 for en-route phase and RNP 1 for approaches phase. ADS-B system is used as the surveillance system and its updating time is 5 s. Communication

system used to transmit resolution advisory is CPDLC, and its transaction time is 6 s.

2. Aircraft’s position uncertainty sources have been discussed. The uncertainty sources include flight technical error, display system error, path definition error, path steering error, and position estimation error.

3. The Kalman filter has been used to reduce position uncertainty. Firstly, coordinate transformations have been made due to the application of this thesis. Then aircraft dynamic model and the Kalman filter have been introduced. Lastly, position uncertainty has been modelled in both horizontal and vertical planes.

5 Case Study and Results

5.1 Introduction

This chapter uses a simulation to evaluate the separation minimum safety issues. The main purpose is to find a suitable separation minimum which can satisfy the safety requirement of TLS. When aircraft are separated by this minimum distance, the collision risk probability between two aircraft is smaller than TLS, which is regulated by ICAO. Section 5.2 presents the architecture of the simulation. The parameters, which are needed in the simulation, are summarized in Section 5.3. Section 5.4 discusses the results of the simulation. Finally, a summary is given in Section 5.5.

5.2 Procedure of Case study

The separation minimum evaluation procedure can be divided into four steps: firstly, models and parameters are developed to describe the performance of CNS, such as navigation accuracy, communication transaction time and surveillance delay time; secondly, a new method, based on the CNS performance parameters, is built to estimate the position of the aircraft; then the Reich model is used to evaluate the collision risk for the parallel air route separation minimum; finally, the collision risk is compared to target level of safety (TLS) of 5×10^{-9}. If the collision risk is smaller than TLS, the safety is guaranteed; otherwise, there will be a potential collision in the future, and a resolution advisory should be given. Therefore, the separation should be enlarged in order to ensure the safety issue. The Kalman filter software has been discussed in Section 4.5.

The risk assessment procedure in lateral, longitudinal and vertical planes can be demonstrated by Figure 5-1.

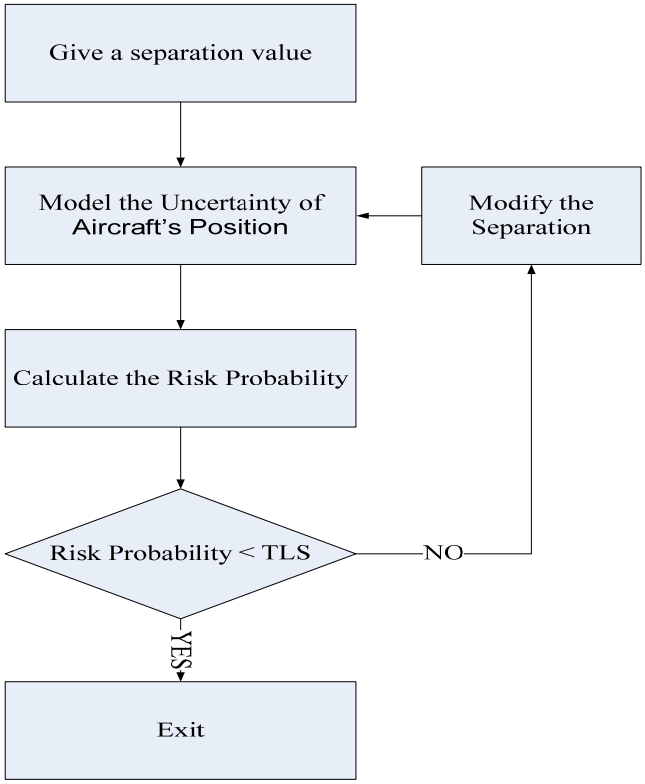

Figure 5-1 Risk Assessment Procedure

5.3 Reich Model Parameters

Aircraft which fly in the air routes are shown in Table 5-1. These aircraft's data are made based on assumption, because actual data should be based on historical observation data, and there is a lack of observation conditions.

B737-700 aircraft dimensions are given in Figure 5-2 as a demonstration.

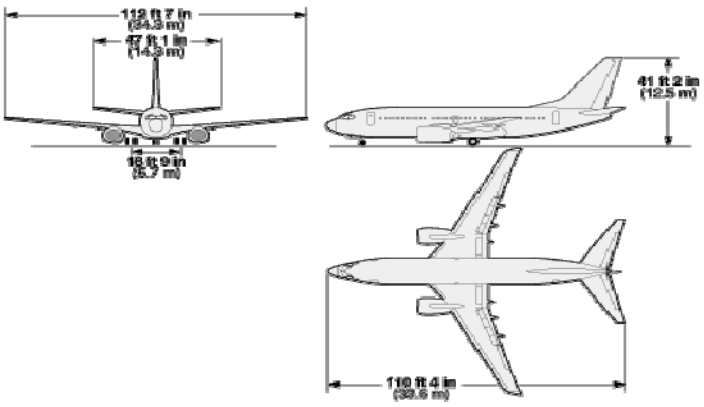

Figure 5-2 B737-700 Aircraft Dimensions

Table 5-1 Aircraft Population Information

Aircraft	Length λ_x (ft)	Width λ_y (ft)	Height λ_z (ft)	Cruising Speed (knots)
B737-700	110.40	112.70	41.20	495
A320	123.00	111.00	38.00	472
A310	153.08	144.00	51.83	484
A340	194.83	197.83	54.75	495
Average	145.12	136.89	45.27	486.5

Relative velocity and average number of aircraft data, which are derived from historical observation data, are given in Table 5-2 [43].

Table 5-2 Reich Model Parameters

Parameters	Value	Parameters	Value
$\left\|\bar{V}\right\|$	475 knots	$E_y(same)$	0.2562
$\left\|\Delta\bar{V}\right\|$	20 knots	$E_y(opp)$	0
$\left\|\bar{\dot{y}}\right\|$	20 knots	$E_z(same)$	0
$\left\|\bar{\dot{z}}\right\|$	1.5 knots	$E_z(opp)$	0.144
$E_x(same)$	0.61	$\tilde{S}_x$	80 NMI
$E_x(opp)$	0.01		

5.4 Separation Minimum Safety Assessment

5.4.1 Lateral Collision Risk

In order to assess lateral collision risk, lateral probability of overlap should be calculated first. In Section 4.4, aircraft's position distribution is modelled by zero mean Gaussian distribution, and its variances are described in equation 4-30, equation 4-31 and equation 4-32. Therefore, aircraft's position probability density is given by

$$P(y) = \frac{1}{\sqrt{2\pi}\sigma_y} e^{-\frac{y^2}{2\sigma_y^2}}$$

Lateral probability of overlap is shown as follows

$$P(S_0) = \int_{-\lambda_y}^{\lambda_y} \int_{-\infty}^{\infty} f^1(y) f^2((S_0 + \left|\dot{\bar{y}}\right| * (T + \tau)) + y_1 - y) dy_1 dy \quad \textbf{(5-1)}$$

Where T is ADS-B updating time, and τ is communication system transaction time.

Substituting equation 5-1 and the parameters in Table 5-2 into equation 3-7, lateral collision risk probability is generated and shown in Figure 5-3.

In the left side figures, y axis is the collision risk probability value, calculated from the Reich model, and x axis is the separation minimum value. It is easy to see that the collision risk probability decreases as the separation increases. For convenience, the y axis value is transmitted by logarithmic function, and the result is shown in the right side figures. The blue line represents the TLS of 5×10^{-9} . If the probability value is equal to or smaller than TLS, the corresponding value on the x axis is the separation minimum. Therefore for RNP 5, the separation minimum, without using the Kalman filter, is 19.4 NMI. However, the separation minimum by using the Kalman filter reduces to 14.8

NMI. For RNP 1, the separation minimum without using the Kalman filter is 4.8 NMI, and the value decreases to 4.4 NMI by using the Kalman filter.

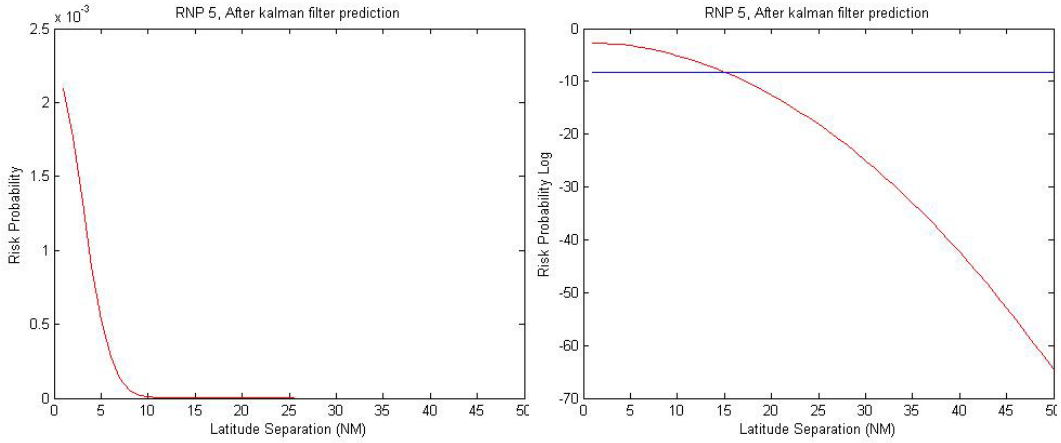

(a) Separation Minimum With Using Kalman filter

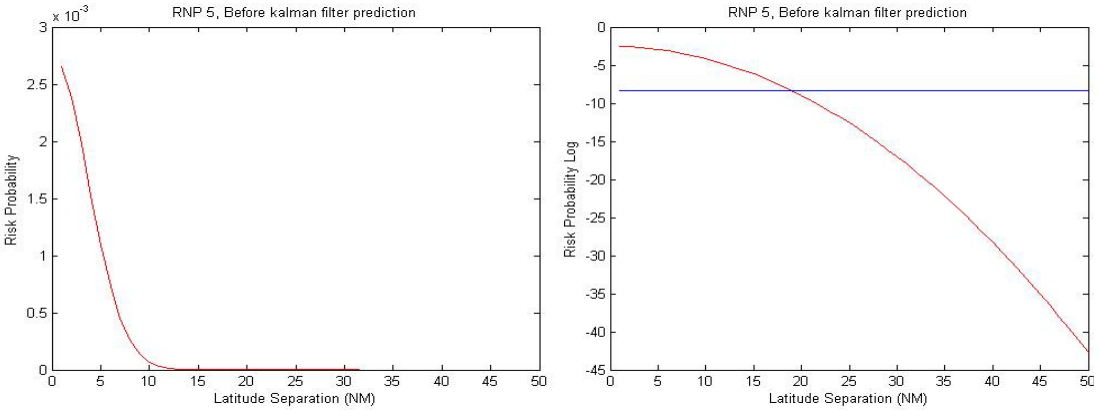

(b) Separation Minimum Without Using Kalman filter

Figure 5-3 Lateral Collision Risk Assessment for RNP 5

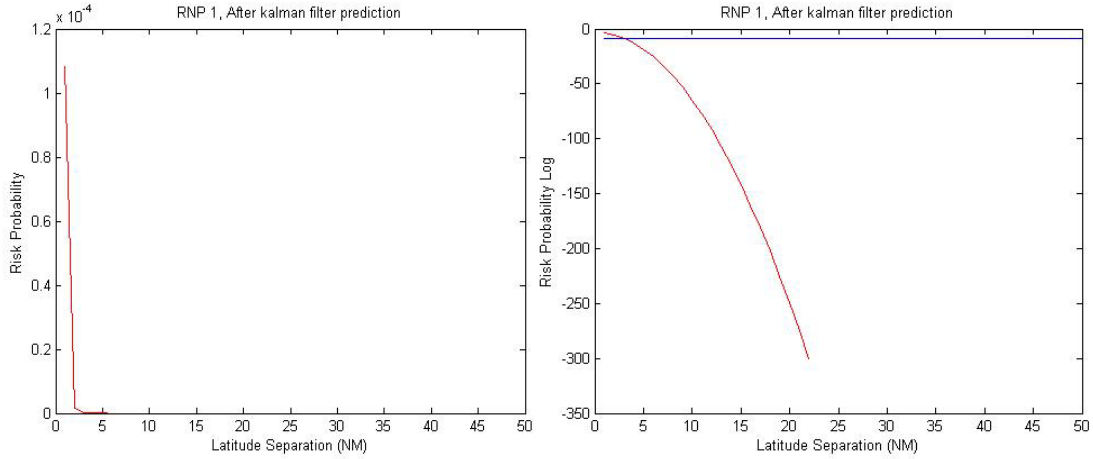

(a) Separation Minimum With Using Kalman filter

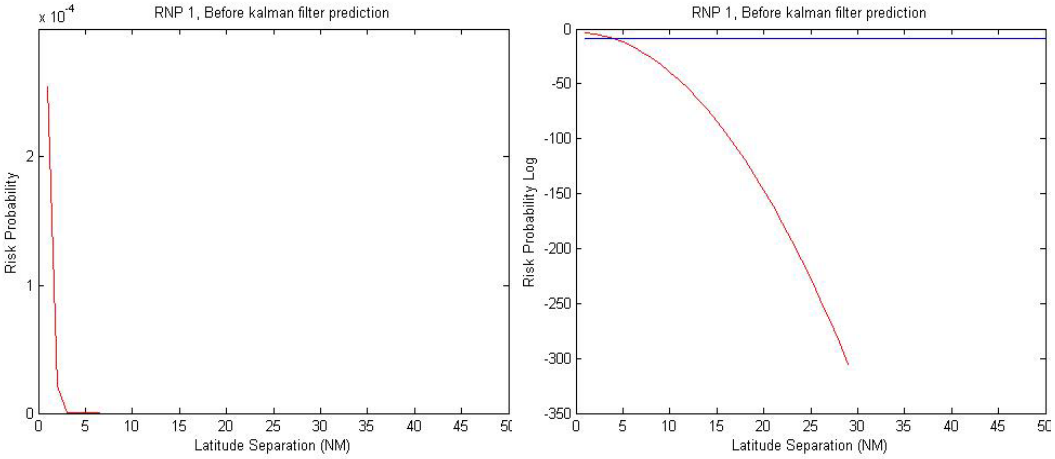

(b) Separation Minimum Without Using Kalman filter

Figure 5-4 Lateral Collision Risk Assessment for RNP 1

5.4.2 Longitudinal Collision Risk

The process, used to evaluate longitudinal collision risk, is similar to the process to assess lateral collision risk. Aircraft's position probability density is given by

$$P(x) = \frac{1}{\sqrt{2\pi}\sigma_x} e^{-\frac{x^2}{2\sigma_x^2}}$$

Longitudinal probability of overlap is shown as follows

$$P(S_0) = \int_{-\lambda_x}^{\lambda_x} \int_{-\infty}^{\infty} f^1(x) f^2((S_0 + \left|\Delta \bar{V}\right| * (T + \tau)) + x_1 - x) dx_1 dx \quad \textbf{(5-2)}$$

Substituting equation 5-2 and the parameters in table 5-2 into equation 3-8, collision risk probability is shown in Figure 5-5.

For RNP 5, the separation minimum without using the Kalman filter is 19.4 NMI. However, the separation minimum by using the Kalman filter reduces to 14.8 NMI. For RNP 1, the separation minimum without using the Kalman filter is 4.8 NMI, and the value decreases to 4.4 NMI by using the Kalman filter.

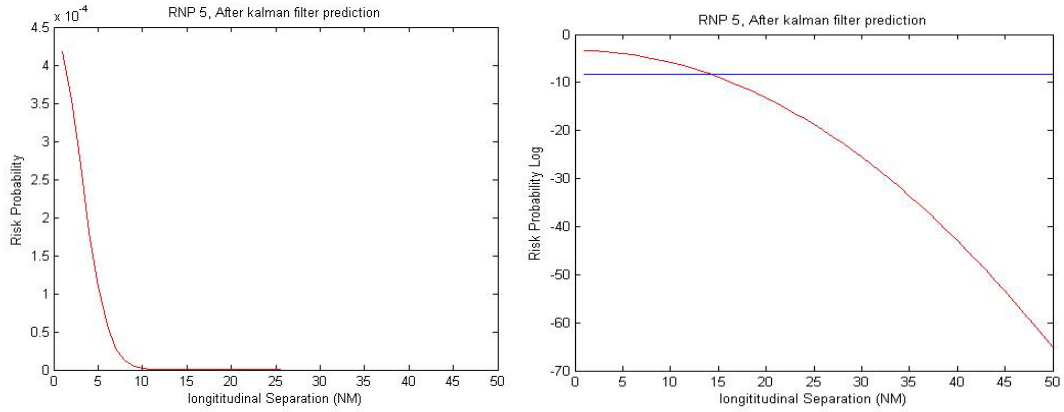

(a) Separation Minimum With Using Kalman filter

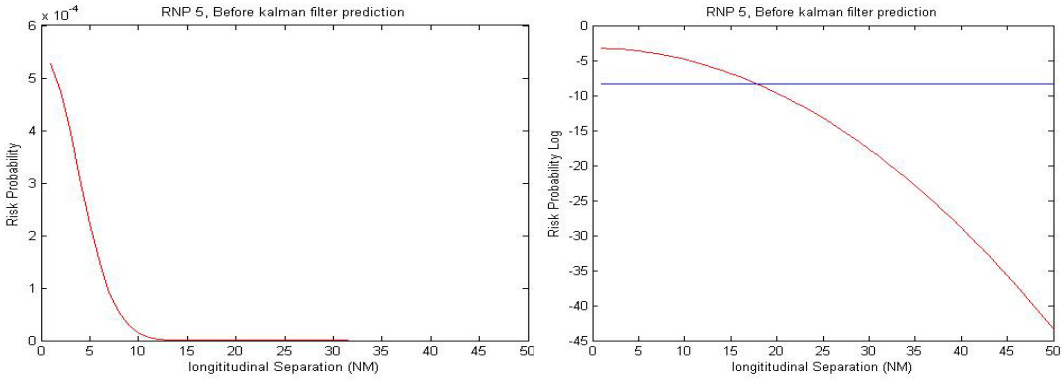

(b) Separation Minimum Without Using Kalman filter

Figure 5-5 Longitudinal Collision Risk Assessment with RNP 5

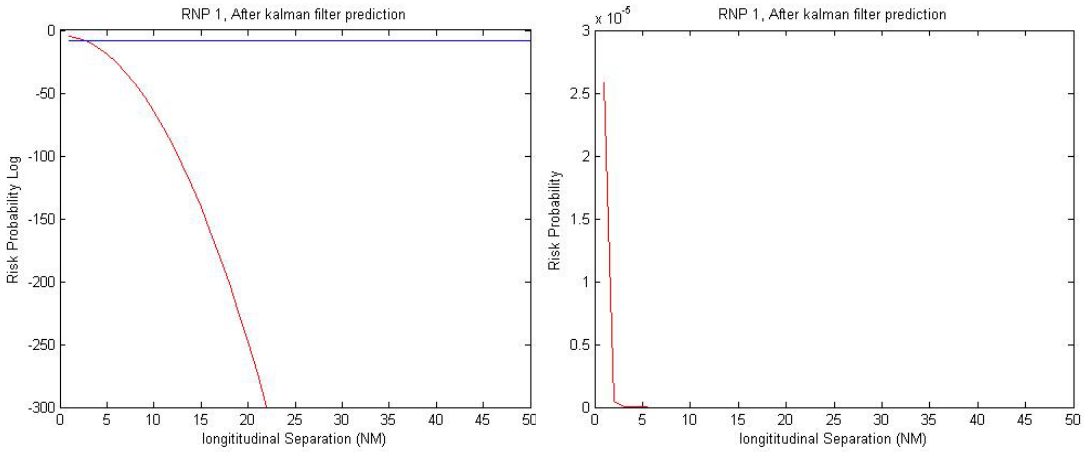

(a) Separation Minimum With Using Kalman filter

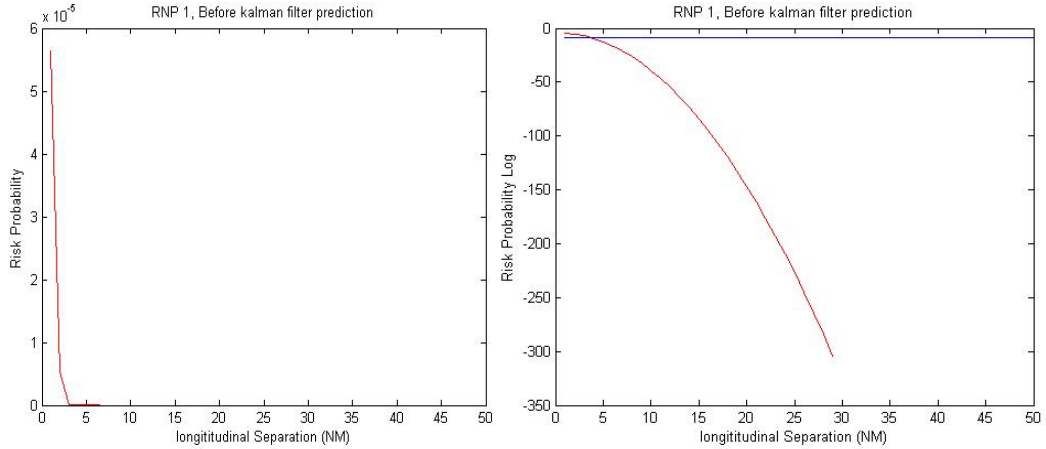

(b) Separation Minimum Without Using Kalman filter

Figure 5-6 Longitudinal Collision Risk Assessment with RNP 1

5.4.3 Vertical Collision Risk

Aircraft's position probability density in vertical plane is given by

$$P(z) = \frac{1}{\sqrt{2\pi}\sigma_z} e^{-\frac{z^2}{2\sigma_z^2}}$$

Vertical probability of overlap is shown as follow

$$P(S_0) = \int_{-\lambda_z}^{\lambda_z} \int_{-\infty}^{\infty} f^1(z) f^2((S_0 + |\bar{\dot{z}}| * (T + \tau)) + z_1 - z) dz_1 dz \quad \textbf{(5-3)}$$

Substituting equation 5-3 and the parameters in Table 5-2 into equation 3-9 Vertical collision risk probability is shown in Figure 5-7.

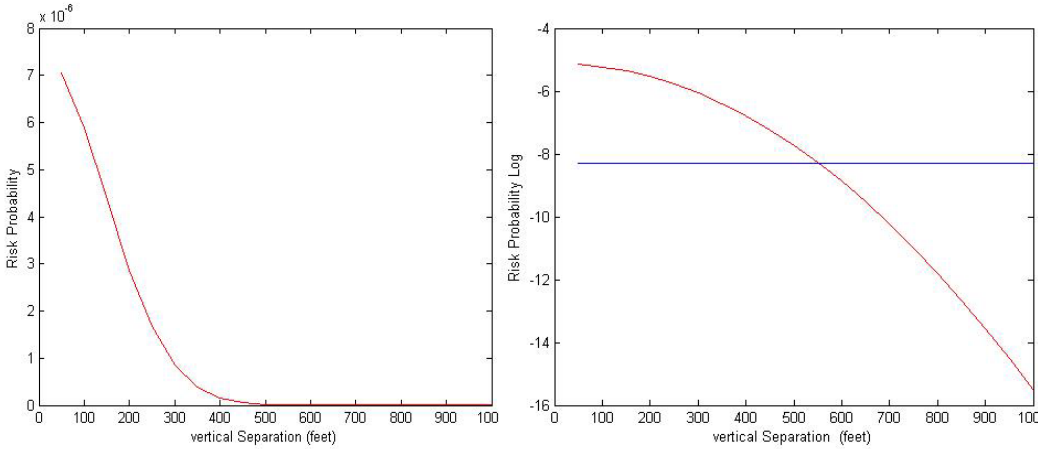

Figure 5-7 Vertical Collision Risk Assessment

From Figure 5-7, it can be seen that the separation minimum is 600 feet, which is smaller than 1000 feet regulated by ICAO.

The lateral, longitudinal and vertical separation minimums are summarized in Table 5-3 and Table 5-4.

Table 5-3 Separation Minimum for RNP 5

Separation Minimum	Not Using Kalman Filter and AS-B updating time	Using Kalman Filter and AS-B updating time
Lateral	18.4 NMI	14.2 NMI
Longitudinal	19.1 NMI	14.8 NMI
Vertical	1000 feet	600 feet

Table 5-4 Separation Minimum for RNP 1

Separation Minimum	Not Using Kalman Filter and AS-B updating time	Using Kalman Filter and AS-B updating time
Lateral	3.82 NMI	2.74 NMI
Longitudinal	3.9 NMI	2.89 NMI
Vertical	1000 feet	600 feet

5.5 Summary

This chapter has provided a case study of separation minimum safety assessment issues. Lateral, longitudinal and vertical separation minimums have been evaluated based on safety requirements. The main points of this chapter are summarized as follows:

1. Procedure of separation minimum safety assessment has been provided.

2. Parameters used in the Reich model have been offered, based on the historical observation data.

3. Separation minimum safety assessment has been carried out in horizontal and vertical planes. The results indicate that the paper provides a feasible method for safety assessment of parallel route separation minimum.

6 Conclusion and Future Work

6.1 Conclusion

Developments of the CNS systems and their effects on separation minimum assessment are discussed in this thesis. A Kalman filter prediction architecture, used to improve trajectory tracking performance, has been developed. Simulation results show that this architecture has a positive effect on the reduction of separation minimum.

The main contributions of this thesis are summarised as follows:

1. Performance-based CNS technologies, including RNP, RCP and RSP, are discussed. RNP is used to model the navigation errors as an input of the Kalman filter.

2. A Kalman filter prediction architecture is developed to improve trajectory tracking performance. In this filter, aircraft motion is considered as a constant velocity model. The simulation shows that trajectory tracking performance has been improved. As a result, the position uncertainty has been reduced.

3. Reich model is used to evaluate the collision risks in lateral, longitudinal and vertical planes, respectively. The results show that the method which is developed in the thesis can reduce separation minimum.

6.2 Future Work

Although, much work has been done in this thesis, further research is necessary in several areas.

1. Aircraft's motion, which is a constant velocity model in this thesis, can represent aircraft's dynamics most of the time. However, when aircraft turn or accelerate, this model has a large bias. Therefore, a multi dynamical model should be developed to describe different aircraft's motions.

2. The failure probability of CNS systems is not considered. In this thesis, an assumption that CNS systems do not fail during flight has been made, but this is not true. So, in the future, collision risk analysis should consider CNS failure modes.

3. The data used in the Reich model is based on the historical observation data. It is suggested that the collision risk evaluation should be updated with new data.

REFERENCES

[1] CAA Report, “Recent Trends in Growth of UK Air Passenger Demand", the United Kingdom’s Civil Aviation Authority, 17 March 2008.

[2] Galotti, V.P.J., “The Future Air Navigation System (FANS)” England: Ashgate Publishing Company Limited, 1999.

[3] FAA, “Instrument Procedure Handbook”, U.S. Department of Transportation, 2007

[4] Reich, P. G．”Analysis of Long—Range Air Traffic Systems：Separation Standards I”．Journal of the Institute of Navigation, 1966, Vol. 19, No. 1, pp. 88-96

[5] Reich, P. G．”Analysis of Long—Range Air Traffic Systems：Separation Standards Ⅱ”．Journal of the Institute of Navigation, 1966, Vol. 19, No. 2, pp. 169-176

[6] Reich, P. G．”Analysis of Long—Range Air Traffic Systems：Separation Standards Ⅲ”．Journal of the Institute of Navigation, 1966, Vol. 19, No. 3, pp. 331-338

[7] ICAO, “Air Traffic Services Planning Manual”, DOC 9426, ICAO, 1992

[8] Penna, D. M. “Longitudinal Separation of North Atlantic Air Traffic”, Civil Aviation Authority, London, 1977, Paper 77028

[9] Brooker, P., Lloyd, D. E. “Collision Risk and Longitudinal Separation Standards for North Atlantic Air Traffic” UK CAA DORA Communication 7801, Issue 2, CAA, London, 1978

[10] Moek, G., Lutz, E., Mosberg, W. “Risk assessment of RNP 10 and RVSM in the South Atlantic Flight Identification Regions”, ARINC Report, USA, 2001

[11] Zhang, Z., Liu, J., Shen, J., “Assessment of Collision Risk on Intersecting Tracks based on Communication Navigation Surveillance Performance”, 2010 2nd International Asia Conference on Informatics in Control, Automation and Robotics (CAR), 2010, pp.58-62

[12] Zhang, Z., Liu, J., “Assessment of Collision Risk of Vertical Separation Based on CNS Performance”, Journal of Civil Aviation University of China, 2010, Vol. 20, pp. 23-27

[13] Shen, J., Zhang, Z., Liu, J, “Study on the safe Separation on Given CNS Position errors and Parallel route”, Aeronautical Computing Technique, 2010, Vol. 13, pp.13-15

[14] Eurocontrol Report, “Radar Sensor Performance Analysis”, European Organization for the Safety of Air Navigation, 1997,

[15] Rockman, J. M., “A Preliminary Mathematical Model for the Radar Separation Minimum”, the MITRE Corporation, 1994

[16] Thompson, S. D., Andrews, J. W., Harris, G. S., Sinclair, K. A., “Required Surveillance Performance Accuracy to Support 3-Mile and 5-Mile Separation in the National Airspace System”, Project Report ATC-323, Washington: Federal Aviation Administration, 2006

[17] Nagaoka, S., Amai, O., Watanabe, Y., “Evaluating the Feasibility of a Radar Separation Minimum for a Long-Range SSR”, Journal of Navigation, 1989, Vol.42, pp.403-416

[18] Gazit, R.Y., Powell, J.D., “The Effect of GPS-based Surveillance on Aircraft Separation Standards”, Position Location and Navigation Symposium, IEEE, 1996, pp.360-367

[19] Jones, S. R., “ADS-B Surveillance Separation Error Sensitivity Analysis”, the MITRE Corporation, 2009

[20] Castle, M. W., Sleight, R., Handy, S. “Evaluation of Separation Performance with ADS-B at the LOUISVILLE KEY Site”, Digital Avionics Systems Conference, 2009. DASC '09. IEEE/AIAA 28th , 2009, pp.3.E.4-1 - 3.E.4-14

[21] Boeing Commercial Airplane Group, “Air Traffic Management Concept Baseline Definition”, NEXTOR Report # RR-97-3, the Boeing Company, October 31, 1997.

[22] ICAO, “ICAO annex 10”, ICAO, 1998

[23] ICAO, “Manual on HF Data Link”, DOC 9741, ICAO

[24] ICAO, “Manual on Required Communications Performance”, OPLINKP/1-WP/33, Version 5.1, 2002

[25] ICAO, “Performance-based Navigation (PBN) Manual”, DOC 9613, the third edition, 2008

[26] ICAO, “Manual on Required Navigation Performance (RNP)”, Doc 9613-AN/937, Second Edition, 1999

[27] ICAO, “Minimum aviation system performance standards for automatic dependent surveillance broadcast (ADS-B)”, DO-242A, June 25, 2002.

[28] ICAO, “Manual on Airspace Planning Methodology for the Determination of Separation Minima”, ICAO Doc 9689-AN/953, 1998

[29] White, B. E., “Tactical Data Links, Air Traffic Management, and Software Programmable Radios” Proceedings 18th Digital Avionics Systems Conference, 1999, Vol.1, pp. 5.C.5-1 - 5.C.5-8

[30] ICAO, “A Unified Framework for Collision Risk Modelling in Support of the Manual on Airspace Planning Methodology for the Determination of Separation Minima”, ICAO, DOC 9689, 2009

[31] Paielli, R. A., Erzberger, H., “Conflict probability estimation for free flight”, AIAA Journal of Guidance, Control, and Dynamics, May-June 1997, vol. 20, no.3, pp. 588-596

[32] Erzberger, H., Paielli, R. A., Isaacson, D. R., Eshow, M. M., “Conflict detection and resolution in the presence of prediction error”, 1st USA/EUR Air Traffic Management R&D Seminar, Saclay, France. June 1997.

[33] Yang, L., Kuchar, J., “Prototype conflict alerting logic for free flight”, AIAA Journal of Guidance, Control, and Dynamics, 1997, Vol. 20 no. 4, pp. 768-773,

[34] Besada Portas, J.A., Garcia Herrero, J., Jimenez Rodriguez, F.J., Casar Corredera, J.R., “Proceedings 17th Digital Avionics Systems Conference, 1998, pp.F43/1 -F43/9

[35] Da Silva, J.L.R., Brancalion, J.F.B., Fernandes, D., “Data Fusion Techniques Applied to Scenarios Including ADS-B and Radar Sensors for Air

Traffic Control", 12th International Conference on Information Fusion Seattle, WA, USA, July 6-9, 2009, pp.1481-1488
[36] Li, X.R., Jilkov, V.P., "Survey of maneuvering target tracking-part I: dynamic models," IEEE Transactions on Aerospace and Electronic Systems, October 2003, Vol.39(4), pp.1333-1364
[37] Lin, X., Zhang, J., Zhu, Y., Liu, W., "Simulation Study of Algorithms for Aircraft Trajectory Prediction Based on ADS-B Technology", Asia Simulation Conference - 7th International Conference on System Simulation and Scientific Computing, 2008, pp.322 - 327
[39] Zhou, H., Kumar, S. P., "A 'current' statistical model and adaptive algorithm for estimating manoeuvring targets", AIAA Journal of Guidance, Control, and Dynamics, Sept.–Oct. 1984, Vol. 7, no. 5, pp. 596–602
[40] Singer, A. R., "Estimating Optimal Tracking Filter Performance for Manned Manoeuvring Targets", IEEE Transactions on Aerospace and Electronic Systems, 1970, Vol. AES-6, pp. 473 - 483
[41] Baud, O., Honore, N., Taupin, O., "Radar / ADS-B data fusion architecture for experimentation purpose", Proceedings of the 9th International Conference on Information Fusion, 2006, pp.1-6.
[42] European Organisation for the Safety of Air Navigation, "Guidance Material for the Flight Inspection of RNAV Procedures", EUROCONTROL, second edition, May 2005.
[43] Harrison, D., Moek, G., "Studies to Investigate the Feasibility of using 1000ft Vertical Separation Minima above FL290, Part II Precision Radar Data Analysis and Collision Risk Assessment". Journal of Navigation, 1992, Vol. 45, pp. 91-106
[44] Moek, G., Smeltink, J. W., "Pre-Implementation Collision Risk assessment for RVSM in the Africa Indian Ocean Region", NLR-CR-2007-637, National Aerospace Laboratory, 2007

APPENDIX A

WGS-84 Parameters

Parameters	Notation	Value
Semi-major axis	R_a	$6378137\ m$
Normalized	C20	-484.16685×10^{-6}
Flattening (ellipticity)	f	$1./298.257223563$
Semi-minor axis	R_b	$R_b = R_a(1-f)$ $= 6356752.3142\ m$
Eccentricity squared	e^2	$e^2 = f(2-f)$ $= 6.69437999013\times10^{-3}$
Angular velocity of the Earth	Ω	7.292115×10^{-5} rad/s
The Earth's gravitational constant	GM	$3986004.418\times10^8\ m^3/s^2$
Gravity at the equator	g_0	$9.780373\ m/s^2$
Gravity formula constant	g_1	0.00193185138639
Velocity of light	C	$299792458\ m/s$

APPENDIX B

Phases of Flight

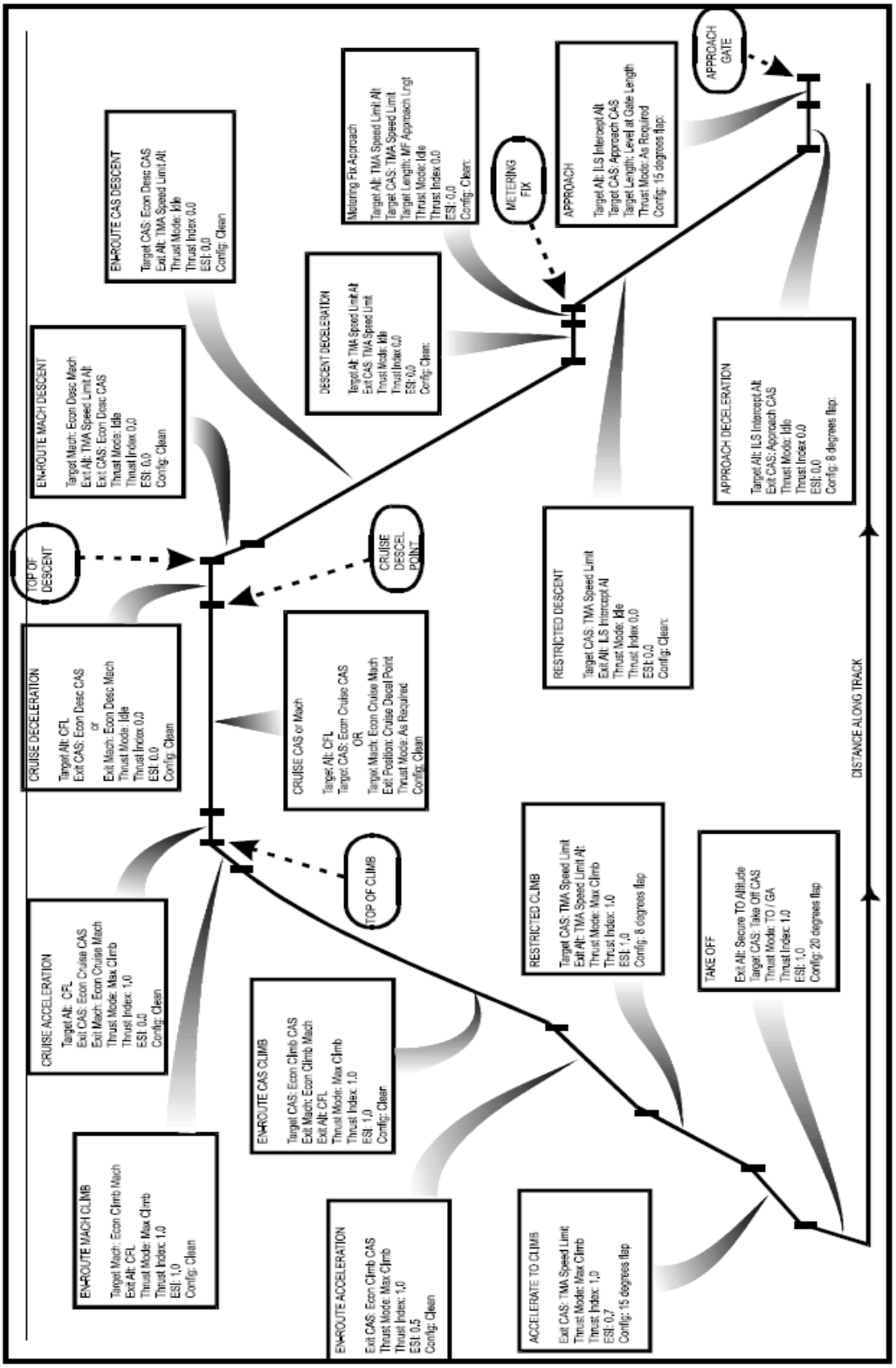

APPENDIX C

1. Trajectory Function MATLAB Program.

```
function [X,Y]=trajectory(T,Time,flag)
% Generate True Trajectory[X,Y]£¬
% T is Update Time
% Time is simulation time
% flag=1 constant velocity, flag=0 acceleration
Number=ceil(Time/T);
flag=1;
% initialize the position m
x0=5000;
y0=0;
% aircraft velocity vx, vy m/s
vx=250;
vy=0;
% accelaration ax, ay m/s*s
ax=5;
ay=0;
%true trajectory
x=zeros(Number,1);
y=zeros(Number,1);
%measured trajectory
X=zeros(Number,1);
Y=zeros(Number,1);
% Genegrated Trajectory
if flag==1
    for i=1:1:Number
        x(i)=x0+vx*i*T;
        y(i)=y0+vy*i*T;
    end
end
```

```
else
      for i=1:1:Number
         x(i)=x0+vx*i*T+0.5*ax*T*T;
         y(i)=y0+vy*i*T+0.5*ay*T*T;
      end
end
% measured trajectory without measured noise
for i=1:1:Number
   X(i)=x(i);
   Y(i)=y(i);
end
```

2. Kalman Filter Function MATLAB Program.

```
function XE=Kalman_filter(Ts,offtime,d,Flag)
% Kalman_filter
% XE                    Estimated value
% Ts                    ADS-B updating time
% offtime               Simulation time
% d                     Variance of measured noise
% Flag                  Flag=1 x axis, Flag=0 y axis
N=ceil(offtime/Ts);
Pv=d*d;
% Process Noise
sigma=1;
% initialize the Kalman filter state
Phi=[1,Ts;0,1];
Gamma=[Ts*Ts/2;Ts];
C=[1 0];
R=Pv;
Q=sigma^2;
Xest=zeros(2,1);
Xfli=zeros(2,1);
Pxe=zeros(2,1);
```

```
Px=zeros(2,1);
XE=zeros(1,N);
% Generate true trajectory
[x,y]=trajectory(Ts,offtime);
  zx(1)=x(1);
  zy(1)=y(1);
% Generate measured trajectory
for i=2:N
  vx(i)=d*randn(1);
  vy(i)=d*randn(1);
  zx(i)=x(i)+vx(i);
  zy(i)=y(i)+vy(i);
end
% Kalman filter prediction
switch Flag
   case 0
      Xfli=[zx(2) (zx(2)-zx(1))/Ts]';
      Px=[Pv,Pv/Ts;Pv/Ts,2*Pv/Ts+Ts*Ts*Q/4];
      K=Phi*Px*C'*inv(C*Px*C'+R);
      for k=3:N
      Xfli=Phi*Xfli+K*(zx(k-1)-C*Xfli);
      K=Phi*Px*C'*inv(C*Px*C'+R);
      Px=(Phi-K*C)*Px+Gamma*Q*Gamma';
      XE(k)=Xfli(1,1);
      end
      XE(1)=zx(1);XE(2)=zx(2);
   case 1
      Xfli=[zy(2) (zy(2)-zy(1))/Ts]';
      Px=[Pv,Pv/Ts;Pv/Ts,2*Pv/Ts+Ts*Ts*Q/4];
      K=Phi*Px*C'*inv(C*Px*C'+R);
      for k=3:N
      Xfli=Phi*Xfli+K*(zy(k-1)-C*Xfli);
```

```
        K=Phi*Px*C'*inv(C*Px*C'+R);
        Px=(Phi-K*C)*Px+Gamma*Q*Gamma';
        XE(k)=Xfli(1,1);
        end

        XE(1)=zy(1);XE(2)=zy(2);
    otherwise
        error('False iuput nargin');
end
```

3. Result Function MATLAB Program.

```
%function [XER,YER]=filter_result(RNP,Ts,mon)
% filter_result
% Ts                ADS-B updating time
% mon               Monte-Carlo repeated times
% d                 variance of measured error
%XER, YER estimated value
clc;
%position measured noise variance
d=0.3*RNP*1852
% Generate true trajectory
[x,y]=trajectory(Ts,offtime);
Pv=d*d;
N=ceil(offtime/Ts);
randn('state',sum(100*clock));
% Measured value
for i=1:N
   vx(i)=d*randn(1);
   vy(i)=d*randn(1);
   zx(i)=x(i)+vx(i);
   zy(i)=y(i)+vy(i);
end
for n=1:mon
```

```
    % Kalman filter
    XE=Kalman_filter(Ts,offtime,d,0);
    YE=Kalman_filter(Ts,offtime,d,1);
    % Variance of filter
    XER(1:N,n)=x(1:N)-(XE(1:N))';
    YER(1:N,n)=y(1:N)-(YE(1:N))';
end
for i=1:1:N
    xstd=0;
    ystd=0;
    for j=1:1:mon
        xstd=xstd+XER(i,j)*XER(i,j);
        ystd=ystd+YER(i,j)*YER(i,j);
    end
    XSTD(i)=sqrt((1/mon)*xstd);
    YSTD(i)=sqrt((1/mon)*ystd);
end
%plot result
figure
plot(x,y,'r');hold on;
plot(zx,zy,'g');hold on;
plot(XE,YE,'b');hold off;
xlabel('x distance m'),grid on;
ylabel('y distance m'),grid on;
legend('True Trajectory','Measured Trajectory','Estimated Trajectory');
 figure
plot(zy,'r');hold on;
plot(YE,'b');hold off;
figure
plot(XSTD)
xlabel('T time s'),grid on;
ylabel('X Deviation m'),grid on;
```

```
figure
plot(YSTD)
xlabel('T time s'),grid on;
ylabel('Y Deviation m'),grid on;
```

APPENDIX D

(Group Design Programme Main Results)

1. Introduction

1.1 General Introduction

The objective of this year's Group Design Project (GDP) is the extension design from last group for a new civil transport aircraft. This aircraft, which was named "Flying crane", should have the following requirements:

- Aimed market: Regional jet airliner
- Seating capacities: 100 ~ 130
- Competitor: B737, A319
- Low cost
- Comfortable
- Reliable

1.2 Task Allocation

Autonomous Traffic Collision Detection and Avoidance System (ATCDAS) Design

- ATCDAS function and safety requirements, including AWAE
- ATCDAS architecture design
- Collision detection and avoidance algorithms
- Software design (C or Ada)
- ATCDAS simulation and evaluation

- Safety assessment
- Integration of ATCDAS software into Net-ASS

Terrain and Weather Surveillance Systems Design (TWSS)

- Analyse and define function and safety requirements of terrain and weather surveillance systems, including AWAE
- Integrated weather, traffic and terrain warning surveillance system architecture design
- Integrated weather and terrain warning surveillance systems designs, such as Terrain Awareness/Warning System (TAWS)
- Terrain detection and avoidance algorithm development
- Simulation and evaluation of terrain detection systems
- Evaluate system performance according to certification regulations, required surveillance performance
- Safety assessment
- Integration of terrain detection and avoidance software into Net-ASS

1.3 Avionics System Design Process

According to ARP (Aerospace Recommended Practice) 4754 requirement, system development process goes concurrently with safety assessment process. With the output from conceptual design, aircraft level requirements and FHA respectively, preliminary design starts with system level function allocation and FHA, then the stage goes further to system architecture and PSSA, which would be the input of detail design.

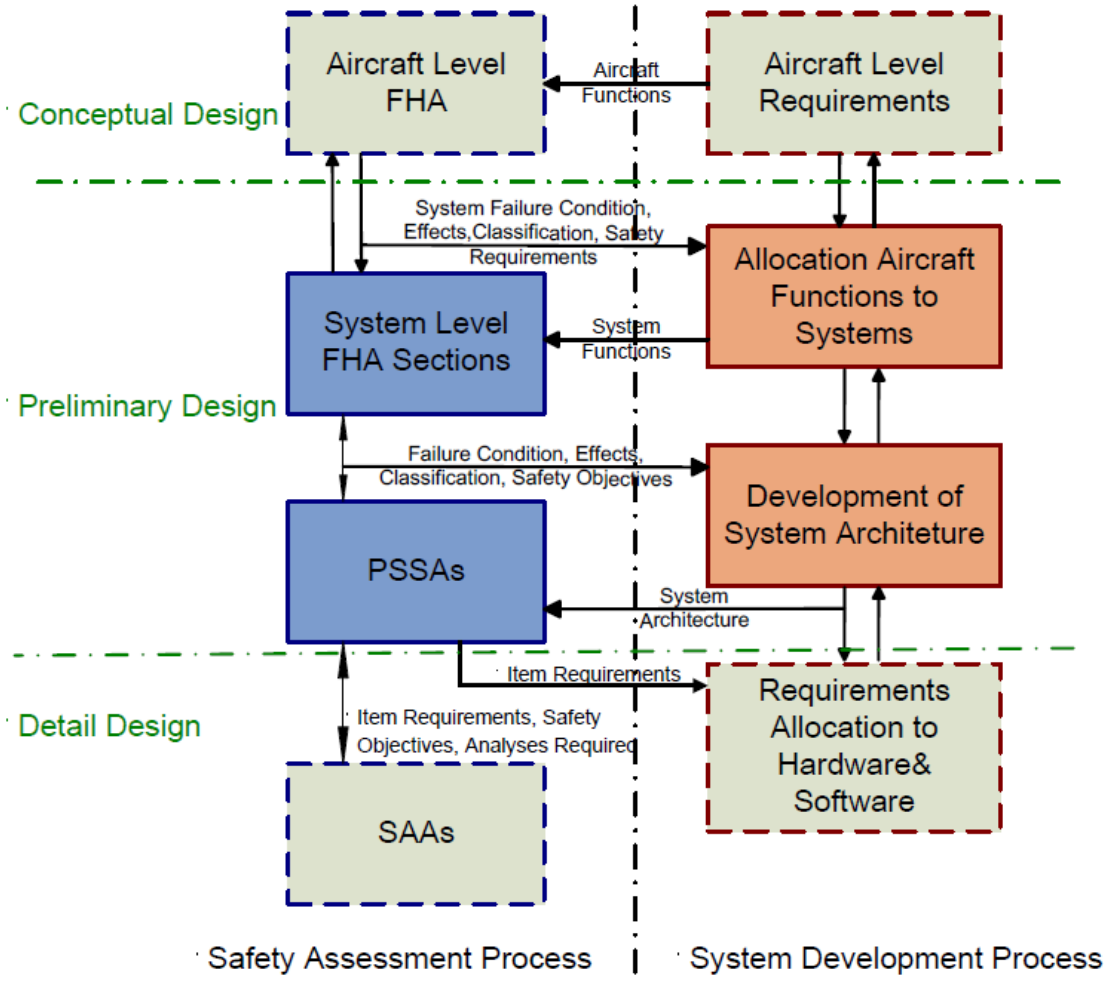

Figure 1 System Design Process

2. Integrated Surveillance System Design

Surveillance is defined as the detection, tracking, characterization, and observation of aircraft, other vehicles, weather and airspace status information and phenomena for the purposes of conducting flight operations in a safe and efficient manner. Design of the surveillance system of flying crane based on the concept of integration. This new, highly integrated system combines weather detection, traffic alert and collision avoidance, terrain awareness and warning functions into a single system.

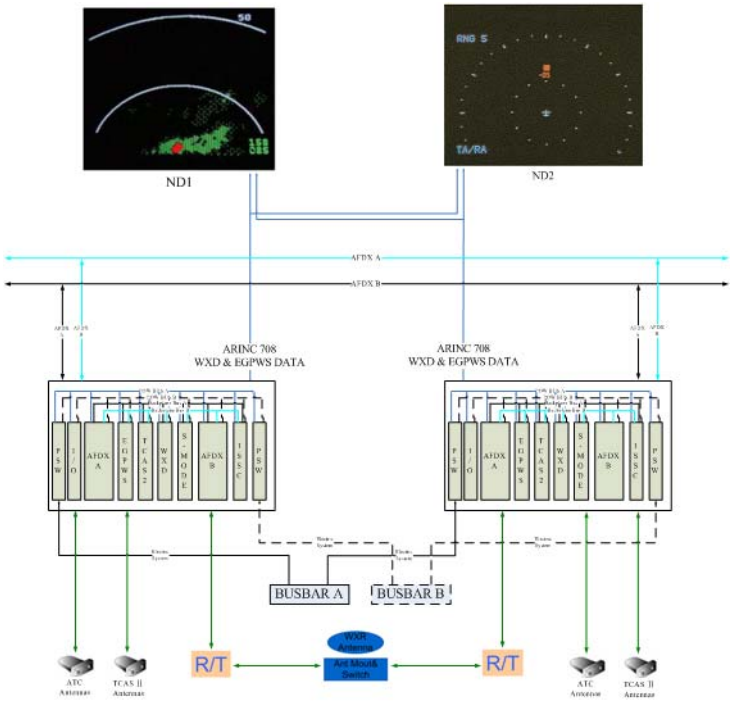

Figure 2 Surveillance System Architecture

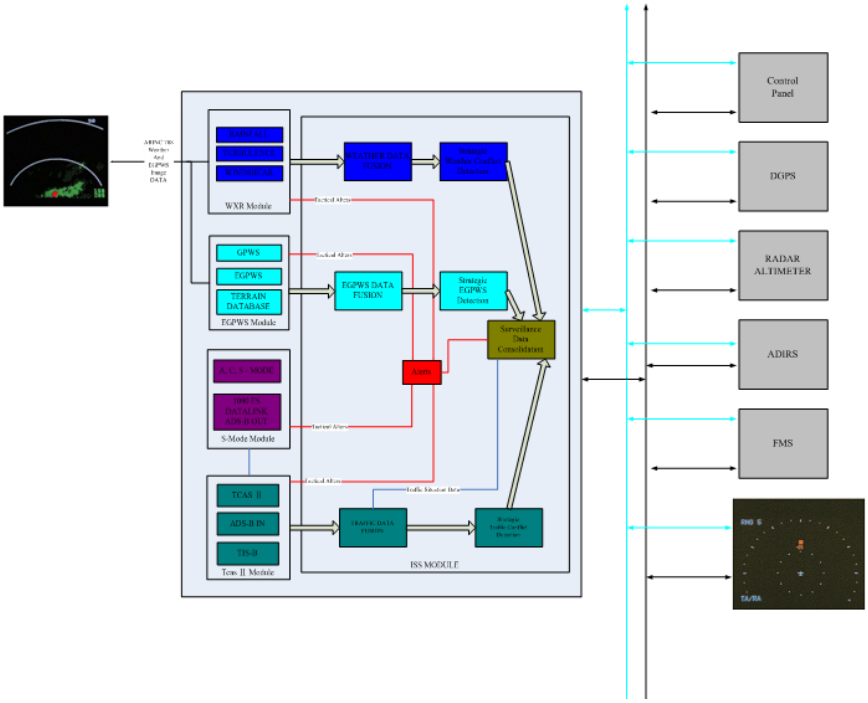

Figure 3 Surveillance System Data fusion Architecture

3. Conflict Detection and Resolution System Design

3.1 Introduction

In the early days of flying, all pilots navigated using ground features such as roads, rail tracks and coastlines.

Adequate collision avoidance for aircraft has been sought for many years and has evolved into its present form as TCAS IV.

TCAS has been extensively analysed, for example by the Radio Technical Commission for Aviation (RTCA). TCAS exchanges information using transponders between aircraft in danger of collision and provides resolution advisory information to the flight crew.

TCAS I1 and its proposed successor TCAS IV use a simple threat detection zone around each aircraft and determines a manoeuvre that ensures adequate separation even if one of the aircraft does not manoeuvre. This provides safe separation even if the link to one aircraft fails. TCAS can provide for non-TCAS aircraft or failure in communications by negotiating sense reversals when the original advisories have been thwarted.

TCAS has some limitations, which are recognised in the literature. For example, it has limited ability to deal with multiple aircraft and the domino effect, where the motion of one aircraft during avoidance affects the other aircraft in the same area. Ongoing work on TCAS is improving its accuracy after implementation.

The premise of this paper is that TCAS has a major weakness in providing aircraft with a very late method of avoiding annihilation. Unlike the proposed method using ADS-B, the information obtained for each aircraft is limited and, thus, the ability to make informed decisions is limited.

The RTCA recognised that advances are needed to improve collision avoidance as packing density increases. They recommend better use of prior knowledge and the need to push the event horizon further.

3.2 TCAS

Traffic alert and collision avoidance system (both abbreviated as TCAS) is an aircraft collision avoidance system designed to reduce the incidence of mid-air collisions between aircraft. It monitors the airspace around an aircraft for other aircraft equipped with a corresponding active transponder, independent of air traffic control, and warns pilots of the presence of other transponder-equipped aircraft which may present a threat of mid-air collision (MAC). It is a type of airborne collision avoidance system mandated by the International Civil Aviation Organization to be fitted to all aircraft with a maximum take-off mass (MTOM) of over 5700 kg (12,586 lbs) or authorized to carry more than 19 passengers.

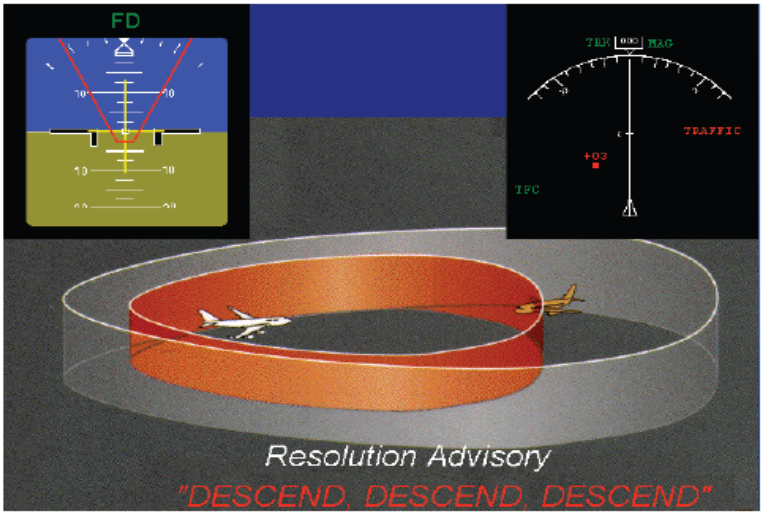

Figure 4 TCAS Model

3.2.1 TCAS- Ⅰ

TCAS I is the first generation of collision avoidance technology. It is cheaper but less capable than the modern TCAS II system, and is mainly intended for general aviation use. TCAS I systems are able to monitor the traffic situation around a plane (to a range of about 40 miles) and offer information on the approximate bearing and altitude of other aircraft. It can also generate collision warnings in the form of a "Traffic Advisory" (TA). The TA warns the pilot that another aircraft is in near vicinity, announcing "traffic, traffic", but does not offer any suggested remedy; it is up to the pilot to decide what to do, usually with the

assistance of Air Traffic Control. When a threat has passed, the system announces "clear of conflict".

3.2.2 TCAS-II

TCAS II is the second and current generation of instrument warning TCAS, used in the majority of commercial aviation aircraft. It offers all the benefits of TCAS I, but will also offer the pilot direct, vocalized instructions to avoid danger, known as a "Resolution Advisory" (RA). The suggestive action may be "corrective", suggesting the pilot change vertical speed by announcing, "Descend, descend", "climb, climb" or "Adjust Vertical Speed Adjust" (meaning reduce vertical speed). By contrast a "preventive" RA may be issued which simply warns the pilots not to deviate from their present vertical speed, announcing, "Monitor vertical speed" or "maintain vertical speed". TCAS II systems coordinate their resolution advisories before issuing commands to the pilots, so that if one aircraft is instructed to descend, the other will typically be told to climb - maximising the separation between the two aircraft.

3.2.3 TCAS-III

TCAS III was the "next generation" of collision avoidance technology which underwent development by aviation companies such as Honeywell. TCAS III incorporated technical upgrades to the TCAS II system, and had the capability to offer traffic advisories and resolve traffic conflicts using horizontal as well as vertical manoeuvring directives to pilots. For instance, in a head-on situation, one aircraft might be directed, "turn right, climb" while the other would be directed "turn right, descend." This would act to further increase the total separation between aircraft, in both horizontal and vertical aspects. Horizontal directives would be useful in a conflict between two aircraft close to the ground where there may be little if any vertical manoeuvring space. All work on TCAS III is currently suspended and there are no plans for its implementation.

3.2.4 ADS-B

An ADS-B-equipped aircraft determines its own position using a global navigation satellite system and periodically broadcasts this position and other relevant information to potential ground stations and other aircraft with ADS-B-in equipment. ADS-B can be used over several different data link technologies, including Mode-S Extended Squitter (1090 ES) operating at 1090 MHz, Universal Access Transceiver (978 MHz UAT), and VHF data link (VDL Mode 4).

ADS-B provides accurate information and frequent updates to airspace users and controllers, and hence supports improved use of airspace, reduced ceiling/visibility restrictions, improved surface surveillance, and enhanced safety, for example through conflict management.

Under ADS-B, an aircraft periodically broadcasts its own state vector and other information without knowing what other aircrafts might be receiving it, and without expectation of an acknowledgment or reply. ADS-B is automatic in the sense that no pilot or controller action is required for the information to be issued. It is dependent surveillance in the sense that the surveillance-type information so obtained depends on the suitable navigation and broadcast capability in the source aircraft. International aviation standards for the individual ADS-B data link technologies have been standardized by the International Civil Aviation Organization (ICAO).

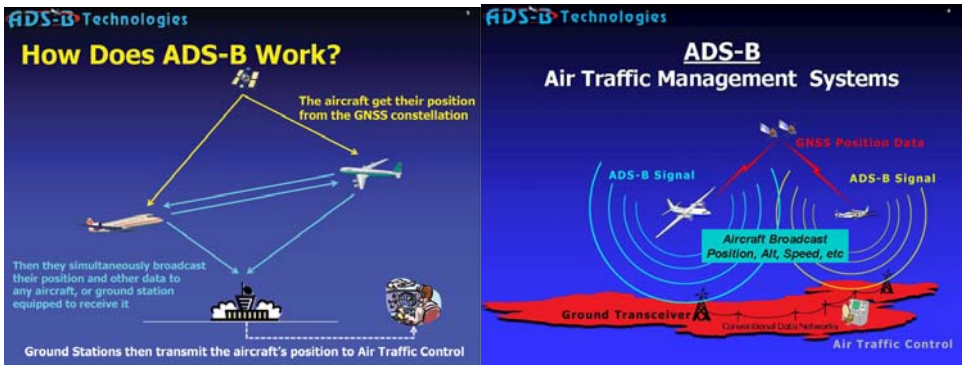

Figure 5 ADS-B Architecture

Table 1 ADS-B data

Number of bits	Contents
5	Format type code
2	Surveillance status
1	Single antenna flag
12	Altitude
1	Time
1	CPR format
17	CPR encoded latitude
17	CPR encoded longitude
56 bits total	

Number of bits	Contents
5	Format type code
7	Movement
1	Status
7	Ground track
1	Time
1	CPR format
17	CPR encoded latitude
17	CPR encoded longitude
56 bits total	

Number of bits	Contents
5	Format type code
3	Subtype
1	Intent change flag
1	IFR capability flag
3	Velocity uncertainty
10 + 1	East-West velocity + sign
10 + 1	North-South velocity + sign
9 + 1 + 1	Vertical rate + sign + source
2	Turn indicator
7 + 1	Geometric height diff. from barometric + sign
56 bits total	

Number of bits	Contents
5	Format type code
3	Aircraft category
6	Callsign Character 1
6	Callsign Character 2
6	Callsign Character 3
6	Callsign Character 4
6	Callsign Character 5
6	Callsign Character 6
6	Callsign Character 7
6	Callsign Character 8
56 bits total	

Number of Bits	Contents
5	Format Type = 29
2	SubType=0
18	Target Altitude and Flags
14	Target Heading/Track
7	NACp, NICb, SIL
5	Reserved
2	ACAS status and RA status
3	A/c emergency/priority status
56	Total

3.2.5 TIS-B

TIS-B is the broadcast of traffic information to ADS-B-equipped aircraft from ADS-B GBTs. The source of this traffic information is derived from air traffic surveillance radars. TIS-B is intended to provide ADS-B-equipped aircraft with a more complete traffic picture in situations where not all nearby aircraft are equipped with ADS-B. This advisory-only application will enhance a pilot's visual acquisition of other traffic. TIS-B service is becoming available in selected locations where there is both adequate radar surveillance coverage and adequate broad-cast coverage from GBTs.

3.3 Conflict Detection and Resolution Architecture

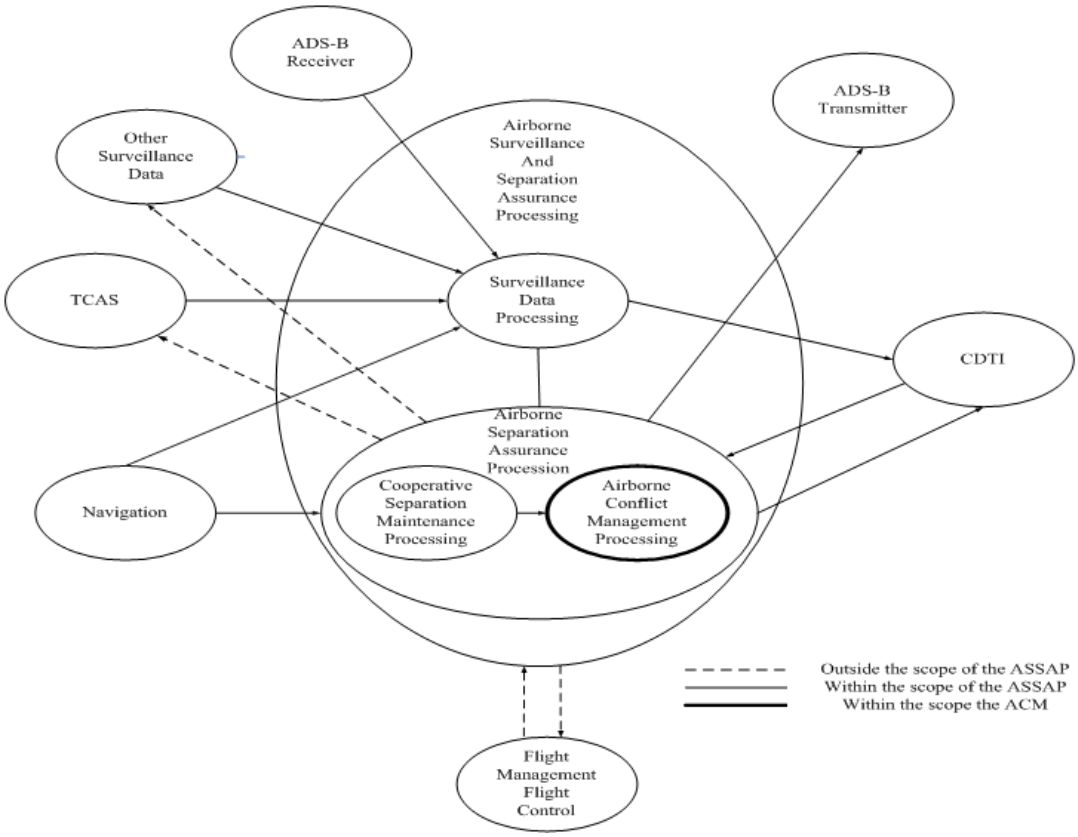

Figure 6 Conflict Detection and Resolution Architecture

3.4 Conflict Detection and Resolution Algorithm

The algorithm generates resolution trajectories in several steps that include iteration loops, as seen in Fig. The input to the algorithm is data for a pair of aircraft that a conflict detection system predicts will lose separation within a time interval of interest. The time to first loss must also be provided. This time is a parameter of great importance to the resolution process. The time to first loss (TFL) is a relative time defined as the difference between the time when separation is predicted to be lost and the current time. TFL plays a crucial role in determining the priority of a conflict relative to other conflicts. It can also influence the resolution strategy.

The detection system must also provide similarly detailed information for other conflicts (referred to as secondary conflicts) that are predicted to occur downstream of the primary conflict. These secondary conflicts must also be resolved if they will involve either of the two primary conflict aircraft and if they

occur within a specified TFL. Secondary conflicts, which occur with increased frequency in dense traffic, add complexity to the resolution process.

Other inputs to the algorithm are manoeuvre constraints. These constraints, if they are active, specify the types of manoeuvre s that should not be used for resolution. Avoidance of nearby airspace boundaries, weather cells, and turbulence may necessitate such constraints. Another type of constraint can exclude one of the aircraft from being chosen as the manoeuvre aircraft such as a descending aircraft close to an arrival fix.

The Resolution Aircraft and Manoeuvre Selector (RAMS) orchestrate the resolution process. As the first step, RAMS identifies the type of the conflict by matching its characteristics against a master set of all conflict types. (The types included in the set will be described in the next section.) Once the conflict type has been established, RAMS has sufficient information to select both the preferred manoeuvre aircraft and the preferred resolution manoeuvre . In addition to these preferred solutions, RAMS determines a set of alternative resolution manoeuvre s and associated manoeuvre aircraft. Finally, RAMS prioritizes these alternative sequences by assigning preference rankings to the alternative manoeuvre s and to the associated manoeuvre aircraft. Higher priority is given to those manoeuvre s that are generally known to create less delay, and that deviate less from the nominal flight plan trajectory or, if delay is not a significant factor, to those manoeuvre s that follow rules controllers would typically use to resolve a similar type of conflict. The set of prioritized manoeuvre s serves as a reservoir for choosing alternative resolutions when a particular preferred resolution fails to resolve a conflict, or when it is found to be deficient for any of several reasons described below.

The prioritized set of resolution manoeuvre types and associated resolution aircraft provide the input to the Resolution Manoeuvre Generator (RMG) shown in Fig. RMG contains a collection of analytical formulae and heuristics for calculating the parameters of a simplified resolution trajectory for any manoeuvre type specified by RAMS. RMG also contains rules and procedures for choosing the coordinates of the return waypoint, which is defined as the

point where the resolution trajectory merges back onto the original flight plan trajectory.

This point can be located far down range if no constraints are violated. The simplified trajectories serve as templates that provide essential input data from which the complete 4D resolution trajectories can be calculated.

The next step in the resolution process is to generate the complete 4D trajectory that corresponds to input data provided by RMG. This function is performed by a complex algorithm referred to as a 4D trajectory synthesizer (TS). It uses detailed models of aircraft performance, operational procedures, and the atmosphere, including winds aloft, to generate the 4D trajectories that the resolution aircraft can actually fly. This process is computationally and logically complex, because it involves integrating point mass aircraft equations of motion that use models of drag and thrust adapted for each aircraft type.

The RMG thus sends the parameters it calculates for the initially selected manoeuvre.

A conflict check of the trial resolution trajectory is necessary for two reasons:

First, to verify the trial resolution trajectory has successfully resolved the original (primary) conflict. Verification is necessary because the simplifications, approximations and rules of thumb used by the RMG can introduce significant differences between the trial resolution manoeuvre and the accurately computed 4D trajectory produced by TS. These differences can result in the primary conflict remaining unresolved in the trial resolution trajectory.

Second, to rule out the possible presence of secondary conflicts (which are illustrated in Fig. A conflict caused by a third aircraft whose trajectory intersects the trajectory of the primary conflict downstream is referred to as a downstream secondary conflict. Downstream secondary conflicts are encountered more frequently as the time horizon for conflict detection or the density of traffic is increased. A conflict involving a fourth aircraft found along the trial resolution trajectory is referred to as a trial resolution secondary conflict. Trial resolution

secondary conflicts can arise along any trial trajectory, since each resolution is designed to resolve only the primary conflict.

If the trial resolution trajectory is free of conflicts for the specified resolution time horizon, the algorithm promotes the trial resolution trajectory to the status of acceptable resolution trajectory. The ground system can now uplink this trajectory to the conflict aircraft and, after receiving a “will comply” message back from the aircraft, update the data base of currently approved 4D trajectories for aircraft in the resolution airspace.

If the trial resolution trajectory is found to have conflicts within the specified resolution time horizon, a fault message along with appropriate diagnostic information is sent back to the RMG, which will pick the next-in-priority trial resolution manoeuvre and send it to the TS for synthesizing another trial trajectory. This iterative process continues until either an acceptable resolution trajectory is found or the reservoir of available trial resolution manoeuvre s is exhausted. If no resolutions are found, the RMG has additional methods to extend the search for resolutions as described below.

Two parameters in the RMG are used to exercise control over the resolution process and to search for additional resolutions. The first parameter is the resolution initiation time horizon (RIH) and the second is the conflict free time horizon (CFH).

The RIH is defined as the earliest time before loss of separation is predicted to occur when a conflict first becomes eligible for resolution. For conflicts predicted by the CD, to the non-preferred aircraft and the corresponding sequence of trial manoeuvre s are given for a few important conflict types. This table is a simplified representation of the logic coded into RAMS.

An examination of the preferences listed in the second column of Table 1 reveals that for non-arrival conflicts, altitude changes are favoured over horizontal and speed changes as the preferred initial choice for resolution manoeuvre s. This strategy is referred to as an altitude-first resolve as

distinguished from a horizontal-first resolve. A comparison of average delays obtained for these two strategies in fast-time simulations revealed a significant advantage in delay reduction for the altitude-first resolve. Thus, whenever circumstances permit and no manoeuvre constraints are violated, all feasible altitude manoeuvre s will be tried first for the preferred aircraft and then for the non-preferred aircraft before horizontal manoeuvre s are tried for either aircraft. Resolution strategies vary considerably among controllers, with some favouring horizontal and some favouring vertical resolutions. An advantage of an automated algorithm is the ability to implement a strategy that provides consistent efficiency benefits. An exception to the altitude-first rule is made for encounters where one of the conflict aircraft is a descending arrival. For such encounters, a horizontal manoeuvre referred to as a path stretch is used (this is explained in the next section). Finally, it should be mentioned that the software gives users the option of specifying either of the two strategies.

The preferred resolution manoeuvre s used to resolve arrival vs. arrival conflicts converging onto a common fix were chosen to be similar to the proposed trajectories used to control arrival traffic onto a metering fix. The table distinguishes between several types of arrival vs. arrival conflicts. If both arrivals are in cruise, then speed changes in cruise and/or in descent are the preferred manoeuvre s. For these cases, the sequence order at the arrival fix helps determine the preferred manoeuvre aircraft. If only one aircraft is in cruise at the time.

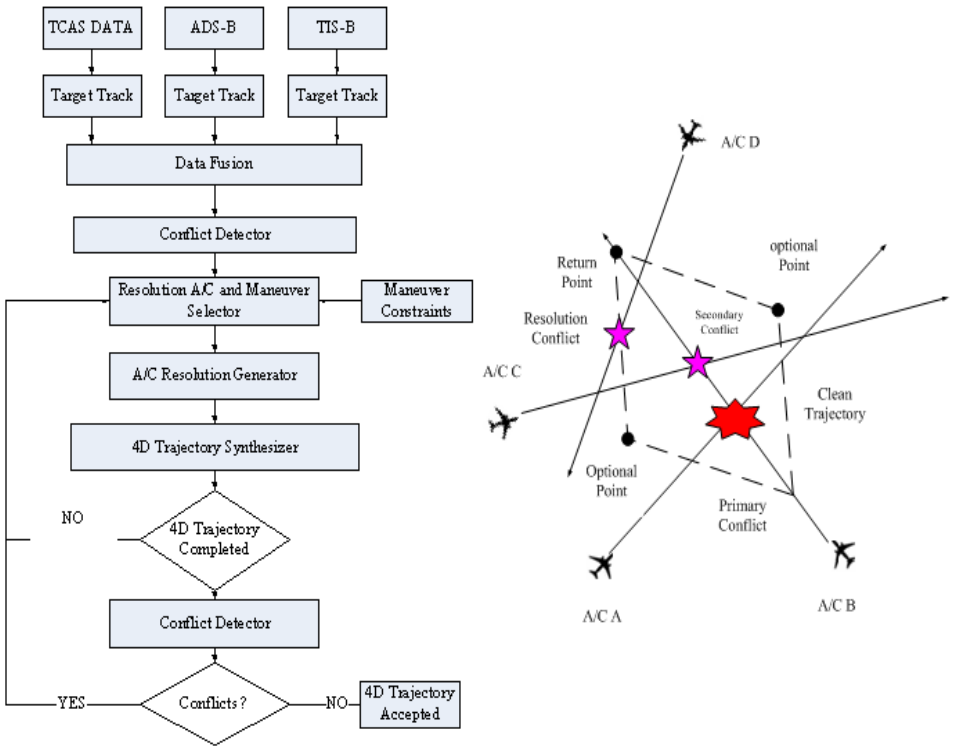

Figure 7 Conflict Detection Theory

3.5 Resolution

Consider two aircraft, A and B, with known positions, flying at the same flight level in a uniform wind field. The aircraft airspeeds are constant and known. The aircraft headings and the wind field are also known, so that ground speeds and tracks may be calculated. Let the position vectors be rA and rB and define the line-of-sight (LoS) vector as

$$\mathbf{s} = \mathbf{r}_B - \mathbf{r}_A$$

If the (ground) velocity vectors of the aircraft are vA and vB, define the relative velocity vector as

$$\mathbf{v}_R = \mathbf{v}_A - \mathbf{v}_B$$

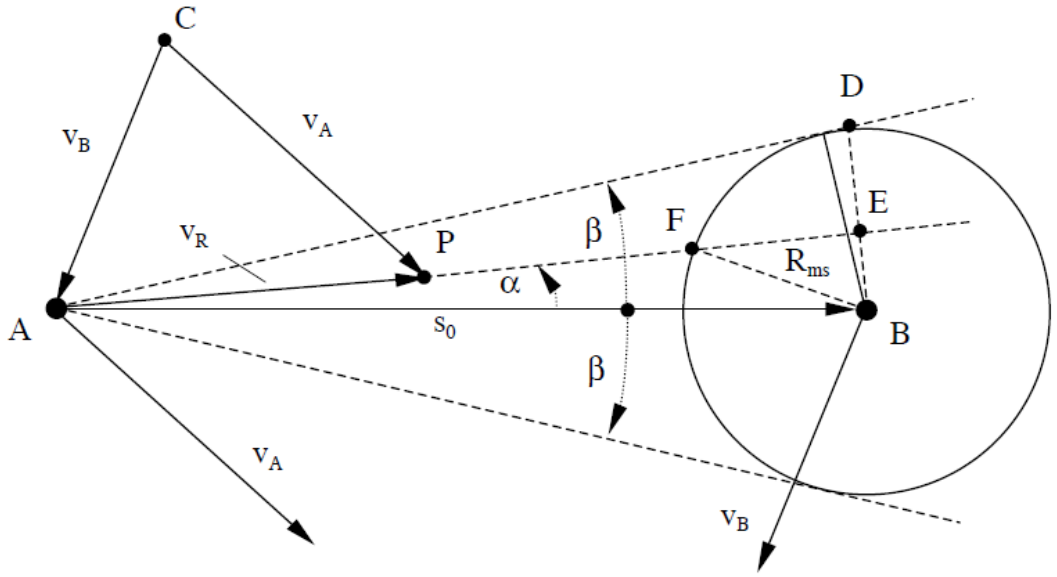

Figure 8 Position and velocity geometry for a level conflict scenario

Conflict Parameters:

$$\beta = \pm \sin^{-1}(R / S_0)$$

$$S_0 = [(X_B - X_A)^2 + (Y_B - Y_A)^2]^{1/2}$$
$$\psi_0 = \tan^{-1}((Y_B - Y_A) / (X_B - X_A))$$

$$\psi_R = \tan^{-1}(N / E)$$
$$V_R = (N^2 + E^2)^{1/2}$$
$$N = V_A \sin\psi_A - V_B \sin\psi_B$$
$$E = V_A \cos\psi_A - V_B \cos\psi_B$$

$$R_{ms} = S_0 \sin\alpha; t_{ms} = S_0 \sin\alpha / V_R$$

$$d_{AF} = S_0 \cos\alpha - (R^2 - R_{ms}{}^2)^{1/2}$$
$$t_{AF} = d_{AF} / V_R$$

$$t_{AF} = d_A / V_A$$
$$t_{AF} = d_B / V_B$$

Resolution schemes that have one aircraft making a heading change have been devised. These may be preferable to providing simultaneous advisories to both aircraft in conflict. Refer to the expanded velocity diagram of Fig, where the information shown in Fig has been simplified. This diagram makes it possible to easily visualize a resolution performed by aircraft A, either by turning ccw (vector vA rotates about point C) until the relative velocity vector lines up with the upper dashed tangent line at point c, or turning cw until the relative velocity vector lines up with the lower dashed line at point e. Notice that in this example, A is the faster aircraft: there will be one valid solution for each tangent line.

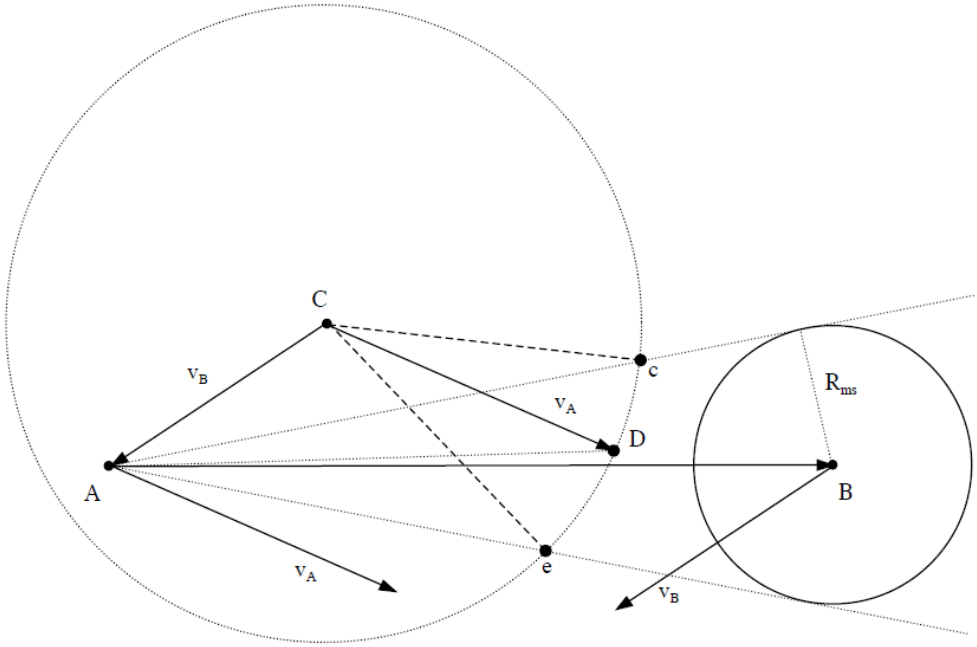

Figure 9 Heading changes for aircraft A to resolve a conflict

The resolved heading for the faster aircraft is obtained by applying the Law of Sines to the new velocity triangle (either ACc or ACe). The result is

$$V_A / \sin(\psi_B - \psi_R^*) = V_B / \sin(\psi_A^* - \psi_R^*)$$

$$\psi_A^* = \psi_R^* + \sin^{-1}[\frac{V_B}{V_A}\sin(\psi_B - \psi_R^*)]$$

3.6 Simulation

3.6.1 Trajectory Tracking

At last, in the figure, we can see that the trajectory tracking performance has been improved after the Kaman filter has been used.

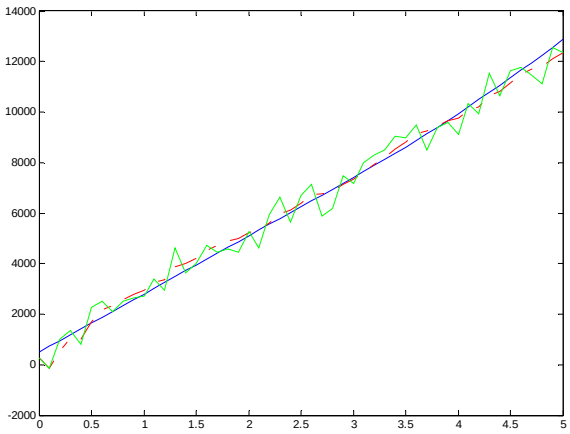

Figure 10 Trajectory Tracking

3.6.2 Conflict Simulation

The results is shown in Fig4.7, the value of blue line is greater than the conflict warning threshold, so the conflict has been resolved.

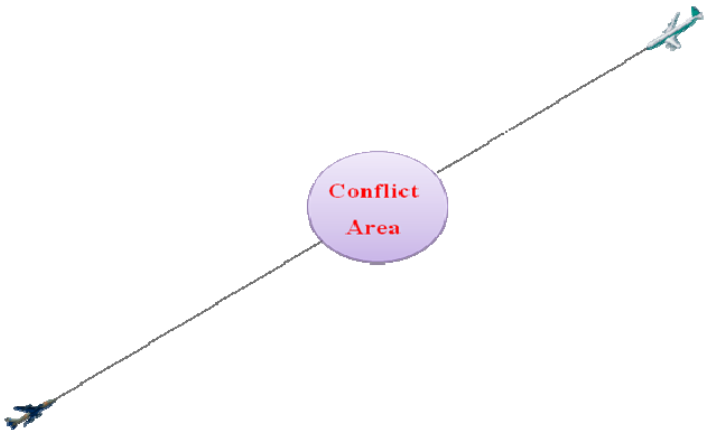

Figure 11 Simulation Scenarios

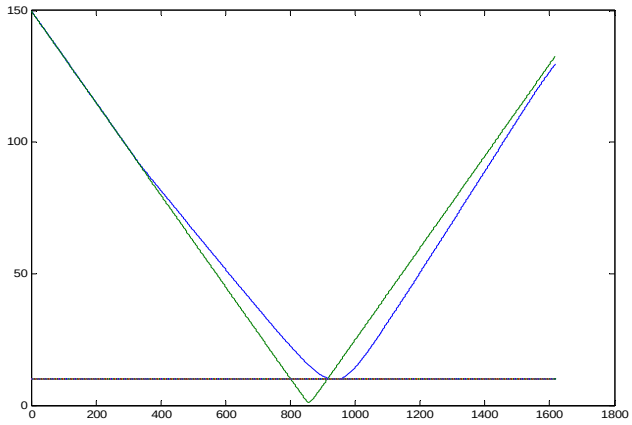

Figure 12 Horizontal Resolution Simulation Results

4. Conclusion

At the beginning, Airbus A320 and Boeing 737 are set as our flying crane's major competitors. As for surveillance system in particular, with the study of these aircrafts, almost all of these functions on those two kinds of aircraft could be embodied in flying crane. In addition, some new concept and design such as integrated surveillance system are also implemented. Likewise, the design process is based on the compliance of airworthiness with safety assessment. With these fly-safe and functional features, flying crane would probably make itself to be one of the most serious competitors in this area.